

UNIVERSIDADE FEDERAL DO PARANÁ

MALTON CARVALHO FRAGA

TAFONOMIA ATUALÍSTICA DE OFIUROIDES



CURITIBA  
2025

MALTON CARVALHO FRAGA

TAFONOMIA ATUALÍSTICA DE OFIUROIDES

Tese apresentada ao Programa de Pós-graduação em Geologia do Setor de Ciências da Terra da Universidade Federal do Paraná como requisito parcial à obtenção de título de Doutor em Geologia.

Orientadora: Profa. Dra. Cristina Silveira Vega

CURITIBA  
2025

DADOS INTERNACIONAIS DE CATALOGAÇÃO NA PUBLICAÇÃO (CIP)  
UNIVERSIDADE FEDERAL DO PARANÁ  
SISTEMA DE BIBLIOTECAS – BIBLIOTECA DE CIÊNCIA E TECNOLOGIA

Fraga, Malton Carvalho  
Tafonomia atualística de ofiuroides / Malton Carvalho Fraga. – Curitiba,  
2025.  
1 recurso on-line : PDF.

Tese (Doutorado) - Universidade Federal do Paraná, Setor de Ciências  
da Terra, Programa de Pós-Graduação em Geologia.

Orientador: Cristina Silveira Vega

1. Equinodermos. 2. Fossilização. 3. Soterramento. 4. Tafonomia. 5.  
Ofiuroides. I. Universidade Federal do Paraná. II. Programa de Pós-  
Graduação em Geologia. III. Vega, Cristina Silveira. IV. Título.

Bibliotecário: Elias Barbosa da Silva CRB-9/1894



MINISTÉRIO DA EDUCAÇÃO  
SETOR DE CIÊNCIAS DA TERRA  
UNIVERSIDADE FEDERAL DO PARANÁ  
PRÓ-REITORIA DE PÓS-GRADUAÇÃO  
PROGRAMA DE PÓS-GRADUAÇÃO GEOLOGIA -  
40001016028P5

## TERMO DE APROVAÇÃO

Os membros da Banca Examinadora designada pelo Colegiado do Programa de Pós-Graduação GEOLOGIA da Universidade Federal do Paraná foram convocados para realizar a arguição da tese de Doutorado de **MALTON CARVALHO FRAGA**, intitulada: **TAFONOMIA ATUALÍSTICA DE OFIUROIDES**, sob orientação da Profa. Dra. CRISTINA SILVEIRA VEGA, que após terem inquirido o aluno e realizada a avaliação do trabalho, são de parecer pela sua APROVAÇÃO no rito de defesa.

A outorga do título de doutor está sujeita à homologação pelo colegiado, ao atendimento de todas as indicações e correções solicitadas pela banca e ao pleno atendimento das demandas regimentais do Programa de Pós-Graduação.

CURITIBA, 02 de Abril de 2025.

Assinatura Eletrônica  
02/04/2025 17:58:26.0  
CRISTINA SILVEIRA VEGA  
Presidente da Banca Examinadora

Assinatura Eletrônica  
03/04/2025 11:37:14.0  
JULIANA DE MORAES LEME BASSO  
Avaliador Externo (UNIVERSIDADE DE SÃO PAULO)

Assinatura Eletrônica  
03/04/2025 14:52:14.0  
MARCELLO GUIMARÃES SIMÕES  
Avaliador Externo (UNIVERSIDADE EST. PAULISTA JÚLIO DE  
MESQUITA FILHO/BOTUCATU)

Assinatura Eletrônica  
04/04/2025 18:21:03.0  
ROBSON TADEU BOLZON  
Avaliador Externo (UNIVERSIDADE FEDERAL DO PARANÁ)

Assinatura Eletrônica  
02/04/2025 22:04:05.0  
ISMAR DE SOUZA CARVALHO  
Avaliador Externo (UNIVERSIDADE FEDERAL DO RIO DE JANEIRO)

## **AGRADECIMENTOS**

A Deus, pela manutenção da vida.

–

### **SUPORTE FINANCEIRO:**

Coordenação de Aperfeiçoamento de Pessoal de Nível Superior (CAPES)  
Programa de Apoio à Pós-graduação (PROAP)

–

### **ASSISTÊNCIA DE CAMPO:**

Laudicéia Fraga, Mauro Fraga, Nicole Stakowian & Rodrigo Guimarães

–

### **APOIO LABORATORIAL:**

Cristina Vega & Robson Bolzon  
Dhiego Silva & Jennyfer Pietsch  
Carolina Freire & Nicole Stakowian  
Caro Valenzuela & Adelita Rodrigues  
Thiago Silva, Juliana Costa & Deonir Agustini  
Liz Agnol, Lucas Szekut, Gabriel Martins & Henrique Rieger

–

### **SUPORTE TÉCNICO-CIENTÍFICO:**

Cristina Vega | Universidade Federal do Paraná  
Fernando Vesely | Universidade Federal do Paraná  
Ismar Carvalho | Universidade Federal do Rio de Janeiro  
Jeffrey Thompson | University of Southampton  
Jih-Pai Lin | National Taiwan University  
Juliana Leme | Universidade de São Paulo  
Marcello Simões | Universidade Estadual Paulista  
Michela Borges | Universidade Estadual de Campinas  
Przemysław Gorzelak | Polish Academy of Sciences  
Robson Bolzon | Universidade Federal do Paraná  
Samuel Zamora | Instituto Geológico y Minero de España

–

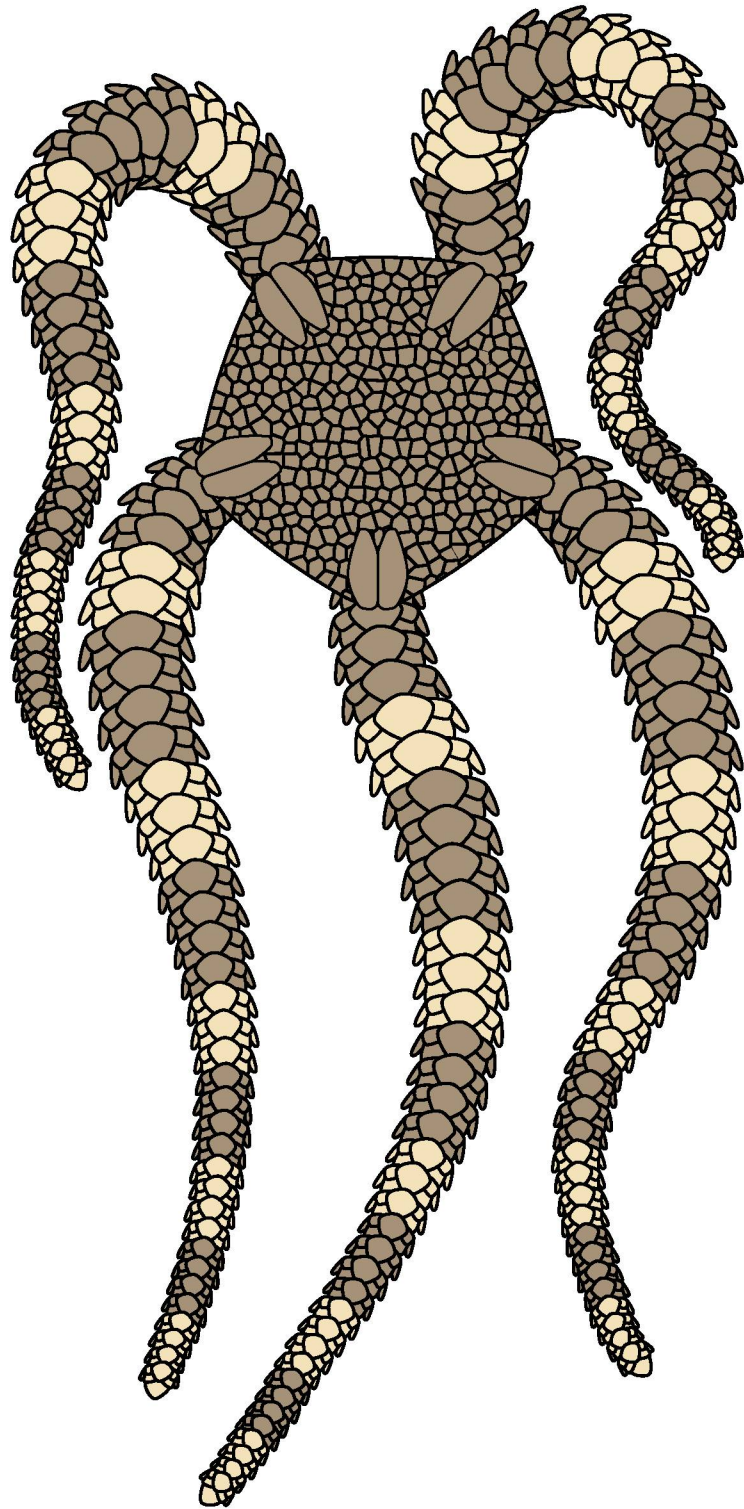
### **CONDUÇÃO DE TÉCNICAS ANALÍTICAS:**

Centro de Microscopia Eletrônica (CME-UFPR)  
Laboratório de Pesquisas Hidrogeológicas (LPH-UFPR)  
Instituto Laboratório de Análises de Minerais e Rochas (iLAMIR-UFPR)  
Laboratório de Fisiologia Comparativa da Osmorregulação (LABOSMO-UFPR)

–

### **CONCESSÃO DE ESPAÇO E FERRAMENTAS DE PESQUISA:**

Laboratório de Paleontologia (LABPALEO-UFPR)



*Fale com a terra, e ela o instruirá*  
**Jó 12:8**

## RESUMO

Ofiuroides são um grupo de equinodermos muito importante para rastrear condições excepcionais de fossilização. Isso deve-se ao fato de eles terem um hábito de vida livre que favorece o escape do soterramento, além de um esqueleto multi-elemental muito delicado que rapidamente desarticula após a morte. No entanto, embora esses princípios sejam consolidados na paleontologia, estudos de tafonomia atualística ainda são escassos para ofiuroides modernos, retendo muitas interpretações no campo da especulação. Por isso, o objetivo da tese foi explorar como diferentes variáveis ambientais podem influenciar no potencial de fossilização desses equinodermos em bacias marinhas. Para isso, 34 experimentos laboratoriais avaliaram o papel de diferentes tipos de fluxos deposicionais, agentes bioestratinômicos e processos diagenéticos na preservação de espécimes de *Amphipholis januaris*, coletados no Complexo Estuarino de Paranaguá, no Paraná. Do ponto de vista deposicional, os resultados evidenciaram que leitos de 10 cm de espessura são o limite-chave para o soterramento de espécimes vivos na maior parte dos casos. A deposição de leitos arenosos resultou em taxas maiores de autotomia, enquanto leitos lamosos beneficiaram a preservação de esqueletos intactos. No entanto, a deposição de lama não mostrou nenhum efeito entorpecente como anteriormente sugerido para equinodermos. O efeito anestésico foi observado somente sob sedimentos ricos em água doce intersticial, paralisando os espécimes e impedindo o escape devido às mudanças na salinidade. Do ponto de vista bioestratinômico, a acidificação, a energia da água, a produção de bolhas, a atividade microbiana, o crescimento de algas e a atividade de necrófagos foram os principais agentes de destruição das carcaças. Ainda assim, os experimentos apontaram que alterações bruscas na salinidade e na temperatura podem ser eficientes para limitar a distribuição de necrófagos e microrganismos, enquanto fundos escuros e estagnados podem proteger as carcaças de correntes e da desestabilização ocasionada pelo crescimento de algas filamentosas. Diferente da ideia de que a anoxia pode beneficiar a preservação, os resultados também destacaram que fundos pobres em oxigênio não limitam a desarticulação causada por micronecrófagos anaeróbicos. As condições anóxicas ainda aceleraram a produção de bolhas no sedimento e favoreceram a acidificação da coluna d'água, destruindo o esqueleto carbonático dos ofiuroides. Por fim, do ponto de vista diagenético, a preservação das partes moles foi controlada principalmente pela estrutura esquelética e pelo tipo de sedimento de soterramento. Enquanto as vísceras alojadas no disco foram mais propensas à compressão e à polimerização, as propriedades antibacterianas de argilas caulínicas foram bem-sucedidas em preservar compressões carbonáceas maiores e mais espessas ao longo das carcaças de ofiuroides. Tais resultados podem servir como um guia na interpretação tafonômica de fósseis de equinodermos e de outros organismos multi-elementais preservados em várias unidades geológicas marinhas, além das limitações de idade ou localização.

**Palavras-chave:** Equinodermos, Soterramento, Desarticulação, Fossilização.

## ABSTRACT

Ophiuroids are a highly significant group of echinoderms for tracing exceptional fossilization conditions. This is due to their free-living habit, which facilitates escape from burial, as well as their highly delicate multi-element skeleton, which rapidly disarticulates after death. However, although these principles are well established in palaeontology, actualistic taphonomic studies on modern ophiuroids remain scarce, leaving many interpretations in the realm of speculation. Therefore, the aim of the thesis was to explore how different environmental variables may influence the fossilization potential of these echinoderms in marine basins. To achieve this, 34 laboratory experiments assessed the role of different types of depositional flows, biostratinomic agents, and diagenetic processes in the preservation of *Amphipholis januarii* specimens, collected from the Paranaguá Estuarine Complex in Paraná, Brazil. From a depositional perspective, the results indicated that 10 cm-thick beds represent the critical threshold for the burial of live specimens in most cases. The deposition of sandy beds resulted in higher rates of autotomy, whereas muddy beds favoured the preservation of intact skeletons. However, mud deposition did not exhibit any numbing effect as previously proposed for echinoderms. The anaesthetic effect was observed only under sediments rich in interstitial fresh water, paralysing the specimens and preventing escape due to changes in salinity. From a biostratinomic perspective, acidification, water energy, bubble production, microbial activity, algae growth, and scavenger activity were the main agents of carcass destruction. Nonetheless, the experiments also pointed that abrupt changes in salinity and temperature can effectively limit the distribution of scavengers and microorganisms, while darker and stagnant bottoms can protect carcasses from currents and from destabilization caused by the rapid growth of filamentous algae. Contrary to the notion that anoxia can favour preservation, the results highlighted that oxygen-poor bottoms do not limit disarticulation by anaerobic microscavengers. The anoxic conditions themselves also lead to the liberation of bubbles in the sediment and boosted the acidification of the water column, destroying the ophiuroid skeleton. Finally, from a diagenetic perspective, soft tissue preservation was primarily controlled by skeletal structure and the type of burial sediment. While viscera housed in the flexible disc were more prone to compression and polymerization, the antibacterial properties of kaolinitic clays successfully preserved larger and thicker carbonaceous compressions along the ophiuroid carcasses. These results may serve as a guide for the taphonomic interpretation of echinoderm fossils and other multi-element organisms preserved in different marine geological units, beyond limitations of age or locality.

**Key-words:** Echinoderms, Burial, Disarticulation, Fossilization.

## LISTA DE FIGURAS

<b>Figura 1.</b> Representação idealizada do esqueleto multi-elemental dos ofiuroides.....	11
<b>Figura 2.</b> Espécie-modelo utilizada nos experimentos atualísticos.....	13
<b>Figura 3.</b> Coleta manual de espécimes de ofiuroides enterrados do sedimento.....	15
<b>Figura 4.</b> Simulação de soterramento com um fluxo de lama rico em água doce.....	16
<b>Figura 5.</b> Estrutura laboratorial usada nos experimentos bioestratinômicos.....	17
<b>Figura 6.</b> Exemplo de fóssil artificial produzido nos experimentos diagenéticos.....	18
<b>Figura 7.</b> Setup of the experiment aquarium (90 cm long x 15 cm wide x 30 cm high).....	22
<b>Figura 8.</b> Salinity and oxygenation curves during the initial hours after burial.....	24
<b>Figura 9.</b> Burial model of live free-living echinoderms under different turbidites.....	27
<b>Figura 10.</b> Collection site of the ophiuroid specimens.....	36
<b>Figura 11.</b> Six idealised decay stages for the multi-element skeleton of asterozoans.....	37
<b>Figura 12.</b> Experimental setup and ophiuroid samples.....	38
<b>Figura 13.</b> Decay pattern of <i>Protoreaster nodosus</i> .....	42
<b>Figura 14.</b> Decay pattern of <i>Amphipholis januarii</i> and <i>Ophiolepis superba</i> .....	44
<b>Figura 15.</b> Decay pattern of <i>Amphipholis januarii</i> under different marine conditions - A.....	45
<b>Figura 16.</b> Decay stages of asterozoans under conditions without macroscavengers.....	47
<b>Figura 17.</b> Microscopic decay patterns in arm segments of <i>Amphipholis januarii</i> - A.....	48
<b>Figura 18.</b> Decay pattern of <i>Amphipholis januarii</i> under different marine conditions - B.....	51
<b>Figura 19.</b> Microscopic decay patterns in arm segments of <i>Amphipholis januarii</i> - B.....	53
<b>Figura 20.</b> Decay pattern of <i>Amphipholis januarii</i> under different marine conditions - C.....	54
<b>Figura 21.</b> Decay stages of ophiuroids under conditions with macroscavengers.....	57
<b>Figura 22.</b> Decay pattern of <i>Amphipholis januarii</i> under macroscavengers.....	58
<b>Figura 23.</b> Decay pattern of <i>Amphipholis januarii</i> under polychaete activity.....	60
<b>Figura 24.</b> Rapid burial of a benthic community by a muddy extrabasinal turbidite.....	64
<b>Figura 25.</b> Provenance of the Devonian ophiuroids.....	71
<b>Figura 26.</b> Provenance of the artificial fossil ophiuroids.....	72
<b>Figura 27.</b> Chemical distributions in carbonaceous compressions of <i>Encrinaster pontis</i> .....	75
<b>Figura 28.</b> BSE images in natural and artificial fossil ophiuroids.....	76
<b>Figura 29.</b> Signatures under Raman spectroscopy.....	77
<b>Figura 30.</b> Chemical patterns of decayed remains under organic-poor kaolinitic clay.....	79
<b>Figura 31.</b> Chemical patterns of decayed remains under organic-rich kaolinitic clay.....	80

## LISTA DE TABELAS

<b>Tabela 1.</b> Main attributes and results of burial experiments.....	23
<b>Tabela 2.</b> Main attributes of decay experiments without macroscavengers.....	39
<b>Tabela 3.</b> Decay agents and limiting conditions for multi-element skeletons.....	61
<b>Tabela 4.</b> Main attributes of the diagenetic experiments.....	73

## SUMÁRIO

<b>1. INTRODUÇÃO</b> .....	10
1.1 CONTEXTO E PROBLEMÁTICA.....	10
1.2 OBJETIVOS.....	12
1.3 ESTRUTURA DA TESE.....	14
<b>2. MATERIAIS E MÉTODOS</b> .....	14
2.1 COLETA DOS ESPÉCIMES.....	14
2.2 EXPERIMENTOS DE SOTERRAMENTO.....	14
2.3 EXPERIMENTOS DE BIOESTRATINOMIA.....	15
2.4 EXPERIMENTOS DE DIAGÊNESE.....	16
2.5 ANÁLISES LABORATORIAIS.....	17
<b>3. RESULTADOS E DISCUSSÕES</b> .....	19
3.1 ARTIGO 1.....	19
3.2 ARTIGO 2.....	33
3.3 ARTIGO 3.....	68
<b>4. CONSIDERAÇÕES FINAIS</b> .....	87
<b>REFERÊNCIAS</b> .....	91
<b>ANEXOS</b> .....	103

# 1. INTRODUÇÃO

## 1.1 CONTEXTO E PROBLEMÁTICA

Os ofiuroides são uma classe de equinodermos extremamente abundante nos mares atuais. Com mais de 2000 espécies catalogadas, eles são distribuídos em todos os oceanos, desde regiões costeiras a planícies abissais, ao longo de mares polares a equatoriais (Stöhr et al., 2012). Diferente das estrelas-do-mar, eles possuem um disco central bem delimitado, de onde normalmente partem cinco braços longos e flexíveis (Figura 1). Embora certas espécies habitem tocas, todos os ofiuroides podem usar do movimento coordenado entre os braços para locomoção, ajudando-os a rastejar pelo fundo marinho de forma ágil e eficiente (Barnes, 1987; Tomholt et al., 2020; Goharimanesh et al., 2023). Além disso, eles também podem ser encontrados em grandes números, algumas vezes em aglomerações de milhares de indivíduos por m<sup>2</sup> (Warner, 1971; Broom, 1975). Contudo, apesar da extensa distribuição dos grupos modernos, os representantes fósseis são escassos no registro geológico devido ao baixo potencial de fossilização desses equinodermos (Lewis, 1980; Donovan, 1991; Brett et al., 1997; Ausich, 2021; Fraga & Vega, 2022).

Diferente de outros organismos bentônicos sésseis, os ofiuroides são bem-sucedidos em escapar da maioria dos eventos de soterramento rápido. Eles podem flexionar os braços e escavar acima no sedimento, reduzindo as chances de soterramento de espécimes vivos articulados (Brett et al., 1997; Ishida & Fujita, 2001). Eles ainda podem recorrer à autotomia quando o processo de escavação é obstruído, liberando voluntariamente alguns segmentos de braço para facilitar o escape da coluna de sedimento (Ishida & Fujita, 2001; Reid et al., 2019; Fraga & Vega, 2022). Curiosamente, mesmo após a morte, o potencial de preservação desses equinodermos ainda é muito limitado. Entre grupos fósseis existentes, o esqueleto multi-elemental dos ofiuroides pode incluir dezenas de milhares de pequenos ossículos carbonáticos fracamente articulados (Figura 1) (Lewis, 1980; Donovan, 1991; Brett et al., 1997; Ausich, 2021). Esse arranjo esquelético é um dos mais complexos conhecidos na natureza, e rapidamente entra em colapso após a morte, diferente de outros organismos com partes duras maiores e mais resistentes (Fraga & Vega, 2022).

Porém, embora essas percepções sejam consolidadas na paleontologia, estudos de tafonomia atualística ainda são escassos para ofiuroides modernos. E, na falta de correlatos atuais, muitas interpretações no registro geológico permanecem no campo da especulação. Do ponto de vista deposicional, um caso importante ocorre em bacias epicontinentais, onde os tempestitos são apontados como o principal agente para soterramento de equinodermos articulados (Lewis, 1980; Brett & Baird, 1986; Speyer & Brett, 1988; Brett et al., 1997; Ausich, 2021), mesmo na falta de evidências diretas da atuação de ondas de tempestade. De forma semelhante, a deposição de lama também tem sido atribuída como o “calcanhar de Aquiles”

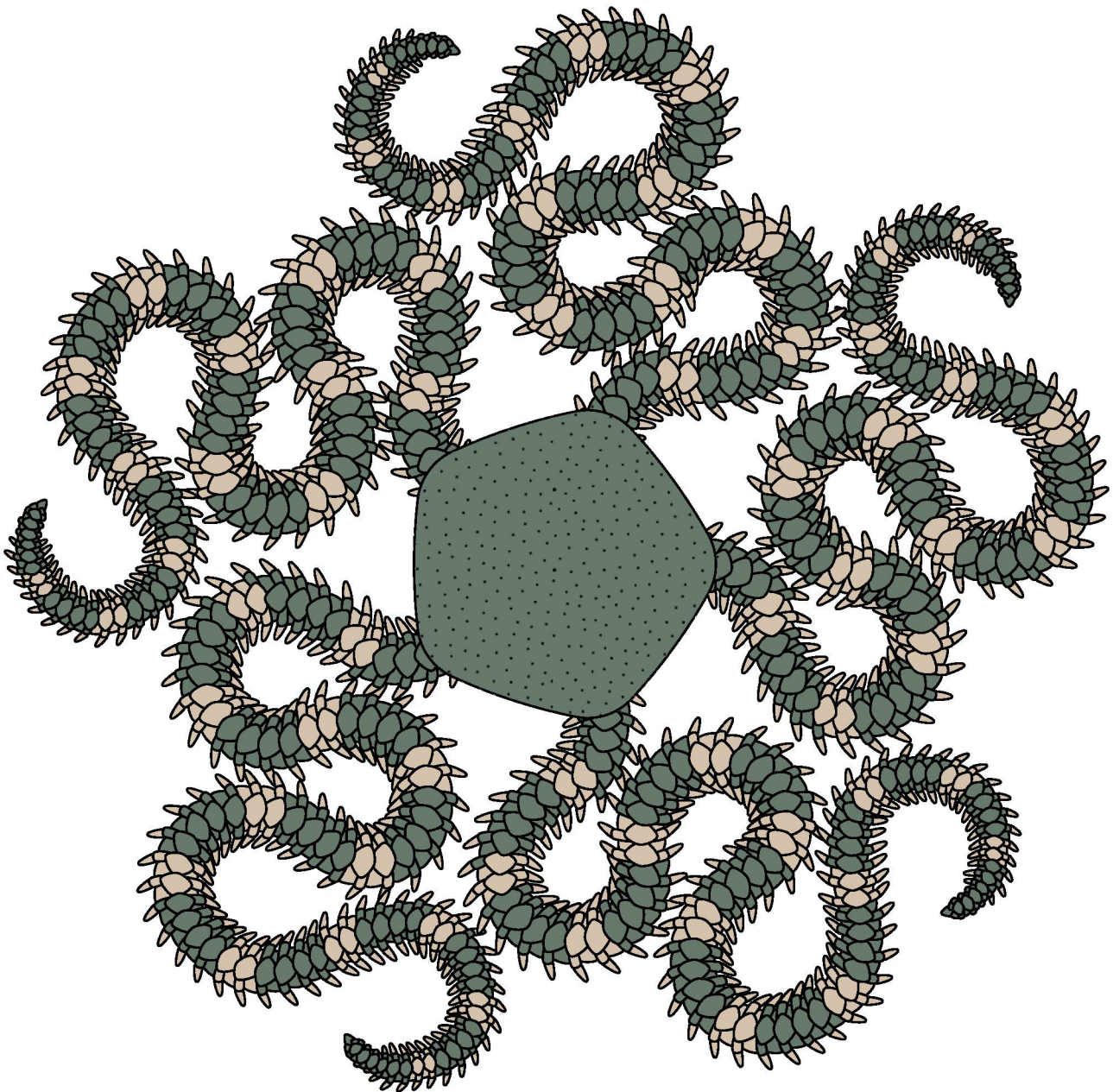


**Figura 1.** Representação idealizada do esqueleto multi-elemental dos ofiuoides. Observe a presença de um disco central bem marcado, por onde partem cinco braços longos e flexíveis. Note também que o corpo pode abranger dezenas de milhares de pequenos elementos carbonáticos fracamente articulados.

dos equinodermos, considerando um suposto efeito anestésico das partículas de argila sobre os canais do sistema ambulacral (Rosenkranz, 1971; Seilacher, 1982; Seilacher et al., 1985). Enquanto isso, outras alternativas para o soterramento rápido continuam subestimadas, como o potencial entorpecimento em massa causado pela água doce intersticial transportada em turbiditos extrabaciais<sup>1</sup> (Fraga & Vega, 2022).

Apesar de algumas pesquisas terem avaliado a degradação em laboratório, lacunas importantes também existem do ponto de vista bioestratigráfico, principalmente para equinodermos. A maior parte dos estudos tem focado no transporte de carcaças sob fluxos tur-

<sup>1</sup> Gerados fora da bacia marinha, normalmente por descargas fluviais (Zavala & Arcuri, 2016)

bulentos (Allison, 1986; Kidwell & Baumiller, 1990; Greenstein et al., 1995; Kerr & Twitchett, 2004; Gorzelak & Salamon, 2013; Salamon et al., 2014), mas o decaimento sob condições de baixa energia segue pouco explorado. De maneira similar, a oxigenação tem sido investigada sobretudo por simulações de anoxia ou normoxia (Allison, 1988b; Kidwell & Baumiller, 1990), mas sem informações sobre a faixa de hipoxia entre esses extremos. Os experimentos de temperatura também têm se concentrado em testes de curta duração (Kidwell & Baumiller, 1990) ou em alterações de tecidos moles (Kerr & Twitchett, 2004), restringindo o entendimento das mudanças a longo prazo nas partes duras. Por outro lado, o efeito de outras variáveis marinhas importantes ainda demanda atenção, como a salinidade, o sedimento, a luminosidade e a atividade de necrófagos sobre as carcaças.

Além disso, os ofiuroides também carecem de pesquisas focadas em transformações diagenéticas. Mesmo que alguns experimentos tenham avaliado mudanças químicas e cristalográficas ao longo do esqueleto carbonático de equinodermos soterrados (Dickson, 2001; Nebelsick, 2004), nenhum estudo atualístico foi publicado sobre o processo de preservação de tecidos moles nesses invertebrados. Esse fato é importante porque há um registro notável de fósseis de equinodermos com a preservação excepcional de restos orgânicos. Os exemplos englobam desde a piritização dos sistemas digestivo e ambulacral em ofiuroides e estiloforídeos (Glass & Blake, 2004; Glass, 2006; Clark et al., 2017; Saleh et al., 2023) à infiltração calcítica e ferruginosa em crinoides e estrelas-do-mar (Haugh, 1975; Haugh & Bell, 1980; Sutton et al., 2005). Interessantemente, mesmo compressões carbonáceas também tem sido descritas para alguns fósseis de ofiuroides (Fraga & Vega, 2022), destacando um potencial atípico para querogenização em grupos sem partes fortemente esclerotizadas ou cuticularizadas.

## 1.2 OBJETIVOS

Considerando a escassez de estudos atualísticos com equinodermos, o principal objetivo dessa tese foi de explorar como diferentes variáveis marinhas podem influenciar no potencial de fossilização de ofiuroides modernos com o auxílio de experimentos tafonômicos laboratoriais. Ao todo, 34 experimentos examinaram o impacto de eventos de soterramento, processos bioestratinômicos e transformações diagenéticas na preservação de espécimes vivos e carcaças frescas de *Amphipholis januarii* (Figura 2), um pequeno ofiuroide escolhido como espécie-modelo para o estudo atualístico. A partir disso, espera-se que os resultados obtidos sirvam como um guia para pesquisas futuras, auxiliando na interpretação tafonômica de diversas unidades geológicas onde fósseis de equinodermos e outros organismos multi-elementais são preservados, além das limitações de idade e de localização geográfica. Seguindo esse princípio, três objetivos específicos foram estabelecidos a fim de fracionar os



**Figura 2.** Espécie-modelo utilizada nos experimentos atualísticos. A espécie corresponde a *Amphipholis januarii*, um pequeno ofiuoide extremamente abundante nos fundos lamosos ao longo do Complexo Estuarino de Paranaguá, no litoral do estado do Paraná, Brasil.

experimentos laboratoriais do ponto de vista deposicional [1], bioestratinômico [2] e diagenético [3], tal como especificado abaixo:

[1] Revisar a influência da salinidade, da oxigenação, da granulometria do sedimento e da espessura do leito depositado sobre o comportamento de escape de espécimes vivos de ofiuoídes soterrados. A partir disso, analisar o potencial de preservação de fósseis articulados sob turbiditos intrabacinais<sup>2</sup> e extrabacinais.

[2] Revisar a influência da luz, da energia, da salinidade, do sedimento, da oxigenação, da temperatura e da atividade de necrófagos sobre a degradação de carcaças frescas de ofiuoídes expostas no fundo marinho. A partir disso, avaliar agentes destrutivos e atalhos de preservação relevantes para pequenos esqueletos multi-elementais.

[3] Revisar a influência do tipo de sedimento e do período de maturação no processo de formação de compressões carbonáceas ao longo de carcaças frescas de ofiuoídes soterrados. A partir disso, descrever o potencial de querogenização de tecidos moles em fósseis de equinodermos.

---

<sup>2</sup> Gerados na bacia marinha, como por tempestades e deslizamentos submarinos (Zavala & Arcuri, 2016)

### 1.3 ESTRUTURA DA TESE

O documento da tese foi organizado em quatro seções. A primeira delas, apresentada acima, compreende um panorama geral do tema, da problemática e dos principais objetivos. A segunda seção abrange uma síntese dos métodos usados na pesquisa. Seguindo as normas do Programa de Pós-graduação em Geologia da UFPR, a terceira seção, de resultados e discussões, engloba na íntegra os três artigos derivados da pesquisa. O primeiro artigo intitulado "*How does rapid burial work? New insights from experiments with echinoderms*" foi publicado no volume 67 de abril de 2024 da *Palaeontology*. O segundo artigo nomeado "*Decay and preservation in marine basins: A guide to small multi-element skeletons*" foi publicado no volume 196 de janeiro de 2025 do *International Biodeterioration & Biodegradation*. O terceiro artigo denominado "*Carbonaceous compressions in echinoderms: insights from fossils and diagenetic experiments*" foi publicado no volume 114 de janeiro de 2025 do *International Journal of Earth Sciences*. Por fim, a quarta seção da tese reúne uma lista com as principais considerações alcançadas pela pesquisa.

## 2. MATERIAIS E MÉTODOS

### 2.1 COLETA DOS ESPÉCIMES

Os experimentos foram baseados em espécimes de *Amphipholis januarii*, um pequeno ofiuoide semi-infaunal abundante ao longo dos bancos lamosos do Complexo Estuarino de Paranaguá, no litoral do Paraná (Figura 2) (Borges & Amaral, 2005; Bueno et al., 2018). Com auxílio de um pequeno barco de pesca alugado para acessar a região, centenas de espécimes adultos foram manualmente coletados vivos em períodos de maré baixa, quando partes do fundo do estuário emergem e os ofiuroides se enterram no sedimento para escapar da radiação solar (Figura 3). Todos os espécimes coletados foram alocados e transportados em caixas plásticas parcialmente preenchidas com o sedimento encharcado do estuário para diminuir o estresse e evitar a autotomia dos segmentos de braço. Alguns galões de lama e água salgada também foram amostrados na região para manipulação em laboratório. Ao todo, 12 coletas de campo foram realizadas, todas licenciadas pelos Sistema de Autorização e Informação em Biodiversidade (SISBIO) e Sistema Nacional de Gestão do Patrimônio Genético e do Conhecimento Tradicional Associado (SISGEN).

### 2.2 EXPERIMENTOS DE SOTERRAMENTO

Em laboratório, 10 espécimes ativos, capazes de virar rapidamente quando colocados com ventre para cima, foram usados em cada um dos nove experimentos de soterramento. As simulações foram geradas em um aquário marinho de 40 litros, com 30 cm de altura, 15 cm de largura e 90 cm de comprimento. Após três horas de aclimação dos espécimes,



**Figura 3.** Coleta manual de espécimes de ofiuroide enterrados no sedimento. O período de maré baixa expõe temporariamente grandes partes do fundo lamoso do Complexo Estuarino de Paranaguá, facilitando a coleta de espécimes bentônicos sem a necessidade de equipamentos de mergulho.

uma mistura de sedimento foi derramada no topo de uma rampa de vidro, com 10° de inclinação, previamente fixada no aquário (Figura 4). A mistura foi preparada para representar um fluxo de lama fluida com concentração de 0.3 kg/L, assim como observado em ambientes naturais (cf. Rijn, 2023). O sedimento usado na mistura de soterramento variou entre argila dolomítica e areia fina de quartzo. Por sua vez, o fluido intersticial variou entre água doce ( $\pm 0,5$  ppt) e água salgada natural (30 ppt). Enquanto isso, a espessura final do leito depositado alternou entre 1, 5 e 10 cm. Todos os ambientes de soterramento foram observados durante 48 horas, com registros periódicos das oscilações de salinidade e oxigenação. Apenas espécimes que expuseram completamente o disco acima do leito de soterramento foram classificados como tendo escapado com sucesso. A metodologia completa é apresentada na Seção 3.1 do Artigo 1.

### 2.3 EXPERIMENTOS DE BIOESTRATINOMIA

Cinco carcaças frescas de ofiuroides foram usadas em cada um dos 21 experimentos bioestratinômicos realizados em laboratório. As carcaças foram inseridas no fundo de aquá-



**Figura 4.** Simulação de soterramento com um fluxo de lama rico em água doce. Observe que a pluma de sedimentos se comporta como um fluxo hiperpicinal, soterrando os espécimes de ofiuroides a medida que percorre o fundo do aquário, sobre o leito pré-depositado de areia.

rios marinhos previamente instalados, com 15 cm de altura, 30 cm de largura e 30 cm de comprimento (Figura 5). Um ambiente padrão foi criado para simular a degradação em um fundo marinho idealizado, com substrato siliciclástico (areia fina de quartzo) e água quente (25°C), fluente (5 cm/s), euhalina (30 ppt), oxigenada (>5 mg/L) e rica em micronecrófagos. A partir disso, 20 simulações analisaram os efeitos da alteração na energia (0, 5 ou 10 cm/s), salinidade (15, 30 ou 45 ppt), luz (com ou sem fotoperíodo), temperatura (5, 15, 25 ou 35°C), substrato (lama, areia ou oóides), oxigenação (anoxia, hipoxia ou normoxia), presença de micronecrófagos (água natural ou artificial estéril) e atividade de macronecrófagos (moluscos, anelídeos, artrópodes e equinodermos). As carcaças de ofiuroides foram examinadas diariamente durante 15 a 45 dias sob essas diferentes condições. A metodologia detalhada é apresentada na Seção 3.2 do Artigo 2.

## 2.4 EXPERIMENTOS DE DIAGÊNESE

Quatro experimentos diagenéticos também foram realizados em laboratório para avaliar os processos de degradação e preservação em ofiuroides soterrados. Essas simulações



**Figura 5.** Estrutura laboratorial usada nos experimentos bioestratinômicos. Observe que cinco aquários foram instalados para permitir a condução simultânea de vários experimentos diferentes. Após isso, todos os aquários eram limpos e reestruturados para que novos ciclos de experimentos fossem realizados.

foram conduzidas em aquários cilíndricos, com 10 cm de diâmetro e 30 cm de altura, ambos previamente preenchidos com um leito de 10 cm de substrato pré-depositado e uma coluna de 8 cm de água salgada natural (30 ppt). Uma carcaça fresca de ofiuroide foi posicionada no fundo de cada um dos aquários e, em seguida, soterrada por 10 cm de lama. O sedimento de soterramento variou entre caulinita e uma mistura (1:1) de caulinita e lama marinha natural, peneirada em uma malha granulométrica de 125  $\mu\text{m}$ . Os experimentos foram lacrados e mantidos no escuro a 25°C para maturação diagenética por um período de 30 a 90 dias. Após essa etapa, os aquários foram abertos e mantidos a 35°C para secagem gradual do sedimento durante 30 dias. Por fim, um pequeno martelo e talhadeira foram utilizados para abrir os blocos secos de lama, possibilitando a análise dos fósseis artificiais ali preservados (Figura 6). A metodologia completa é apresentada na Seção 3.3 do Artigo 3.

## 2.5 ANÁLISES LABORATORIAIS

Diferentes técnicas laboratoriais foram conduzidas para auxiliar na interpretação dos dados da pesquisa. Amostras de sedimento foram quimicamente avaliadas sob Fluorescên-



**Figura 6.** Exemplo de fósil artificial produzido nos experimentos diagenéticos. Observe o espécime de *Amphipholis januarii* preservado após 60 dias em sedimento composto por uma mistura (1:1) de caulinita e lama marinha natural.

cia de Raios-X em um Panalytical Axios Max do Instituto Laboratório de Análise de Minerais e Rochas (iLAMIR-UFPR), enquanto amostras de água salgada foram detalhadas em laudos hidrológicos disponibilizados pelo Laboratório de Pesquisas Hidrogeológicas (LPH-UFPR). Para investigação microscópica da estrutura esquelética de *A. januarii*, um espécime foi explorado sob Microtomografia Computadorizada de Raios-X (Micro-CT) em um Skyscan 1172 providenciado pelo iLAMIR-UFPR. Entre carcaças frescas a degradadas, diversas amostras de *A. januarii* ainda foram avaliadas sob Microscopia Eletrônica de Varredura (MEV) e Espectroscopia por Energia Dispersiva (EDS) em um Tescan Vega3 LMU viabilizado pelo Centro de Microscopia Eletrônica (CME-UFPR). Além disso, algumas amostras querogenizadas também foram exploradas sob Espectroscopia Raman em um Microcópico WiTeC Alpha300R Confocal cedido pelo CME-UFPR.

### 3. RESULTADOS E DISCUSSÕES

#### 3.1 ARTIGO 1

## HOW DOES RAPID BURIAL WORK? NEW INSIGHTS FROM EXPERIMENTS WITH ECHINODERMS

by MALTON CARVALHO FRAGA<sup>1\*</sup> and CRISTINA SILVEIRA VEGA<sup>1</sup>

<sup>1</sup>Departamento de Geologia, Setor de Ciências da Terra, Universidade Federal do Paraná, Curitiba, PR, Brazil; malton.fraga@ufpr.br, cvega@ufpr.br

\*Corresponding author

**Abstract** - This research explores the significance of rapid burial in preserving fossils, with a particular focus on free-living echinoderms. Experiments were based on ophiuroids to simulate burial under different turbiditic flows. The results showed that a bed thickness of around 10 cm is a limit for the preservation of whole skeletons in most cases. The type of sediment can affect the integrity of the buried skeletons, with sand deposition resulting in higher rates of autotomy. However, mud deposition did not show any numbing effect, as previously believed for echinoderms. In contrast, freshwater-rich sediments can play a critical role, paralyzing specimens and preventing escape postures through rapid changes in salinity. From this, the study highlights the importance of extrabasinal turbidites, generated outside the marine basin, in the fossilization of marine invertebrates. Such sediments are rich in fresh water and can be more efficient burial traps compared to other intrabasinal deposits generated by storm waves or submarine landslides.

**Keywords:** ophiuroid, escape posture, turbidite, intrabasinal, extrabasinal, experimental taphonomy.

### Introduction

Burial is a critical factor in the preservation of most fossils. On the one hand, low burial rates keep the remains of organisms under the destructive effects of biostratinomy, resulting in the decay of soft parts and disarticulation of hard elements (Brandt, 1989; Brett & Baird, 1986). But a rapid and definitive burial, especially before death, is a shortcut that can interrupt the action of waves and currents, decrease the oxygenation of the sediment, restrict the activity of scavenging metazoans, and accelerate the diagenetic changes of the buried re-

mains (Brett & Baird, 1986, 1993; Speyer & Brett, 1988; Donovan, 1991; Parry et al., 2017). These rapid depositional events can produce obrution beds with well-preserved fossils, including delicate records of soft-bodied and multi-elemental organisms (Seilacher et al., 1985; Allison, 1988).

Although this exceptional preservation is often attributed to the rapid burial of live specimens, the type of depositional process associated is still an underexplored variable in taphonomic studies. An important case occurs in epicontinental basins, where tempestites are considered the main burial agent of articulated invertebrates (Lewis, 1980; Brett & Baird, 1986; Speyer & Brett, 1988; Brett et al., 1997; Ausich, 2021), even in the absence of direct sedimentological evidence of storm influence. However, although storm waves also can produce potential burial events, they carry a paradox: post-depositional reworking is high in proximal sandy tempestites, while the frequency and thickness of beds are limited in distal muddy tempestites, narrowing the fossilization potential in both depositional scenarios (Fraga & Vega, 2022).

In the case of free-living echinoderms, such as asteroids and ophiuroids, even a rapid influx of sediment still depends on a special condition to prevent the escape of specimens buried alive. The burial thickness can have an important effect in this scenario, hindering escape when the sediment column overload exceeds a critical point (Schäfer, 1972; Nichols et al., 1978). Another limiting effect is historically inferred to as mud deposition events, in which clay particles could obstruct the madreporite, suffocating the water vascular system of echinoderms (Rosenkranz, 1971; Seilacher, 1982; Seilacher et al., 1985). However, since modern echinoderms can remain active for prolonged periods without access to madreporite (e.g., Ferguson, 1992, 1995), it is uncertain whether mud obstruction alone could rapidly inhibit escape behaviours.

A more recent alternative for the burial may be also related to sediment flows derived from river discharges, which are well known for their extensive sedimentary contribution to modern seas. These events can generate long-duration hyperpycnal flows capable of transferring large loads of freshwater-rich sediments to distal regions beyond the storm wave base, sometimes hundreds of kilometres from the river mouth (Mulder et al., 2003; Mulder & Chapron, 2011; Zavala et al., 2011; Zavala & Arcuri, 2016; Zavala, 2020). Considering that fresh water is an anaesthetic for echinoderms (Saldanha, 1972; Hendler et al., 1995), these hyperpycnal flows may have the potential for mass immobilization of live specimens, favouring preservation under thinner burial beds (Fraga & Vega, 2022).

However, due to the lack of experimental studies, many effects of these processes are still speculative for the burial of free-living echinoderms. Therefore, here we review the influence of salinity, oxygenation, sediment size, and thickness of the deposited bed on the

burial potential of modern ophiuroids. The results are based on laboratory simulations of extrabasinal turbidites, to encompass freshwater-rich hyperpycnal flows generated outside marine basins, and intrabasinal turbidites, to cover depositional events generated within the marine basins, such as those derived from storm waves and submarine landslides. From this, we hope to explore how echinoderms can be buried alive and how different depositional events can influence the preservation of these delicate organisms in the geological record.

## Material and Method

The experiments were based on *Amphipholis januarii*, a small semi-infaunal ophiuroid abundant along the Paranaguá Estuarine Complex, on the coast of Paraná, in southern Brazil. With the help of a small boat to access the region, some specimens were collected manually during low tide intervals, when parts of this estuary are emersed for a few hours and the ophiuroids burrow into the sediment to avoid solar radiation. The specimens were transported in a thermal box partially filled with soggy sediment from the site. Some gallons of natural saline water were also sampled in the estuary for laboratory use. A total of nine field collections were conducted, one before each burial experiment, all licensed by the Brazilian regulatory systems for biodiversity and genetic heritage, SISBIO and SISGEN, respectively.

In the laboratory, the ophiuroids were carefully inspected to remove dead, moribund, or autotomized specimens. After initial screening, 10 adult and active specimens, capable of quickly turning over when placed on their backs, were selected to be used in each of the experiments. These specimens were acclimatized for 3 h inside a 40 L aquarium with an internal ramp, previously filled with 2 cm thick quartz sand substrate and natural saline water from the collection site (Fig. 7A). A thermostat was installed to maintain the temperature at 25°C, while a dissolved oxygen sensor was attached next to the substrate to analyse the oxygenation (Table S1). The ophiuroids remained free during the acclimatization, some buried themselves in the sand substrate, while others walked more actively through the aquarium.

After the acclimatization interval, the ophiuroids were again inspected and any specimen that had gone up the ramp was relocated to the bottom of the aquarium, in the region of the sand substrate. Once this pre-depositional scenario was established, the burial process was started, always on the same day that the ophiuroids were collected. The main attributes of the nine experiments are indicated in Table 1. The sediment used in the burial flow varied between dolomitic clay or fine quartz sand, the same as the aquarium substrate. The interstitial fluid used in the burial mixture was fresh water ( $\pm 0.5$  ppt) or natural saline

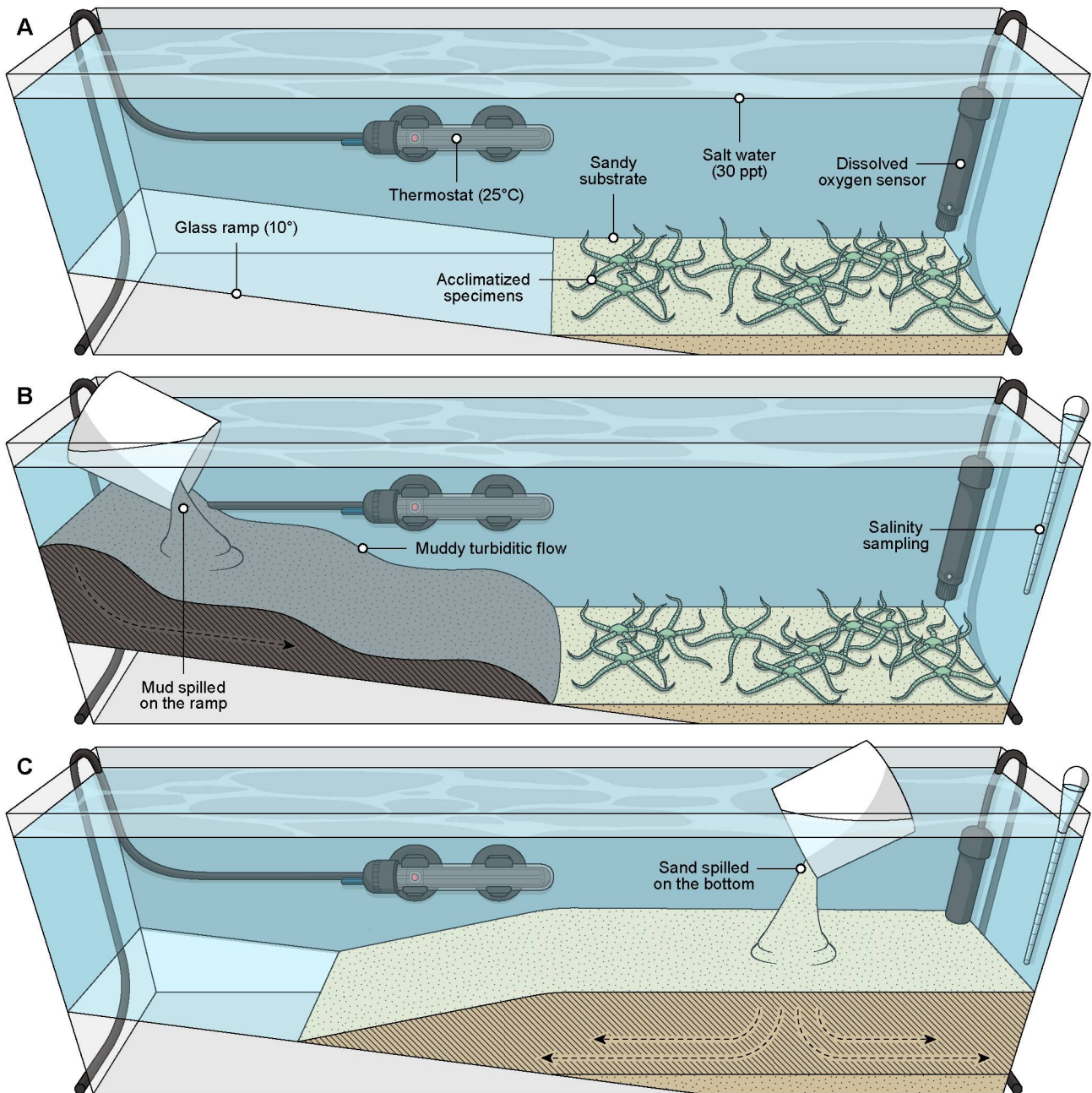


**Figure 7.** Setup of the experiment aquarium (90 cm long x 15 cm wide x 30 cm high). A, overview during the acclimatization phase of the ophiuroid specimens. B, burial methodology based on the production of a muddy turbiditic flow. C, burial methodology based on the deposition of fine quartz sand directly on the bottom.

water (30 ppt), the same as in the aquarium water. In turn, the final thickness of the burial bed varied between 1, 5, or 10 cm, with a margin of error of  $\pm 0.5$  cm in the 10 cm experiments.

In the mud burial, clay powder and water (fresh or saline) were previously mixed in a plastic bucket and then poured on top of the aquarium ramp. The process resulted in a non-erosive turbiditic flow head, with interstitial fresh or salt water, moving down the ramp and gently burying the specimens in the sand substrate at the aquarium bottom (Fig. 7B, Video S1). However, in previous tests, we were unable to reproduce a sandy turbiditic flow by dumping soggy sand at the top of the aquarium ramp. We were also unable to produce

**Tabela 1.** Main attributes and results of burial experiments. The percentages of burial and escape are the results after 48 h of observation of 10 ophiuroid specimens. Abbreviations: Qs, quartz sand; Dc, dolomitic clay; Sw, saline water; Fw, fresh water.

Main attributes	Burial experiments								
	Intrabasinal turbidites						Extrabasinal turbidites		
Sediment type	Qs	Qs	Qs	Dc	Dc	Dc	Dc	Dc	Dc
Interstitial fluid	Sw	Sw	Sw	Sw	Sw	Sw	Fw	Fw	Fw
Burial thickness (cm)	1	5	10	1	5	10	1	5	10
Escape unharmed (%)	70	30	10	100	100	-	100	30	-
Escape + autotomy (%)	30	70	20	-	-	-	-	10	-
Buried specimens (%)	-	-	70	-	-	100	-	60	100

a cohesive mixture of fresh water and pure quartz sand, so we decided not to conduct experiments to represent sandy extrabasinal turbidites. As an alternative, sand burial was produced only by depositing dry sand directly above the region of the aquarium bottom (Fig. 7C).

After burial, the aquarium was observed continuously during the first 8 h. During this period, the salinity of the water and the internal oxygenation of the burial bed were recorded every 30 min. Two 9 W LED lamps were also turned on just above the aquarium to facilitate photography during these initial hours. The aquarium was subsequently covered with a black cloth and left in semi-dark conditions. After 24 h of burial, all specimens that escaped were carefully removed for inspection of potential autotomy patterns resulting from burial stress. The same process was repeated after 48 h of burial and then the experiments were ended. Only specimens that completely exposed the disc above the burial bed were considered to have escaped. No buried specimens were recovered for further evaluation.

## Results

### *Burial by sandy intrabasinal turbidites*

Three experiments were conducted to represent the burial of echinoderms under sandy flows generated within a marine basin (Table 1). The interstitial fluid of the sediment flow was seawater, without a change in the salinity of the environment. Consolidation of the sand beds was immediate, after just the first few seconds of burial, without significant long-term compaction or dehydration. The deposition of pure sand did not affect the clarity

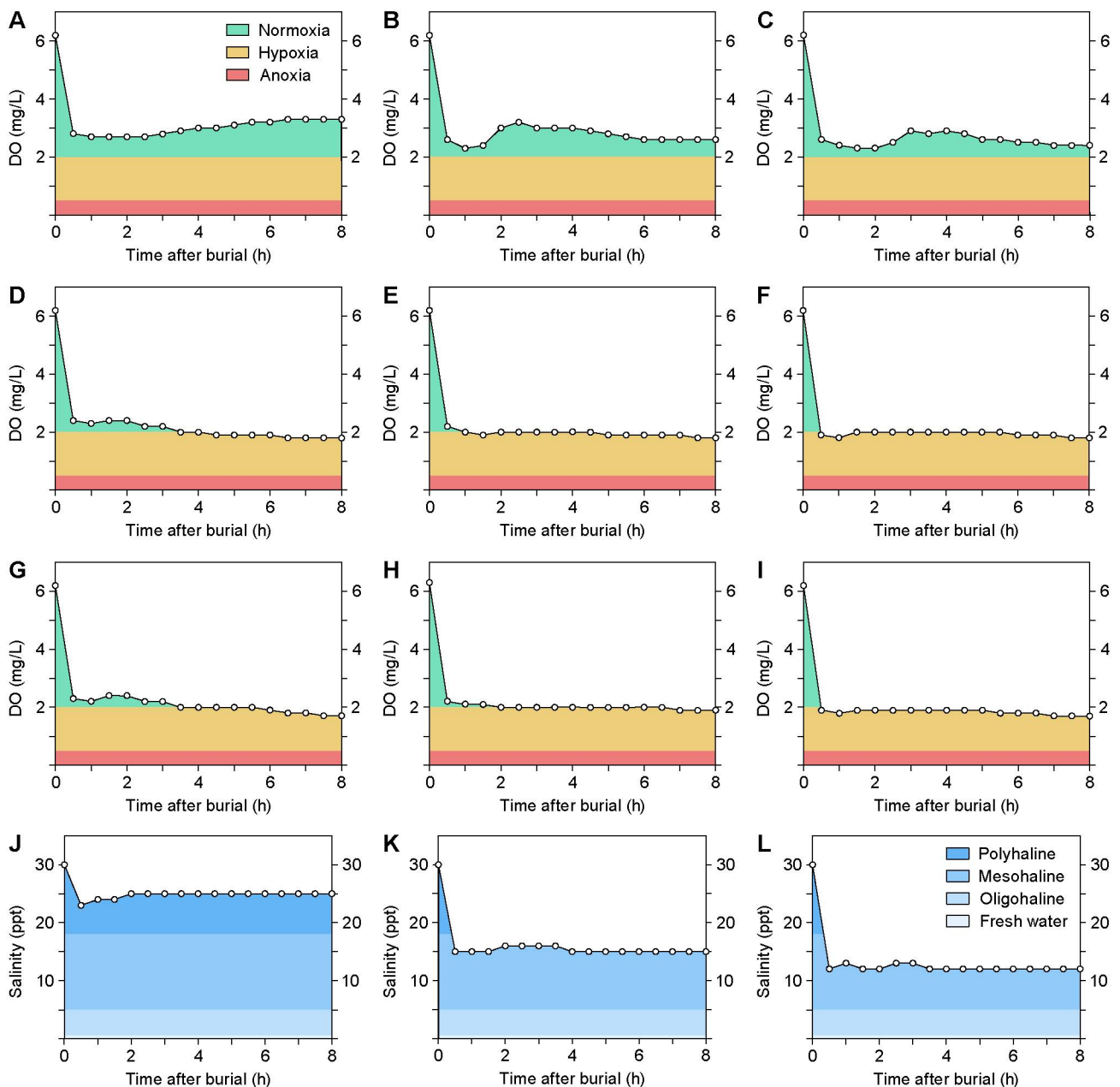


**Figure 8.** Salinity and oxygenation curves during the initial hours after burial. A–C, dissolved oxygen (DO) under sand beds of 1 cm (A), 5 cm (B), and 10 cm (C) with interstitial salt water. D–F, dissolved oxygen under mud beds of 1 cm (D), 5 cm (E), and 10 cm (F) with interstitial salt water. G–L, salinity and dissolved oxygen under mud beds of 1 cm (G, J), 5 cm (H, K), and 10 cm (I, L) with interstitial fresh water.

of the water column, which facilitated the observation of behavioural patterns. The dissolved oxygen below the burial sand followed a similar pattern regardless of bed thickness, with a rapid reduction to restrict normoxic conditions followed by a subtle phase of reoxygenation after the first hours of burial (Fig. 8A-C).

All specimens escaped under the deposition of a 1 cm sand bed (Table 1). Most specimens quickly excavated the sand column and reached the bed surface within a few minutes of burial. Skeletal integrity was relatively high and only 30% of specimens showed mild signs of autotomy, with the loss of one or two arm tips during escape efforts. The results were

also similar under the 5 cm sand bed, with an escape rate of 100% (Table 1). However, the escape velocity was lower under these conditions, and most specimens reached the bed surface only after 3 h of burrowing in the sand. The autotomy proportion was also substantially higher, involving 70% of escapist specimens, ranging from the loss of some arm tips to the loss of several arm segments and the dorsal skin of the disc.

The burial of complete specimens was only recorded from the deposition of 10 cm of sand (Table 1). After burial under this thicker bed, the specimens visible on the sides of the aquarium initiated escape through a main arm segment that excavated at a high angle ( $>60^\circ$ ) toward the top of the bed (Fig. S1A-C). When maximum arm extension was reached, the specimens began to drag the disc and the rest of the arms along the same track. These escape burrows can reach about 6 cm during the first 5 h of burial, but advancement was limited after this interval. Most specimens reached exhaustion during the disc drag and remained buried motionless until the end of the experiment (Fig. S1C). The escape rate dropped to 30% under these burial conditions, maintaining a high proportion of arm autotomy (Table 1).

#### *Burial by muddy intrabasinal turbidites*

Three experiments simulated the burial of echinoderms under muddy flows generated within a marine basin (Table 1). The interstitial saltwater fluid did not change the salinity of the environment in either case. The deposition of the clay flocculates was relatively rapid, generating a bed of fluid mud at the bottom a few minutes after burial. The consolidation of these beds began with a phase of intense dehydration during the first hour of burial, with the formation of small ascending channels to drain interstitial fluids from mud and pre-deposited sand. The final bed thickness was reached after about three hours of gradual compaction. The dissolved oxygen dropped rapidly to restrict normoxic conditions under the thinnest bed (Fig. 8D) and to mild hypoxic conditions under the thickest beds (Fig. 8E-F).

All specimens escaped intact under the deposition of 1 and 5 cm mud beds (Table 1). The escape behaviour was similar in these cases and began quickly after the first minutes of burial. Most specimens visible on the sides of the aquarium used a main arm to excavate the mud column vertically. The first arm tips reached the surface of the bed in less than 20 min. Some specimens also flexed these tips in a wave-like motion to reoxygenate the escape burrow as the disc excavated upwards. Despite the greater turbidity in the mud experiments, the first escapist specimens were fully visible above the mud bed after the first hour of burial under these conditions, when most suspended flocculates had decanted, and the water column began to clear again.

In turn, no specimens escaped from under the 10 cm mud bed (Table 1). Most specimens had a rapid response under these conditions, initiating a high-angle (>60°) excavation with the arms within minutes of mud bed deposition. This behaviour was quite active during the initial hour, resulting in vertical escape burrows of up to 6 cm (Fig. S1D). But the advance of these burrows was drastically reduced after this interval, and the specimens reached exhaustion, remaining trapped in the mud bed. After 24 h of burial, most specimens aborted their escape attempts (Fig. S1E). At the end of the experiment, after 48 h of burial, only sporadic movements of the tube feet were observed in some contracted specimens buried on the sides of the aquarium (Fig. S1F).

### *Burial by muddy extrabasinal turbidites*

Three experiments simulated the burial of echinoderms under muddy hyperpycnal flows derived from river discharges (Table 1). The interstitial fresh water from the burial mud rapidly altered water salinity in all experiments, causing a drop to polyhaline conditions in the deposition of the 1 cm bed (Fig. 8J) and to mesohaline conditions in the deposition of the 5 and 10 cm beds (Fig. 8K-L). However, the consolidation of these mud beds was like the pattern of muddy intrabasinal turbidites, with an initial phase of intense dehydration followed by long-term compaction during the three hours after burial. The variations in dissolved oxygen under the burial beds were also similar, producing a sharp decrease to restrict normoxic and mild hypoxic conditions (Fig. 8G-I).

All specimens showed a rapid pattern of numbness seconds after the deposition of the freshwater-rich mud, with the contraction of the arms around the disc or, in some cases, with the attempt to burrow into the pre-deposited sand substrate. These specimens could remain motionless in these conditions for hours before any attempt to escape was made. Although quite late, all specimens escaped intact under the deposition of the 1 cm mud bed (Table 1). In turn, only 40% of the specimens escaped under the 5 cm mud bed, mostly after 8 h of burial and, in one case, including autotomy of the dorsal disc skin (Table 1). However, all specimens were buried under the deposition of the 10 cm mud bed, and no escape burrows were observed under these conditions (Table 1).

## **Discussion**

### *General considerations*

Our results agree with previous studies that bed thickness is a key factor in rapid burial and that an increase in the overload of the sediment column drastically decreases the escape potential (Schäfer, 1972; Nichols et al., 1978). However, our experiments indicate that 10 cm is a critical thickness for the burial of free-living echinoderms, which is higher than the 5 cm

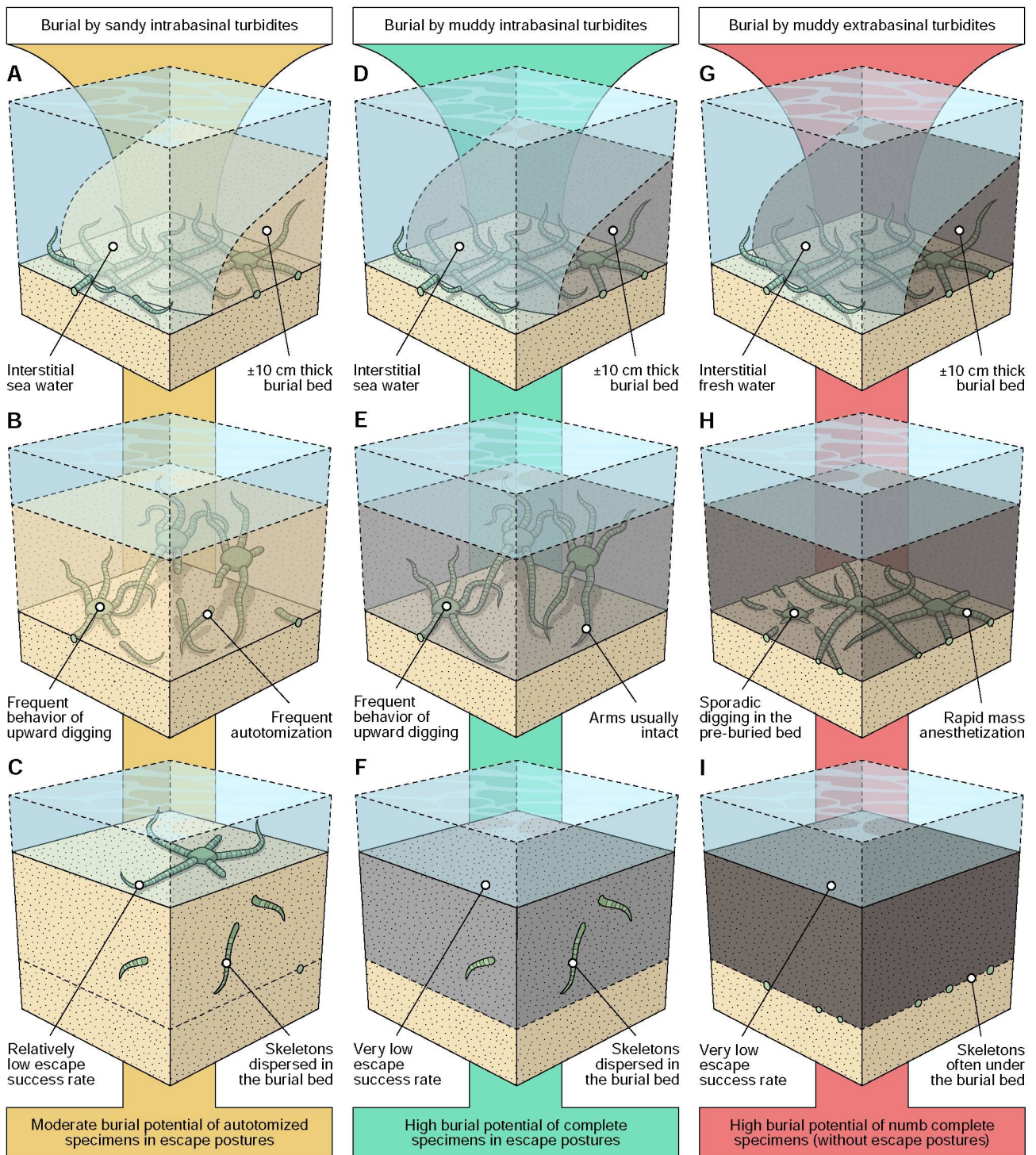


**Figure 9.** Burial model of live free-living echinoderms under different turbidites, considering a critical burial thickness of 10 cm. A–C, burial by sandy intrabasinal turbidites impelling escape attempts and autotomy of arm segments. D–F, burial by muddy intrabasinal turbidites impelling escape attempts but without autotomy. G–I, burial by muddy extrabasinal turbidites repressing escape attempts due to sudden change in salinity.

initially proposed for ophiuroids (Schäfer, 1972) and lower than the 30 cm suggested for other marine invertebrates (Nichols et al., 1978). The deposition of 10 cm thick beds showed a high potential for the burial of live specimens (Fig. 9A-I) regardless of the type of sediment or interstitial fluid, while burial under thinner beds required some more specific conditions to preserve beyond just autotomized parts.

Interestingly, the results also indicated that even rapid deposition does not necessarily lead to anoxia under the buried sediment. All sand beds ( $\leq 10$  cm) reduced oxygenation only to more restrictive normoxic conditions, about 3 mg/L, probably due to the greater ease of diffusion of oxygen from the water column to the sand pores. In turn, all mud beds ( $\leq 10$  cm) were able to produce only mild levels of hypoxia, around 2 mg/L, and even in the long term, some buried specimens still exhibited slight movements of the tube feet, indicating that the process of death from asphyxiation in these conditions may be substantially slow. Thus, it is unlikely that low oxygenation is a factor that prevents escape in the first hours after burial, especially for organisms with lower metabolic rates, such as echinoderms (e.g., Hughes et al., 2011).

On the other hand, the size of the sediment played a significant role in the escape behaviour and integrity of the buried skeletons. Rapid sand deposition produced the highest rates of autotomy among all escapist specimens, possibly as a result of more stressful attempts to excavate in a coarser substrate. This suggests a greater potential for preserving isolated arms and incomplete skeletons under more sand-rich burial beds, as long as there is no reworking by waves, currents or bioturbators. In contrast, the rapid deposition of mud-rich flows can produce burial events subtle enough to maintain the skeletal integrity of most specimens (Fig. 9D-I), favouring the preservation of complete multi-elemental skeletons, with a very low proportion of autotomy.

However, unlike the paradigm that smothering by mud would be the Achilles heel of echinoderms (Rosenkranz, 1971; Seilacher, 1982; Seilacher et al., 1985), our experiments did not show any anaesthetic effect of mud alone on the activity of the specimens. All ophiuroids quickly initiated escape under saltwater-rich mud beds, without any short-term limitation on burrowing speed. The limiting effects of the mud began to become evident only in the long term when the effort of the specimens became insufficient to fluidize the thixotropic (more solid) mud bed. Under these conditions, the escape potential was drastically reduced when the echinoderms did not reach the top of the bed before compaction of the fluid mud, burying the specimens more through fatigue rather than obstruction of their water vascular systems.

Finally, interstitial fresh water was a critical element in the mass numbing of the echinoderms. After the deposition of freshwater-rich flows, even the small change from euhaline to polyhaline conditions was enough to paralyse specimens for hours below the burial column (Fig. 9G-H). This sudden variation in salinity favoured the burial of most specimens under the mud bed of just 5 cm, half the thickness required for burial under mud with interstitial salt water. Therefore, we suggest that the preservation potential of river-derived flows may be up to twice as high as that for other events generated within marine basins, such as

storm waves and submarine landslides. Since these extrabasinal turbidites are the most efficient agents for transferring sediment to marine basins (Zavala, 2020), they also need to be recognized as an important trap for the rapid burial of marine invertebrates.

### *Palaeontological implications*

Although much attention is paid to storms, different depositional agents can produce obrution events in marine geological units. To facilitate identification, these agents can be separated into two main groups, organized according to the origin of the sediment flow. The first encompasses intrabasinal turbidites that remobilize sediments pre-deposited within the marine basin itself, while the second includes extrabasinal turbidites that transport sediments generated by river discharges (Mulder et al., 2003; Mulder & Chapron, 2011; Zavala et al., 2011; Zavala & Arcuri, 2016; Zavala, 2020). Each of these processes has specific sedimentological characteristics, as well as distinct zones of occurrence, which can substantially affect the escape response and the preservation pattern of buried assemblages.

Good examples of intrabasinal turbidites can be deposits formed by submarine landslides and the more distal action of storm waves. Since these events remobilize the seabed, the interstitial fluid of the sediment flow is seawater itself. Echinoderms buried under these conditions can then develop rapid escape behaviours, resulting in skeletons tilted and dispersed in the obrution horizon. The complexity of the postures can also be increased if the specimens are incorporated in more turbulent flows. However, in the absence of an anaesthetic element, the major limiting factor for preservation becomes the thickness of the deposited bed. Thicker intrabasinal turbidites may favour the trapping of live specimens after the exhaustion reached with the escape efforts, but thinner beds may be unsuccessful in burying more than just autotomized parts and other carcass remains.

Similar cases have been well recorded in dozens of geological units from the Eocene to Pleistocene in Japan (Ishida et al., 1996; Ishida & Fujita, 2001; Ishida, 2003; Ishida et al., 2015; Ishida et al., 2024). Ophiuroids can be dispersed at high angles ( $>30^\circ$ ) in silty sandstone beds of these units. Many curved arm postures indicate random escape movements, probably during the rapid burial of the slope by gravity flows, such as submarine landslides. The skeletons can vary from articulated to semi-articulated, highlighting the possibility of arm autotomy during the excavation effort. The thickness of these obrution beds can also be substantially high, around 15–25 cm (Ishida et al., 1996, 2015), which is consistent with the trapping of live specimens mainly due to large sediment overload.

Another relevant case has also been documented in the Lower Devonian Voorstehoek Formation of South Africa (Reid et al., 2019). Hundreds of ophiuroids and stylophorans were preserved in this unit along a 5 cm thick sandy lenticular bed. Many specimens exhibit well-

developed escape behaviours, including inverted postures and arm segments stretched at high angles ( $>30^\circ$ ) to bedding planes. The proportion of incomplete skeletons is high (46%) and abundant isolated arms ( $>600$ ) are preserved near the base of the obrution bed, probably due to a mass autotomy event during stressful deposition of a sandy tempestite. Ripple marks and irregular cross-bedding are also common in adjacent beds and support the scenario of a shallow continental shelf disturbed by periodic storms (Reid et al., 2019).

However, the burial potential of intrabasinal turbidites has limitations and the widespread application of these processes may be a problem in other scenarios. On the one hand, submarine landslides depend on steep and unstable seafloors, where the collapse of sediments can result in gravity flows (Zavala et al., 2011; Zavala & Arcuri, 2016; Zavala, 2020). These processes may be frequent on many continental slopes, but are incompatible with the shallow, low-gradient environment of most epicontinental seas. In turn, although storm disturbance is common in shallower seas, fossil preservation under these conditions is hampered by constant proximal reworking and the low rate and thickness of distal beds (Jelby et al., 2020; Fraga & Vega, 2022). Even an exceptional burial by tempestites on the middle shelf must be treated with caution because, in the absence of numbing agents, the chance of successful escape remains high among free-living organisms.

Therefore, an important alternative for burial involves the action of extrabasinal turbidites. These deposits are generated by hyperpycnal flows associated mainly with medium to large river discharges. The duration of the events can extend from days to months, travelling slowly for hundreds of kilometres even on continental shelves with a low topographic gradient (Mulder et al., 2003; Mulder & Chapron, 2011; Zavala et al., 2011; Zavala & Arcuri, 2016; Zavala, 2020). As a result, hyperpycnal flows can transfer large sediment loads from the continent to distal marine basins, in regions far beyond the base of storm waves. Furthermore, as these flows are rich in interstitial fresh water, derived from the river itself, they also have great potential for mass anaesthesia of stenohaline organisms; a good trap for burying escapist groups.

Even though some echinoderms can tolerate and gradually acclimatize in hyposaline ( $<30$  ppt) and hypersaline ( $>40$  ppt) environments (e.g., Salamon et al., 2012; Russell, 2013), such as the estuarine ophiuroids studied here, the sudden change in salinity has a well-known anaesthetic effect for the entire group (Saldanha, 1972; Hendler et al., 1995). Thus, the rapid burial of the seafloor by an extrabasinal turbidite may help to quickly immobilize entire communities of echinoderms, delaying the development of escape attempts due to the limited osmoregulation of these invertebrates. Unlike intrabasinal turbidites, the numbing by fresh water is the major limiting factor in burial by hyperpycnal flows and may favour the preservation of live specimens even in thinner beds (Fraga & Vega, 2022).

Although this is still a new perception in palaeontology, some analogous deposits have been traced in the epicontinental sequences of the Lower Devonian Ponta Grossa Formation in Brazil (Fraga & Vega, 2022). Many asteroids, ophiuroids, and stylophorans from this unit have been preserved at the base of thin muddy beds, only about 1-3 cm thick. Most specimens are articulated and present resting and walking postures, indicating abruptly buried living assemblages (Fraga & Vega, 2020, 2022). The absence of escape postures under such thin beds draws attention to a potential mass numbness during burial, blocking attempts to excavate the sediment. Plant remains and freshwater microfossils can also be dispersed in these obrution horizons, corroborating a deposition from muddy flows rich in land-derived elements, such as extrabasinal turbidites (see Zavala et al., 2012; Zavala & Arcuri, 2016).

## **Conclusion**

The rapid burial of live specimens is an important step in the fossilization of echinoderms. Even a brief period of a few hours between death and burial can be enough to damage their delicate multi-element skeletons due to the accelerated decay rates of these animals. Thus, the most plausible interpretation for most articulated echinoderm fossils involves death caused by the depositional event itself, under obrution beds. However, since many free-living groups can burrow into the sediment, exceptional preservation still depends on specific conditions: deep burial to prevent escape or at least shallow burial with an anaesthetic element. Under any other thin normal bed, the escape potential of these animals is high and the formation of well-articulated fossils is unlikely.

Based on this, our experiments explore how distinct types of turbidites can impact the preservation potential of free-living echinoderms. In most cases, we observed that a bed thickness of around 10 cm, before diagenetic compaction, is a limit for the burial of whole skeletons. The type of sediment can also interfere with the integrity of buried specimens, with sand causing more stress and autotomy than mud. However, mud deposition alone does not have a short-term smothering effect as previously believed for echinoderms. In turn, freshwater-rich sediments showed a mass numbing effect, quickly preventing escape attempts. Therefore, sediment flows derived from river discharges appear to be excellent traps for anaesthetizing and preserving free-living echinoderms even under thinner burial beds. These results reinforce the need to go beyond storm waves or submarine landslides, also considering extrabasinal turbidites, generated outside the marine basin, as potential burial agents of marine invertebrates in the geological record.

## **Acknowledgements**

We thank the Universidade Federal do Paraná (UFPR) and the Coordenação de Aperfeiçoamento de Pessoal de Ensino Superior (CAPES) for funding the research grant. We also thank the Post-Graduate Support Program (PROAP) for the financial support during fieldwork and the Laboratório de Paleontologia (LABPALEO-UFPR) for making the research structure viable. Special thanks to Michela Borges (MDBio-UNICAMP) for the taxonomic identification of the ophiuroid and to Nicole Stakowian (LFCO-UFPR) for assistance and guidance during field expeditions. Finally, we would like to thank the technical editors for their assistance, and Samuel Zamora and Jeffrey Thompson for their constructive comments.

## **Author contributions**

**Conceptualization** MC Fraga (MCF); **Data Curation** MCF; **Formal Analysis** MCF; **Funding Acquisition** MCF; **Investigation** MCF; **Methodology** MCF, CS Vega (CSV); **Project Administration** MCF; **Resources** MCF; **Supervision** CSV; **Validation** MCF, CSV; **Visualization** MCF; **Writing – Original Draft Preparation** MCF; **Writing – Review & Editing** MCF, CSV.

## **Supplementary data**

<https://doi.org/10.1111/pala.12698>

## 3.2 ARTIGO 2

### **DECAY AND PRESERVATION IN MARINE BASINS: A GUIDE TO SMALL MULTI-ELEMENT SKELETONS**

by MALTON CARVALHO FRAGA<sup>1\*</sup> and CRISTINA SILVEIRA VEGA<sup>1</sup>

<sup>1</sup>Departamento de Geologia, Setor de Ciências da Terra, Universidade Federal do Paraná, Curitiba, PR, Brazil; malton.fraga@ufpr.br, cvega@ufpr.br

\*Corresponding author

**Abstract** - This research explores how decay works and how different variables can affect this process in marine environments. The results are based on asterozoan echinoderms to cover one of the most complex multi-element skeletons in nature. Long-term experiments evaluated the effects of light, energy, salinity, sediment, oxygenation, temperature, and scavenger activity. The results showed that seven major agents can accelerate decay, including algal growth, water energy, microbial activity, microscavengers, macroscavengers, bubble production, and water acidification. Rapid burial of living organisms is the main shortcut to the fossilization of articulated specimens, but burial days to weeks after death can still lead to preservation if exceptional conditions delay the decay agents. Abrupt changes in salinity and temperature can restrict the distribution of scavengers and microorganisms, helping to preserve carcasses in the long term. Deeper or turbid seafloors can prevent small skeletons from destabilising due to the rapid growth of filamentous algae. Stagnant waters can also protect carcasses from waves and bottom currents, while water stratification can attenuate the attack of microscavengers. Although anoxia favours the preservation of soft parts, it is unable to prevent the anaerobic attack of microscavengers, which accelerates the destruction of small hard parts. Microbial reduction in anoxic regions can also drive the production of bubbles and the acidification of the water column, accelerating the destruction and dissolution of carbonate elements. These insights review important taphonomic concepts and provide a useful guide for interpreting the preservation potential of delicate organisms throughout the geological record.

**Keywords:** Asterozoan, Echinoderm, Taphonomy, Fossilization, Disarticulation, Preservation potential.

## Introduction

Fossilization is a fascinating process that allows us to examine the unique characteristics of different life forms that once existed on Earth. However, this process is an exception, not the rule. After death, the decomposition of soft tissues and the disarticulation and fragmentation of hard elements tend to transform all organisms into progressively smaller parts. These changes occur due to the complex physical, chemical, and biological dynamics of most superficial environments on the planet (Schäfer, 1972; Müller, 1979; Brett & Baird, 1986; Speyer & Brett, 1988; Martin, 1999; Behrensmeyer et al., 2000; Purnell et al., 2018). Only under exceptional circumstances can this natural decay sequence be slowed or interrupted, increasing the chances of preserving fossils in the geological record (Seilacher et al., 1985; Allison, 1988a).

Although certain conditions are difficult to replicate, taphonomic experiments are an important way to explore better how decay works and how it can affect at least the early stages of fossilization. In recent decades, many laboratory tests have detailed decay patterns of marine invertebrates, with a particular focus on annelids (Allison, 1986; Allison, 1988b; Briggs & Kear, 1993), molluscs (Chave, 1964; Flessa & Brown, 1983; Salamon et al., 2014; Clements et al., 2017; Gibson et al., 2018), arthropods (Flessa & Brown, 1983; Allison, 1986; Plotnick, 1986; Allison, 1988b; Briggs & Kear, 1994; Klompmaker et al., 2017), and echinoderms (Flessa & Brown, 1983; Lewis, 1986, 1987; Allison, 1990; Kidwell & Baumiller, 1990; Greenstein, 1991; Greenstein et al., 1995; Kerr & Twitchett, 2004; Gorzelak & Salamon, 2013). These investigations provide relevant guidelines on how preservation potential may vary between different groups of organisms.

Despite this, little attention has been paid to how this potential is affected by environmental variables before burial. Although some studies have focused on the role of energy, oxygenation, and temperature, substantial gaps remain in our understanding of biostratigraphy in marine systems. For example, most research on the effects of energy has focused on carcass transport under turbulent flows (Allison, 1986; Kidwell & Baumiller, 1990; Greenstein et al., 1995; Kerr & Twitchett, 2004; Gorzelak & Salamon, 2013; Salamon et al., 2014), but low energy conditions have been little explored. Similarly, research on the impact of oxygenation has been limited to anoxic or high oxic levels (Plotnick, 1986; Allison, 1988b; Kidwell & Baumiller, 1990), without much information on the intermediate ranges between these extremes. Temperature studies have also been restricted to short-term tests (Kidwell & Baumiller, 1990) or analyses focused on soft tissue alteration (Kerr & Twitchett, 2004), obscuring the long-term effects on the decay of hard parts.

Other marine variables require attention, such as salinity, sediment, luminosity, and scavenger activity. Increased salinity was documented as a potential accelerator of the decay

rate (Allison, 1988b, 1990), but the results are grounded on the alteration of buried chitin sacs instead of exposed fresh carcasses. The formation of algal caps in well-lit waters was also suggested as a preservation agent during the decay of some chelicerates, crustaceans, and echinozoans (Kidwell & Baumiller, 1989; Klompmaker et al., 2017), but the same evidence is limited for more complex multi-element organisms. Pioneering studies have also emphasised the relevance of scavengers in the destruction of carcasses (Meyer, 1971; Schäfer, 1972; Plotnick, 1986; Nebelsick & Kampfer, 1994), but ranking disturbance signatures between different scavenger groups remains a challenge.

Based on these gaps, we review the biostratinomic effects of light, energy, salinity, sediment, oxygenation, temperature, and scavenger activity on the decay of echinoderm carcasses. The results are based mainly on experiments with asterozoans to evaluate decay patterns in one of the most complex skeletal arrangements found in nature. From fossil to living species, asterozoans may contain tens of thousands of small, weakly articulated elements of high-magnesian calcite, which quickly collapse after death (Lewis, 1980; Donovan, 1991; Brett et al., 1997; Ausich, 2021). This skeletal fragility makes such echinoderms an accurate taphonomic guide, since they respond better to decay processes than other organisms with larger and more resistant hard parts (Fraga & Vega, 2022). Therefore, we hope to explore how different marine variables can influence the preservation of small multi-element skeletons, impacting the fossilization potential of these delicate organisms in the geological record.

## **Materials and methods**

### *Sampling*

The biostratinomic experiments were based mainly on *Amphipholis januarii*, a small five-armed ophiuroid commonly found along the warm-temperate waters of the Paranaguá Estuarine Complex, on the southern coast of Brazil (Figure 10A; Video S1). Adult specimens were collected alive during low tide peaks, when parts of the estuary bottom are exposed for a few hours and the ophiuroids bury themselves in the sediment to avoid dehydration (Figures 10B-C; S1; S2). The specimens were transported in plastic boxes partially filled with soaked sediment from the site. A few gallons of mud and seawater (30 ppt) were also sampled in the region for laboratory use. In total, 10 field collections were carried out, all licensed by the Brazilian biodiversity and genetic heritage regulatory systems, SISBIO and SISGEN, respectively.

Some specimens from other groups of invertebrates were also obtained to evaluate the disturbance pattern of macroscavengers in some experiments. A sea snail *Phrontis vibex* and a hermit crab *Clibanarius vittatus* were collected alive in the same region as *A. januarii*.

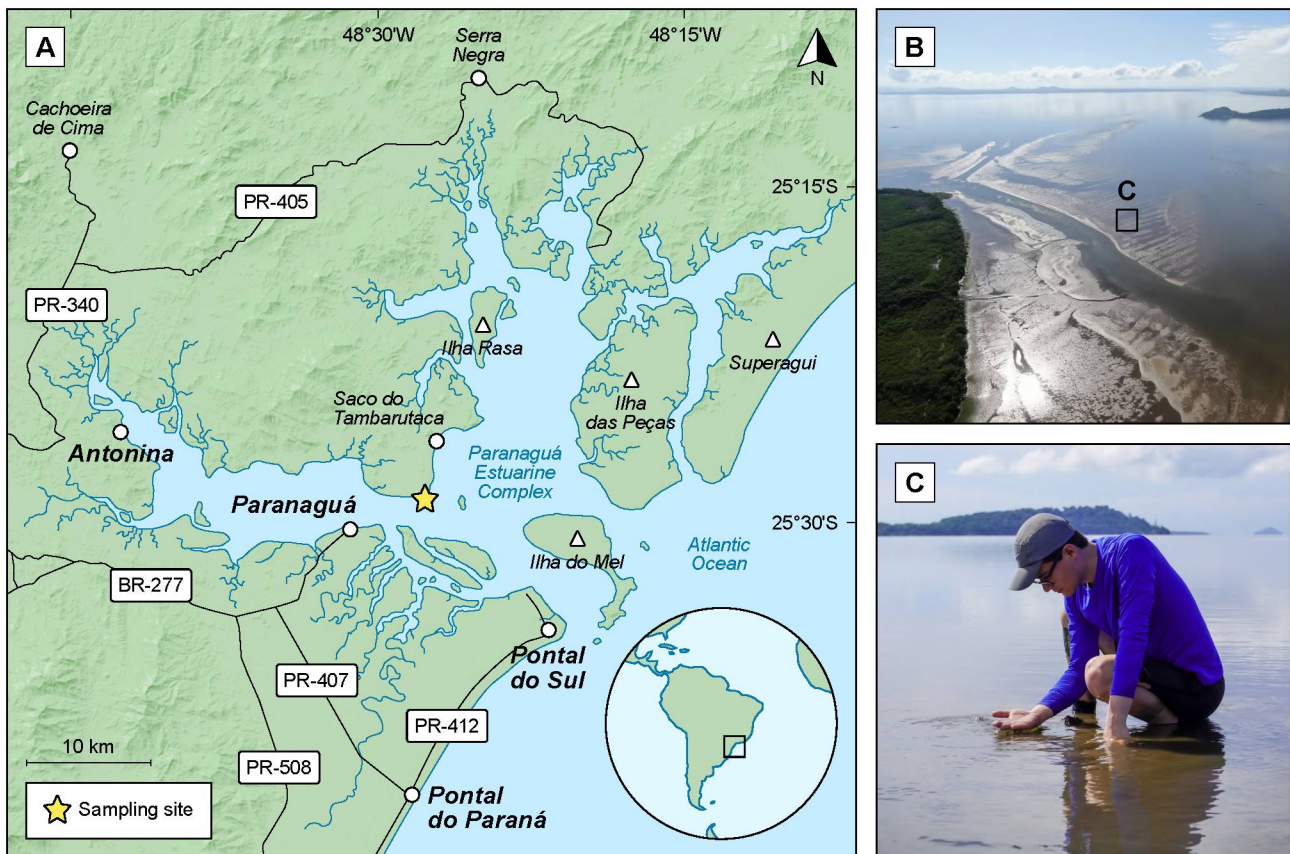


**Figure 10.** Collection site of the ophiuroid specimens. A, Map showing the location of the Paranaguá Estuarine Complex, on the southern coast of Brazil. B, Drone view of the kilometre-long mud banks exposed in the region during low tide peaks. C, Detail of B showing the manual capture of *Amphipholis januarii* specimens buried in the sediment.

A shrimp *Lysmata ankeri*, an ophiuroid *Ophiolepis superba*, an asteroid *Protoreaster nodosus*, and a polychaete *Eurythoe complanata* were purchased alive at a local aquarium store. These individuals, one from each species, were chosen to represent some important phyla of well-known scavengers in modern and extinct marine basins, which include/included many annelids, molluscs, arthropods, and echinoderms. Furthermore, 20 adult specimens of the bivalve *Anomalocardia flexuosa* were collected in the Paranaguá Estuarine Complex to be used as an additional organic source in one of the experiments.

### Decay stages

Some preliminary laboratory tests were conducted to refine the experimental protocol. From these tests, six decay scales (0-5) were created to evaluate the post-mortem alteration of asterozoan echinoderms, with potential application to different asteroids, ophiuroids, stenuroids, and somasteroids (Figure 11A-F). Although other actualist scales have been suggested for some of these organisms (e.g., Schäfer, 1972, Lewis, 1987; Kerr & Twitchett, 2004), they generally focus on soft tissue modifications, such as fluid loss and colour changes, which are more complicated to recognize in fossils. As an alternative, our decay scales

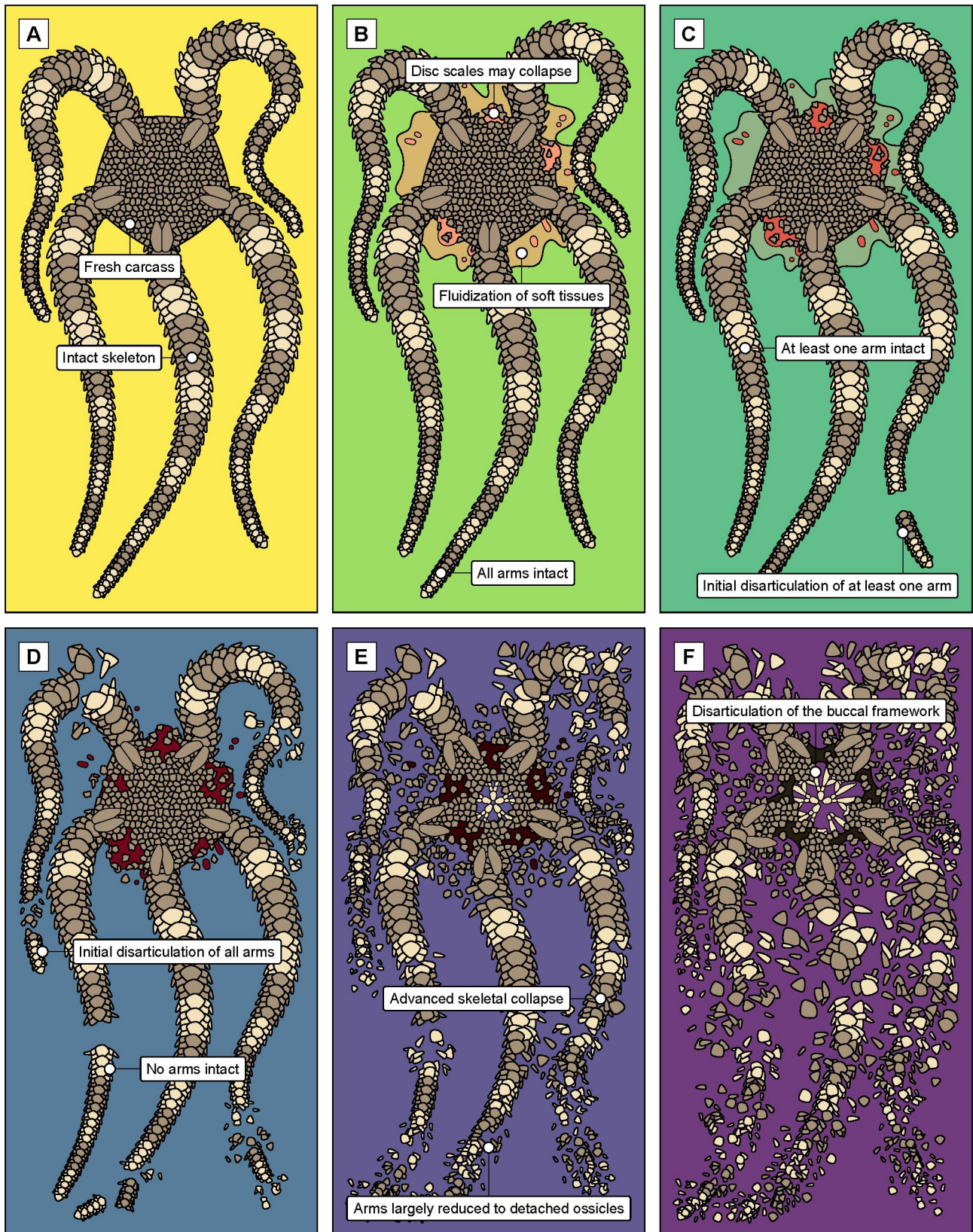


**Figure 11.** Six idealised decay stages (0–5) for the multi-element skeleton of asterozoan echinoderms. A, Decay stage 0. B, Decay stage 1. C, Decay stage 2. D, Decay stage 3. E, Decay stage 4. F, Decay stage 5. Low (stages 1–2), moderate (stage 3), and high (stages 4–5) degrees of skeletal collapse.

include more details of the disarticulation of the skeletal arrangement, considering that modifications of hard parts are a much easier pattern to track in the palaeontological record.

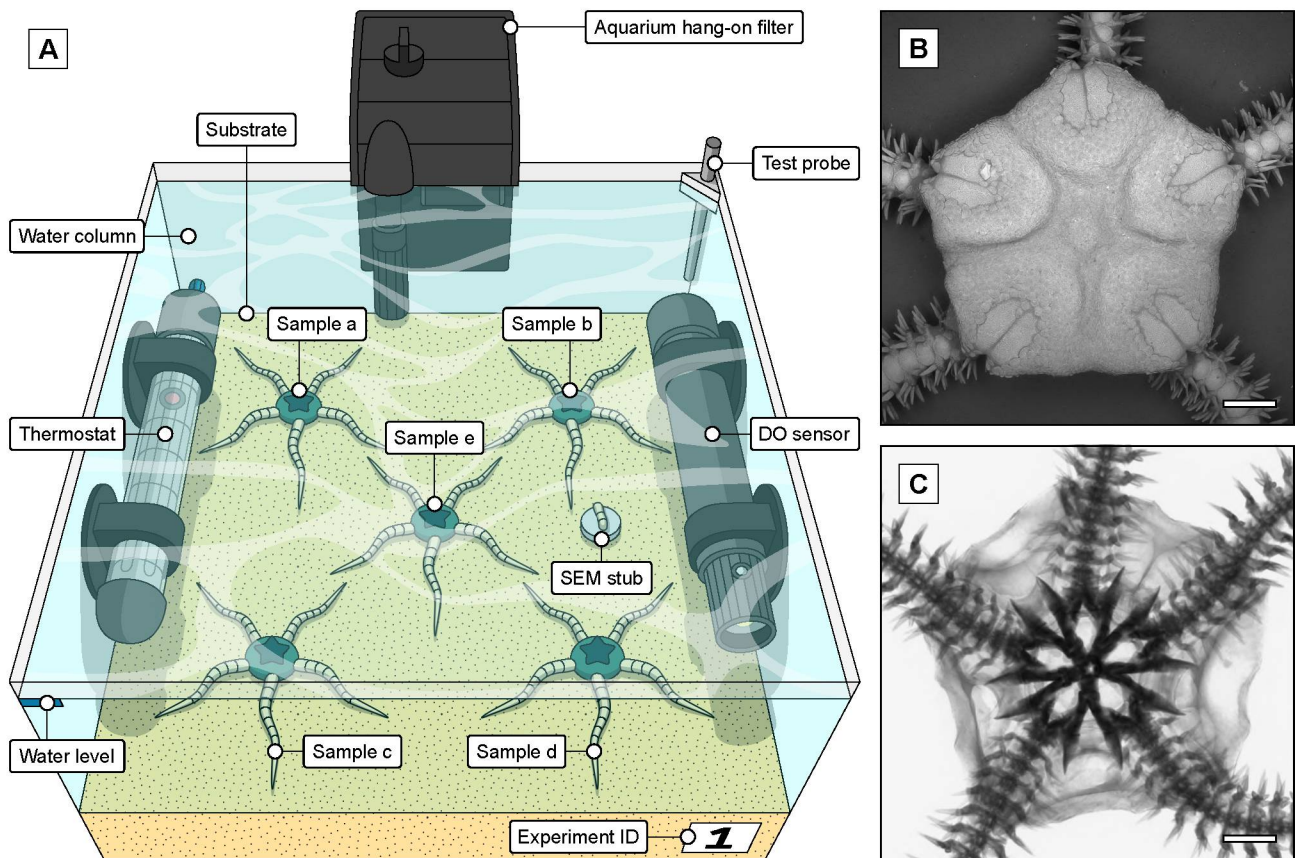


**Figure 12.** Experimental setup and ophiuroid samples. A, Schematic model of the aquarium with the main equipment (see text for details). B, SEM image of the dorsal disc of *Amphipholis januarii*, highlighting the thousands of small, imbricated disc scales. C, Micro-CT image of the disc of *A. januarii*, revealing the denser internal ossicles of the buccal framework. Scale bars indicate 1 mm.

### Main experimental protocol

All decay experiments were conducted in the Laboratório de Paleontologia at the Universidade Federal do Paraná (UFPR), located in Curitiba, Brazil. Once in the laboratory, the ophiuroids were inspected to remove dead, moribund, and autotomised individuals. Only adult specimens, with an intact disc and five preserved arm tips, were selected for the experiments. Preliminary attempts to sacrifice the specimens by leaving them freely in some anaesthetic fluid (e.g., fresh water) resulted in a slower death and, in most cases, with strong coiling of the long arms around the disc. To avoid this, each specimen was stretched out on a dry surface, overlapping arms were carefully untangled, and 5 mL of fresh water at  $\pm 85^{\circ}\text{C}$  was poured onto the disc. Under these conditions, death by thermal shock was instantaneous and the long arms remained relaxed in postures more suitable for later observation.

Five fresh carcasses (a-e) were then placed at the bottom of each previously installed aquarium, always maintaining the same arrangement between the skeletons (Figure 12A). The aquariums measured 30 cm wide, 30 cm long, and 15 cm high and were filled with a 5 cm substrate plus a 9 cm water column (see exceptions below) (Figure S3). In most

**Table 2.** Main attributes of decay experiments without macroscavengers. \*An extra basal layer of organic-rich sediment was added (see text for details).

ID	Light	Water	Energy	Salinity	Sediment	Oxygenation	Temperature
E1	<50 lux	Natural	<5 cm/s	30±1 ppt	Quartz sand	>5 mg/L	25±1°C
E2	<50 lux	Artificial	<5 cm/s	30±1 ppt	Quartz sand	>5 mg/L	25±1°C
E3	<50 lux	Natural	<5 cm/s	30±1 ppt	Quartz sand	>5 mg/L	5±1°C
E4	<50 lux	Natural	<5 cm/s	30±1 ppt	Quartz sand	>5 mg/L	15±1°C
E5	<50 lux	Natural	<5 cm/s	30±1 ppt	Quartz sand	>5 mg/L	35±1°C
E6	<50 lux	Natural	<5 cm/s	15±1 ppt	Quartz sand	>5 mg/L	25±1°C
E7	<50 lux	Natural	<5 cm/s	45±1 ppt	Quartz sand	>5 mg/L	25±1°C
E8	±820 lux	Natural	<5 cm/s	30±1 ppt	Quartz sand	>5 mg/L	25±1°C
E9	±2800 lux	Natural	<5 cm/s	30±1 ppt	Quartz sand	>5 mg/L	25±1°C
E10	<50 lux	Natural	<5 cm/s	30±1 ppt	Oolitic sand	>5 mg/L	25±1°C
E11	<50 lux	Natural	<5 cm/s	30±1 ppt	Marine mud	>5 mg/L	25±1°C
E12	<50 lux	Natural	0 cm/s	30±1 ppt	Quartz sand	>5 mg/L	25±1°C
E13	<50 lux	Natural	<10 cm/s	30±1 ppt	Quartz sand	>5 mg/L	25±1°C
E14	<50 lux	Natural	<5 cm/s	30±1 ppt	Quartz sand	2-4 mg/L	25±1°C
E15	<50 lux	Natural	<5 cm/s	30±1 ppt	Quartz sand*	0 mg/L	25±1°C

cases, a thermostat (Hopar H-386 50W) and a hang-on biochemical filter (Ocean Tech HF-100) were attached to the glass walls to control the temperature and water circulation. Glass lids with ventilation openings were used to slow water evaporation. Deionised water was periodically included to correct salinity only when necessary. Each of the setups underwent a 5-day cycling period to consolidate the microbial colonies before all the decay experiments began. A sheet of kraft paper was used to cover and block out the ambient light in the photoperiod-free aquariums, preventing excessive algae growth.

Two main sets of experiments were prepared: one without and one with macroscavengers. The first set covered 15 experiments (E1-E15) with a duration of 45 days (Table 2). A standard experiment (E1) was performed as a guide to evaluate decay over an idealised seafloor. The setup included a siliciclastic substrate (fine quartz sand) and a warm (25±1°C), euhaline (30±1 ppt), and high oxic (>5 mg/L) natural seawater rich in microscavengers (smaller than about 2 mm). The filter was set to a minimum, resulting in a bottom current of <5 cm/s estimated by observing suspended flocculates. The aquarium remained covered to simulate a dimly lit seafloor, with a peak illuminance of 49 lux close to the substrate, measured once by an LDR light sensor. The decay stages of ophiuroid carcasses (a-e) were recorded

daily, around every 24 hours. At each 5-day interval, specimen "e" was photographed and variations in pH, salinity, temperature, nitrite ( $\text{NO}_2^-$ ), ammonia ( $\text{NH}_3/\text{NH}_4^+$ ), and carbonate hardness (KH) were monitored by some probes and Labcon aquarium chemical tests. Water oxygenation was also measured at the same interval using an external dissolved oxygen (DO) sensor (BLE-9100), always previously calibrated in ambient air.

From this, 14 other experiments (E2-E15) were created by directly changing a main variable (Table 2). Experiment E2 contained artificial seawater obtained by mixing deionised water with dry sea salt (Ocean Tech Reef Salt), restricting microscavengers. Experiments E3 to E5 covered very cold ( $5\pm 1^\circ\text{C}$ , keeping the aquarium inside a fridge) (Figure S4), cold ( $15\pm 1^\circ\text{C}$ ), or very warm ( $35\pm 1^\circ\text{C}$ ) conditions. Experiments E6 and E7 simulated mesohaline conditions ( $15\pm 1$  ppt), from partial dilution with deionised water, or hypersaline conditions ( $45\pm 1$  ppt), from previous gradual evaporation of natural seawater. Experiments E8 and E9 represented a seafloor affected by a 12 h/day photoperiod, with illuminance varying between 820 lux (2 9W LED lamps) or 2800 lux (4 9W LED lamps) (Figures S5; S6). Experiments E10 and E11 alternated between a substrate of oolitic aragonite sand, imported from the Zanzibar Islands in Tanzania, or natural marine mud (Figure S7), collected from the Paranaguá Estuarine Complex in Brazil. Experiments E12 and E13 were conducted under stagnant water, removing the filter, or a higher bottom current ( $>10$  cm/s), setting the filter to the maximum (180L/h).

Two experiments (E14-E15) also evaluated decay under limited oxygenation. The cycling period occurred under high oxic conditions, but the aquariums were sealed with silicone after including ophiuroid carcasses. A 10 cm water column was used to remove air gaps below the glass lid and prevent droplet condensation. However, DO levels reached only low oxic conditions (4-2 mg/L) (E14). We attribute this to the scarcity of aerobic decaying organic matter, limited to small ophiuroid carcasses on a pure sand substrate. As an alternative, experiment E15 was created with a three-level substrate to increase organic load: a 3 cm basal layer of natural marine mud, 20 spaced carcasses of bivalve *A. flexuosa*, and a 2 cm upper layer of pure quartz sand. Water parameters were measured by sampling from a test probe (Figure 12A). Water oxygenation was double-checked using a DO sensor, fixed inside the aquariums, and an additional Labcon O<sub>2</sub> chemical test, carried out on part of the sampled water.

The second set of experiments comprised 6 aquariums with macroscavengers (E16-E21). The setup was the same as for experiment E1, varying only in the inclusion of a scavenger shortly after the inclusion of ophiuroid carcasses. The organisms were a shrimp *L. ankeri* (E16), a sea snail *P. vibex* (E17), an asteroid *P. nodosus* (E18), an ophiuroid *O. superba* (E19), a hermit crab *C. vittatus* (E20), and a polychaete *E. complanata* (E21). As no

additional food source was offered, these experiments were only performed for 15 days to avoid the death of the individuals due to long-term malnutrition. Following the protocol, the decay stages were recorded daily and the water parameters were measured every 5 days. In addition to the periodic recording of carcass "e" (Figure 12A), any other disturbed carcass was also photographed to track scavenger activity. All the scavengers remained alive and active until the end of the experiments.

Two supplementary experiments (E22-E23) were still carried out to evaluate the decay between different asterozoan species. Only two individuals were used, the same as in the macroscavenger analyses: the asteroid *P. nodosus* (E22) (Figure S8) and the ophiuroid *O. superba* (E23). The individuals were sacrificed by immersion in deionised water at  $\pm 85^{\circ}\text{C}$  for 3 seconds. The fresh carcasses were placed at the bottom of two individual aquariums, in the position of specimen "e" from the experiments with *A. januarii* (Figure 12A). The setup was the same as experiment E1. However, experiment E22 lasted 100 days, with photography and periodic water measurements during the initial 45 days and at the end of day 100. Experiment E23 lasted 45 days, with photography and periodic water measurements only during the initial 30 days. The detailed parameters for all the experiments (E1-E23) are given in the Tables S1-S46.

### *Microscopic decay*

Additional samples were prepared to examine some microscopic decay patterns, mainly carbonate dissolution. The samples were obtained by cutting 15 proximal arm segments of *A. januarii*. Each of the segments was fixed on a 12.7 mm aluminium SEM stub with cyanoacrylate-based glue. A stub was then inserted into the bottom of each of the aquariums in experiments E1-E15 (Figures 12A; S9), at the same time as the inclusion of the ophiuroid carcasses. At the end of 45 days of decay under different conditions, the stubs were removed and immersed for 10 minutes in a bowl of deionised water to remove most of the host sodium chloride. After immersion, the stubs were extracted and left to dry at room temperature. The final samples were taken for SEM analysis on a Tescan Vega-3 LMU, from the Centro de Microscopia Eletrônica (CME-UFPR). No metallization was used.

### *Other laboratory analyses*

For a detailed evaluation of *A. januarii*, some fresh carcasses were also inspected by SEM, at the CME-UFPR, and by Micro-CT, at the Instituto Laboratório de Análise de Minerais e Rochas (iLAMIR-UFPR) (Figure 12B-C; Video S2). Both techniques were important for comparing the intact skeleton with the structure of other decayed specimens. Furthermore, a portion of the marine mud used in experiments E11 and E15 was analysed by XRF

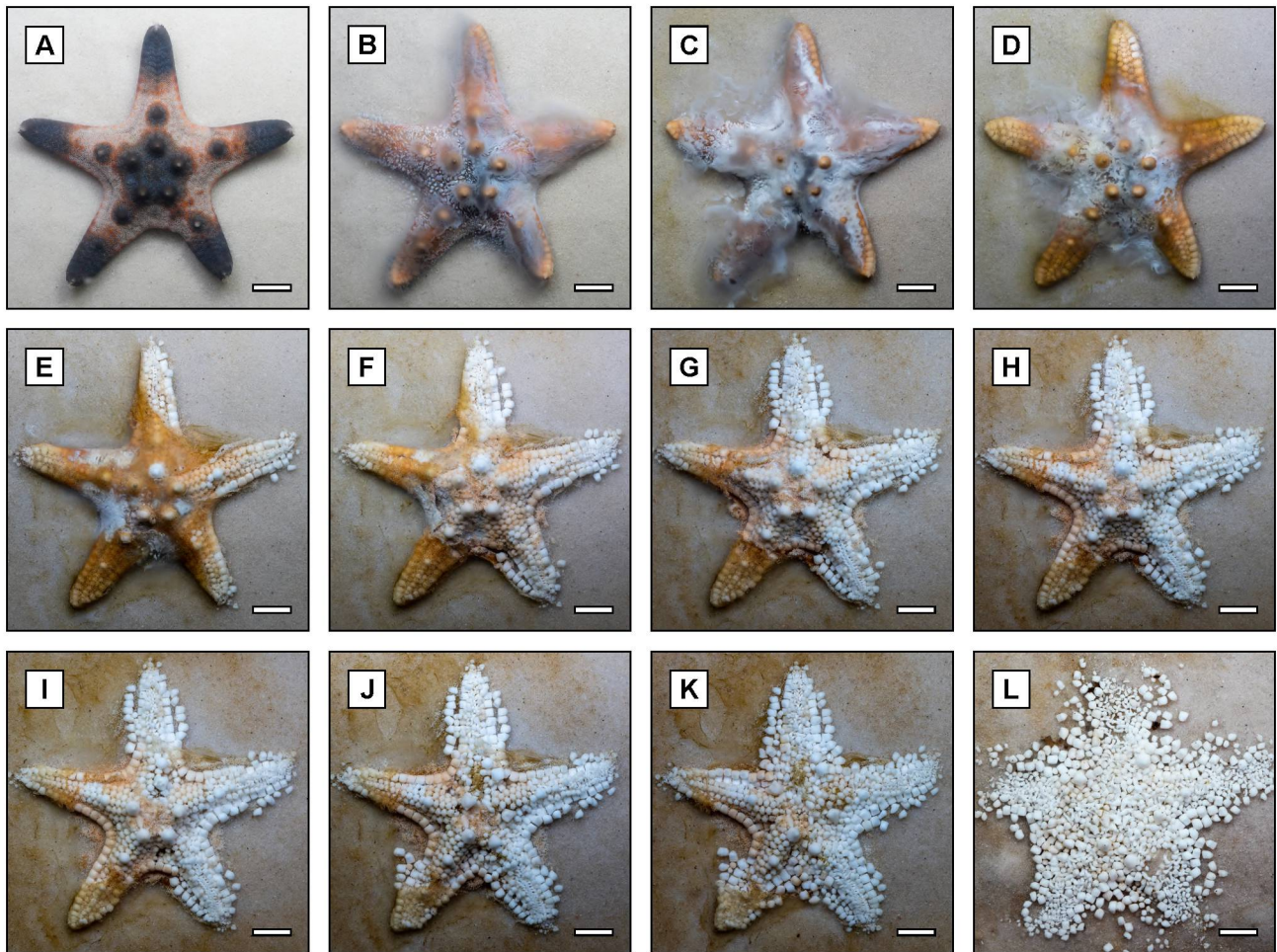


**Figure 13.** Decay pattern of the asteroid *Protoreaster nodosus* under macroscavenger-free marine conditions. A, Day 0 (minutes after death). B, Day 3. C, Day 5. D, Day 10. E, Day 15. F, Day 20. G, Day 25. H, Day 30. I, Day 35. J, Day 40. K, Day 45. L, Day 100. The bottom current was from right to left in all cases. Scale bars indicate 1 cm.

on a Panalytical Axios Max subsidised by iLAMIR. The mud sample was washed with deionised water to remove most of the sodium chloride and then oven-dried before being pulverised for analysis. A detailed physical-chemical analysis of the natural seawater used in aquariums was also carried out in partnership with the Laboratório de Pesquisas Hidrogeológicas (LPH-UFPR). The results of the XRF and hydrochemical tests are listed in Tables S47-S48.

## Results

### *Normal decay sequence*

The alteration of the carcasses begins with the fluidisation of the soft tissues, marking the onset of decay stage 1 (Figure 11B). For smaller skeletons, such as those of *A. januarii*, this process was observed a few hours after death, whereas the first signs were better visible from the end of the first day in *O. superba* and *P. nodosus* (Figures 13A-C). The main damage occurs in the disc, where most of the organic volume of the asterozoans is confined. The

visceral organs begin to degrade into an orange fluid, sometimes escaping through the mouth. A whitish gelatinous coating gradually forms over the discs (Video S3), triggering microbial growth and attack of microscavengers. In the more flexible disc of *A. januarii*, the process also frequently causes rupture of the epidermis and collapse of the disc scales, leading to early disarticulation of the hard parts within decay stage 1 (Figure S10).

Despite this, the first signs of disarticulation usually appear in the small elements of the arm tips during decay stage 2 (Figure 11C). This results in the breaking of the ophiuroid arms into smaller, semi-articulated segments (Figures 14B, J-K; S11). In the asteroid, the main effect was the collapse of the thousands of calcified micro-nodules dispersed in the epidermis of the arms (Figures 13D; S12). Although the proximal arms may also be the target of this initial disarticulation, they are more protected by the viscous coating formed by the fluidisation of the viscera and the overgrowth of microbial colonies (Figure S13). Meanwhile, the distal arm parts remain exposed to direct attack by microscavengers and microvariations in the bottom current, favouring a starting point for skeletal collapse.

In turn, decay stage 3 begins as soon as the disarticulation minimally affects all arms (Figure 11D). From that moment on, no arm segment remains intact. The collapse of the hard parts tends to spread progressively throughout the carcass (Figures 13E-J; 14L-P). However, the disarticulation potential can vary even between arms of the same carcass. Some segments oriented against the direction of the bottom current may present higher decay rates compared to other segments positioned in energetic shadow zones, more protected from water flow. Likewise, highly flexed arm segments can also create points of weakness, leading to the preferential disarticulation of the ossicles in the region. This scenario progresses to the decay stage 4, where all arms are substantially reduced to a series of detached ossicles (Figures 11E; 13E-J; 14C-H). Most of the skeletal arrangement is destroyed under these conditions, making it difficult to recognise the original organism.

The disarticulation of the skeleton advances and increases the number of detached elements. When still present, organic remains are quite limited, usually just small dark masses resulting from the decay of the viscera (Figure S14). At this stage, the buccal framework is usually the main (if not the only) articulated area. The more robust ossicles in this region can stay together longer than any others, protected under the dorsal disc and bonded by the organic remains. The decay stage 5 is only reached when the buccal framework is disarticulated (Figure 11F). The original skeletal arrangement is then completely lost, and the carcasses become nothing more than small bioclasts dispersed in the sediment (Figure 13L). This was the most advanced decay stage observed here under normal marine conditions.

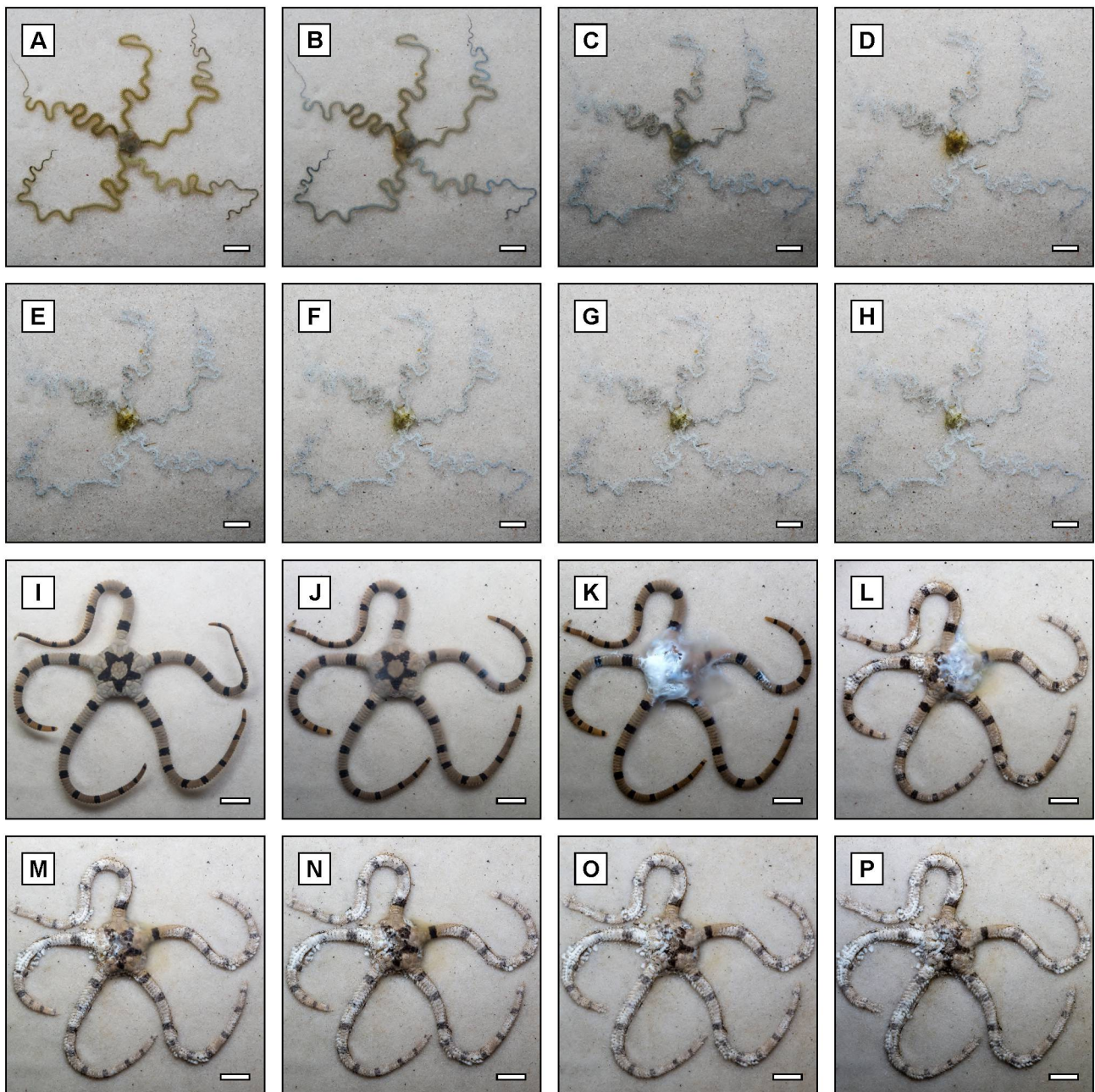


**Figure 14.** Decay pattern of the ophiuroid *Amphipholis januarii* (A–H) and *Ophiolepis superba* (I–P) under macroscavenger-free marine conditions. A, Day 0 (minutes after death). B, Day 5. C, Day 10. D, Day 15. E, Day 20. F, Day 25. G, Day 30. H, Day 45. I, Day 0 (minutes after death). J, Day 2. K, Day 5. L, Day 10. M, Day 15. N, Day 20. O, Day 25. P, Day 30. The bottom current was from right to left (A–H) and left to right (I–P). Scale bars indicate 1 cm.

#### *Influence of microscavengers*

Two experiments (E1–E2) evaluated the impact of microscavengers on decay. The experiment E1 was conducted using natural seawater rich in microplankton. The microbial load was high and led to a rapid proliferation of microbial colonies on carcasses in the initial 3 days. The nitrogen compounds generated by the organic decay were rapidly degraded (Table S1), indicating a sufficiently stable assemblage of ammonia-oxidizing and nitrite-oxidizing bacteria. Microscavengers were abundant and included a variety of ciliates, copepods,

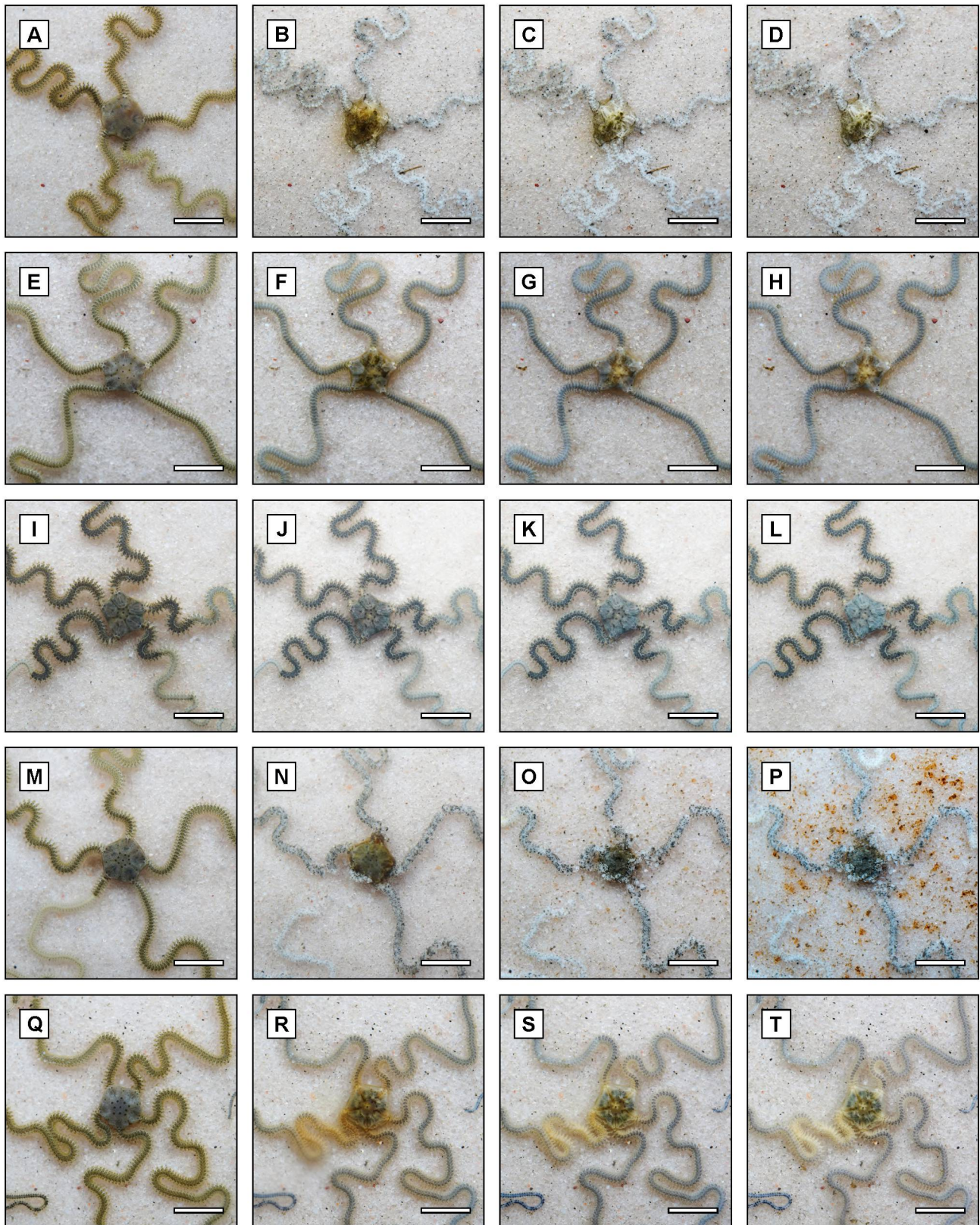


**Figure 15.** Decay pattern of the ophiuroid *Amphipholis januarii* under different marine conditions, without disturbance of macroscavengers. A-D, Decay on an idealised seafloor (E1). A, Day 0 (minutes after death). B, Day 15. C, Day 30. D, Day 45. E-H, Decay in artificial seawater (E2). E, Day 0 (minutes after death). F, Day 15. G, Day 30. G, Day 45. I-L, Decay under very cold conditions (E3). I, Day 0 (minutes after death). J, Day 15. K, Day 30. L, Day 45. M-P, Decay under cold conditions (E4). M, Day 0 (minutes after death). N, Day 15. O, Day 30. P, Day 45. Q-T, Decay under very warm conditions (E5). Q, Day 0 (minutes after death). R, Day 15. S, Day 30. T, Day 45. Scale bars indicate 1 cm.

planarians, and nematodes. These organisms moved frantically over the carcasses, attacking from the disc to the arm tips. This accelerated the decay of soft tissues and the collapse of the delicate skeletal arrangement of *A. januaris* (Figure 15A-D). All carcasses achieved high levels of disarticulation in less than 10 days under these conditions (Figure 16A).

In contrast, experiment E2 was carried out with artificial seawater, drastically restricting the biological load. Ammonia levels generated by organic decay remained high for weeks, while nitrite levels were detectable only from day 15 and remained high until the end of the experiment (Table S2). The long persistence of these nitrogen compounds indicated a much less consolidated assemblage of oxidizing bacteria. This was also supported by the slower development, between the 5th and 10th day, of the whitish microbial caps on the ophiuroid discs. With the lack of microscavengers, the disarticulation of the skeletons was dependent on microbial activity and microvariations in the bottom current. As a result, most of the carcasses remained well-articulated throughout most of the experiment (Figure S15). The main damage was observed in the discs due to the organic degradation and the collapse of some disc scales (Figure 15E-H). Only a few arm tips began to disarticulate after more than 40 days, marking a very late onset of decay stage 2 (Figure 16B).

### *Influence of temperature*

Four experiments (E1, E3-E5) evaluated the impact of temperature on decay. Experiment E3 was carried out in a very cold environment, with water at around 5°C. Ammonia and nitrite were undetectable (Table S3) and no microscavengers were observed throughout the 45 days, indicating a severe restriction on all biological activity. The decay patterns were extremely slow under these conditions. The fluidisation of the viscera was almost imperceptible, without any significant growth of microbial colonies. Even the original colours of the specimens were well-preserved in the long term (Figure 15I-L). The disarticulation was almost exclusively a consequence of water energy. Only two skeletons reached decay stage 2 at different times (Figure 16C), with the breakage of a more unstable arm segment in the bottom current. The rest of the carcasses remained articulated, including even the arm tips and disc scales.

Experiments E4 and E1 simulated cold and warm waters at around 15°C and 25°C, respectively. The decay of nitrogen compounds followed an analogous pattern, with only slightly faster oxidation rates at 25°C (Tables S1, S4). Biological activity was also similar, with rapid microbial growth in the initial 3 days, as well as intense activity of microscavengers until the end of the experiments. The variation in disarticulation rates was small in both scenarios (Figure 16A, D). The arms showed the first signs of breakage around the 5th day, and all the carcasses reached advanced collapse stages on approximately the 10th day.

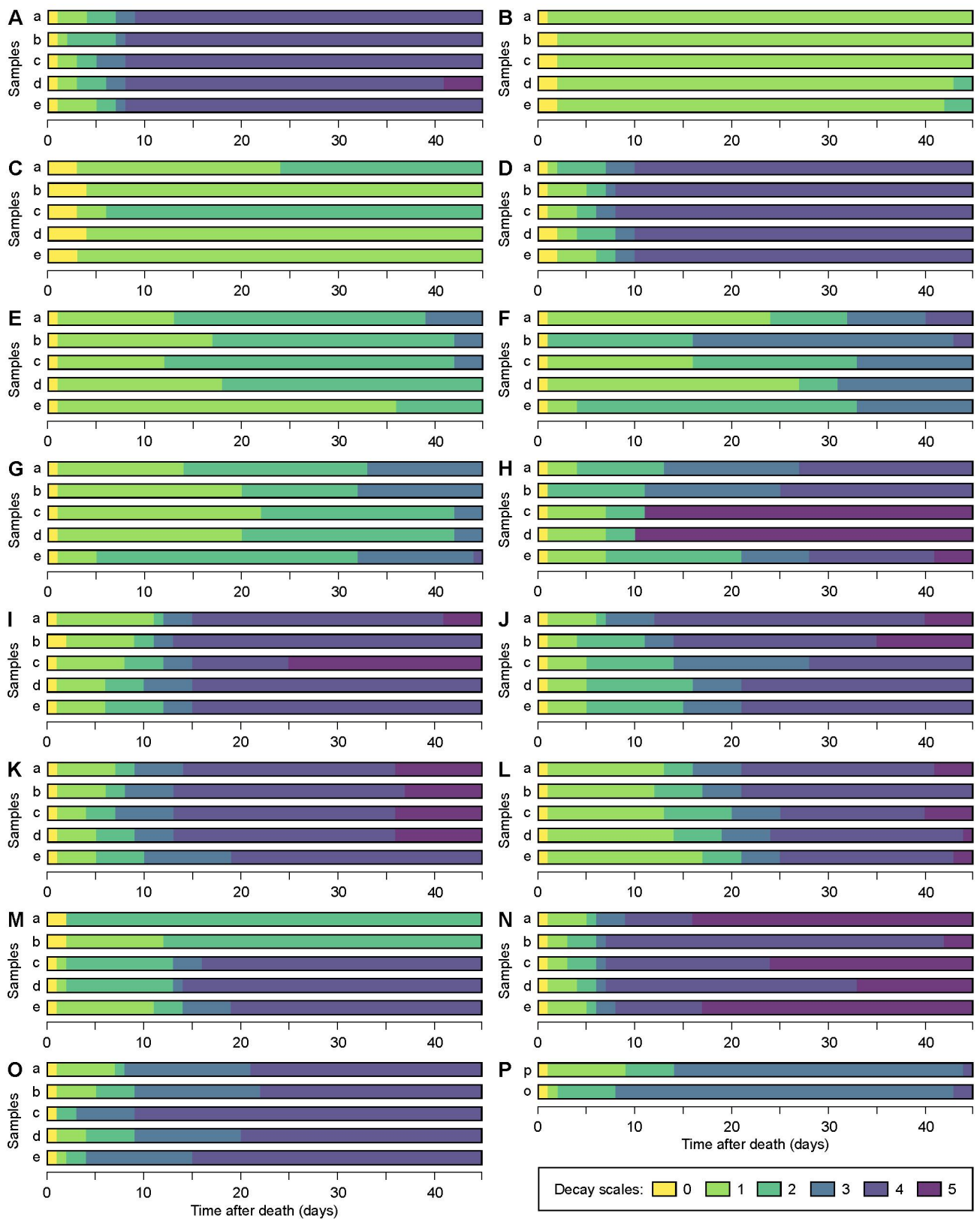


**Figure 16.** Decay stages of asterozoans under different marine conditions, without the disturbance of macrocavengers. A-O, Decay of five specimens (a–e) of the ophiuroid *Amphipholis januarii*. A, Idealised seafloor (E1). B, Artificial seawater (E2). C, Very cold conditions (E3). D, Cold conditions (E4). E, Very warm conditions (E5). F, Mesohaline conditions (E6). G, Hypersaline conditions (E7). H, Lit conditions (E8). I, Well-lit conditions (E9). J, Aragonite substrate (E10). K, Marine mud substrate (E11). L, Stagnant conditions (E12). M, Low bottom current (E13). N, Low oxigenic conditions (E14). O, Anoxic conditions (E15). P, Decay of the asteroid *Protoreaster nodosus* (p) and the ophiuroid *Ophiolepis superba* (o) under idealised seafloor (E22-E23).

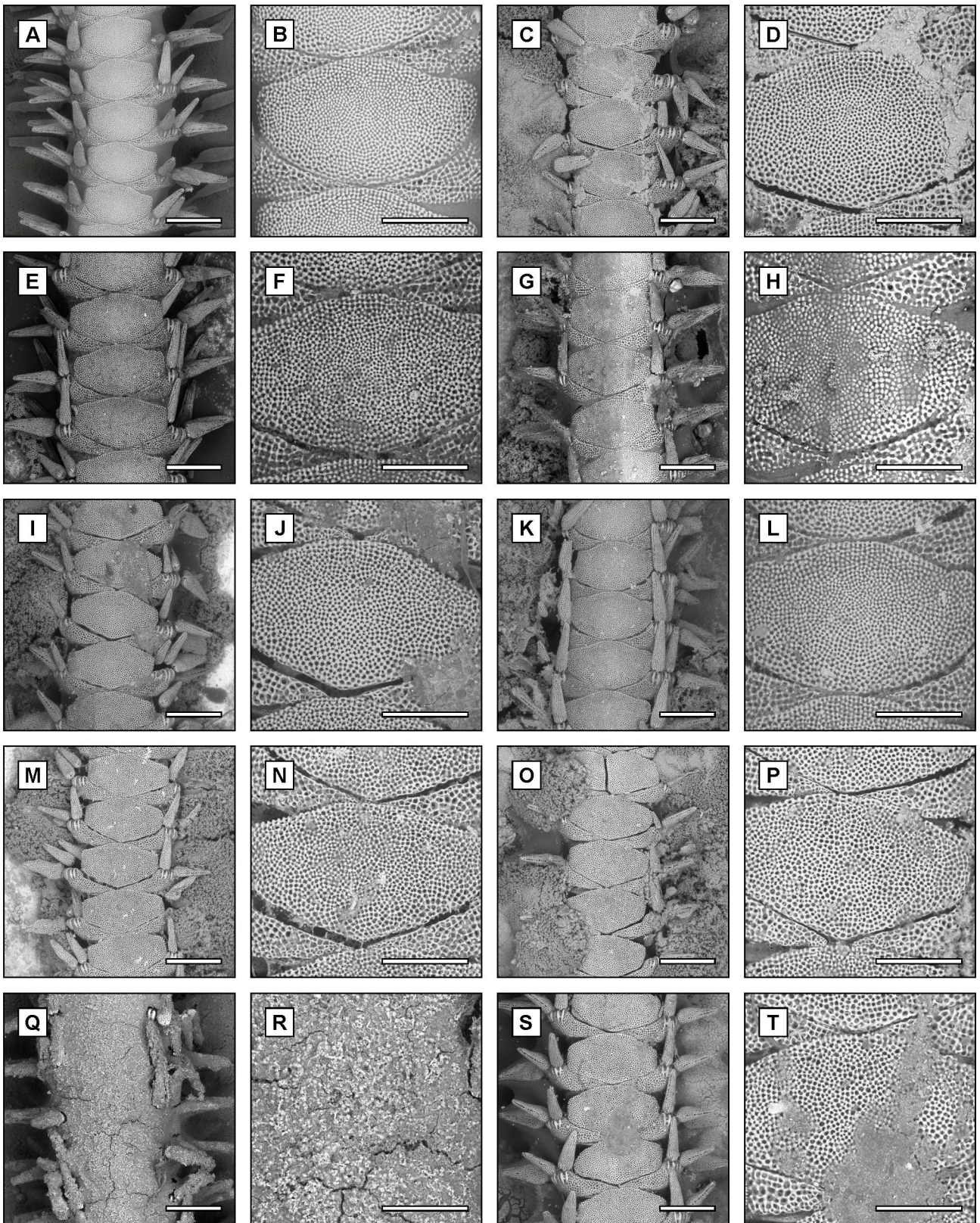


**Figure 17.** Microscopic decay patterns in proximal arm segments of the ophiuroid *Amphipholis januarii*. A, Arm intact, no decay. B, Detail of the centre of "A". C, Decay on an idealised seafloor (E1). D, Detail of the centre of "B". E, Decay in artificial seawater (E2). F, Detail of the centre of "E". G, Decay under very cold conditions (E3). H, Detail of the centre of "G". I, Decay under cold conditions (E4). J, Detail of the centre of "I". K, Decay under very warm conditions (E5). L, Detail of the centre of "K". M, Decay under mesohaline conditions (E6). N, Detail of the centre of "M". O, Decay under hypersaline conditions (E7). P, Detail of the centre of "O". Q, Decay under lit conditions (E8). R, Detail of the centre of "Q". S, Decay under well-lit conditions (E9). T, Detail of the centre of "S". All the arm segments were attached to an aluminium stub with cyanoacrylate-based glue. Note that the

seawater led to the oxidation of the stubs and the associated growth of aluminium oxides in many cases. Scale bars indicate 500  $\mu\text{m}$  (A, C, E, G, I, K, M, O, Q, S) and 250  $\mu\text{m}$  (B, D, F, H, J, L, N, P, R, T).

From this point onwards, the skeletons were reduced to detached elements mainly by the constant disturbance of microscavengers. The biggest variations were only in the long-term preservation of the viscera (Figure 15A-D, M-P). A greater volume of organic remains survived in the discs at 15°C, helping to delay further the collapse of the buccal framework compared to decay at 25°C.

In turn, experiment E5 was calibrated at around 35°C to simulate decay in very warm waters. Nitrogen compounds were undetectable (Table S5) but probably due to the very rapid rate of microbial oxidation. This was supported by the formation of large viscous caps due to the fluidisation of the viscera and the proliferation of microbial colonies. These caps lasted for more than 15 days on most of the carcasses, reducing the attack of microscavengers and the disturbance of the bottom current on the disc and proximal arms (Video S4). Although the presence of microscavengers was high in the early days, it radically declined over the long term in these warmer conditions. Rupture of the epidermis and collapse of the disc scales were frequent in decay stage 1, but the disarticulation typical of decay stage 2 occurred late in the arms. After 45 days, most skeletons showed initial signs of breakage in all arms, but others persisted with at least some arms intact (Figures 15Q-T; 16E).

Due to temperature variations, DO and pH were also indirectly changed in the four experiments (Tables S1, S2-S5). The DO showed small variations, from 5.11 mg/L (E5) to 7.36 mg/L (E3), but always within the high oxic range. The pH also raised by 0.2 points with each 10°C increase in temperature, varying from 7.6 at 5°C to 8.2 at 35°C. However, this change was likely a bias in how the pH test responded to temperature, given that many aquarium chemical kits are calibrated to 25°C. In any case, there was no significant carbonate dissolution during these experiments (Figure 17C-D, G-L). At 5°C, the skeletons only tended to preserve better the soft tissues that fill the stereom pores. This was supported by the greater presence of darker phases on the ossicles, rich in substances with a low mean atomic number (carbonaceous remains) in the BSE analysis (Figure 17G-H).

### *Influence of salinity*

Three experiments (E1, E6-E7) simulated the decay at different types of salinities. Experiments E6 and E7 were performed under mesohaline ( $\pm 15$  ppt) and hypersaline ( $\pm 45$  ppt) conditions, respectively (Tables S1, S6-S7). These variations resulted in a similar decay pattern, with rates much slower than the euhaline conditions ( $\pm 30$  ppt) evaluated in experiment E1. Although the oxidation of the nitrogen compounds was rapid in all three environ-

ments, microbial growth was greatly reduced by both the decrease and the increase in the load of dissolved salts (E6-E7). Only about 10 days of decay in euhaline water were enough for an advanced collapse among all ophiuroid carcasses, destroying most of the soft tissues and skeletal structure (Figures 15A-D; 7A). However, the process was up to more than four times slower with changing salinity (Figures 18A-H; 16F-G).

Under the mesohaline and hypersaline conditions, microscavengers were almost imperceptible, probably due to the osmotic imbalance between the water and these organisms. The environment also led to greater rupture of the epidermis and the collapse of the disc scales after introducing the ophiuroid carcasses, driving early disarticulation within decay stage 1 (Figures 18A; S16). The fluidisation of the viscera generated small caps over the discs, with reduced microbial growth. Most carcasses persisted at this stage for more than 20 days, but initial signs of breakage appeared quickly in some specimens with arms more unstable to the bottom current (Figure 16F-G). After 45 days, most skeletons had achieved an initial collapse, with all arms reduced to small articulated segments. Decay stage 4 was observed late in a few cases. The organic remains persisted better preserved in the long term than under euhaline conditions.

The variations in salinity caused only subtle fluctuations in the chemical parameters compared to the euhaline environment. In the mesohaline experiment (E6), the pH was 7.6 and the KH was 3°dH (Table S6), following the pattern of brackish conditions with a lower proportion of carbonate ( $\text{CO}_3^{2-}$ ) and bicarbonate ( $\text{HCO}_3^-$ ) dissolved in the water. Meanwhile, the pH was 8.2 and the KH was 6°dH in the hypersaline experiment (E7) (Table S7), in keeping with a greater load of dissolved substances. DO levels also oscillated within the high oxic range, varying from 7.07 mg/L in experiment E6 to 5.34 mg/L in experiment E7. However, no substantial pattern of carbonate dissolution was observed due to any of these chemical variations (Figure 17M-P).

### *Influence of luminosity*

Three experiments (E1, E8-E9) evaluated the effects of luminosity on the decay process. Experiment E1 was conducted in a dark aquarium, covered most of the time to simulate a dimly lit seafloor (Table S1). Meanwhile, experiments E8 and E9 were exposed daily to a 12-h photoperiod, reaching a luminosity of about 820 and 2800 lux over the aquarium sediment, respectively (Tables S8-S9). Unlike the dark conditions (E1), algal growth was an important additional element in both lit scenarios (E8-E9). Ammonia and nitrite were almost undetectable in the photoperiod experiments (Tables S8-S9). However, in these cases, this indicates the presence of well-established microbial assemblages, with rapid oxidation of the most toxic nitrogen compounds resulting from decay. Although not measured, even

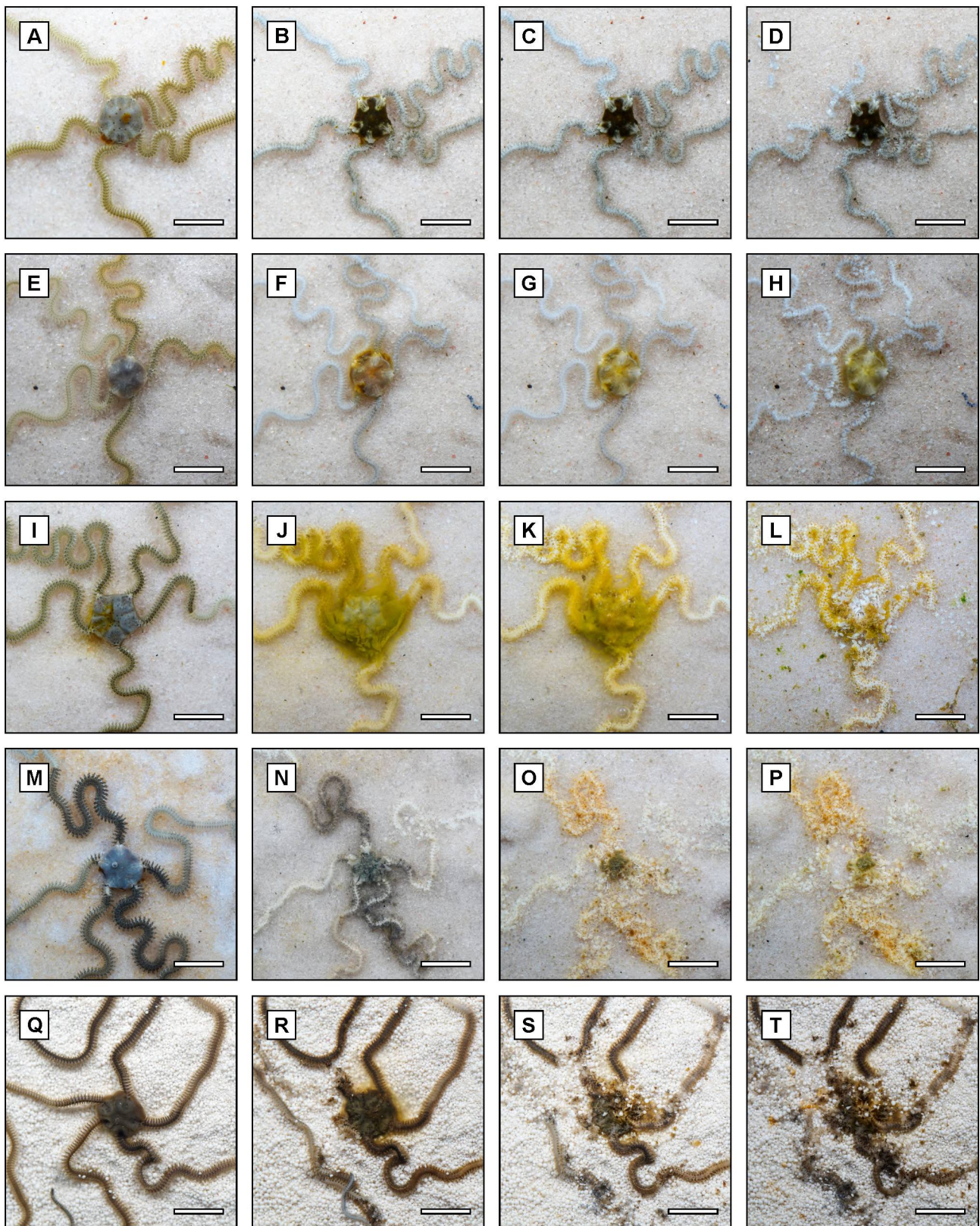


**Figure 18.** Decay pattern of the ophiuroid *Amphipholis januarii* under different marine conditions, without disturbance of macroscavengers. A-D, Decay under mesohaline conditions (E6). A, Day 0 (minutes after death). B, Day 15. C, Day 30. D, Day 45. E-H, Decay under hypersaline conditions (E7). E, Day 0 (minutes after death). F, Day 15. G, Day 30. H, Day 45. I-L, Decay under lit conditions (E8). I, Day 0 (minutes after death). J, Day 15. K, Day 30. L, Day 45. M-P, Decay under well-lit conditions (E9). M, Day 0 (minutes after death). N, Day 15. O, Day 30. P, Day 45. Q-T, Decay in carbonate sediment (E10). Q, Day 0 (minutes after death). R, Day 15. S, Day 30. T, Day 45. Scale bars indicate 1 cm.

the nitrate load ( $\text{NO}_3^-$ ), a product of nitrite oxidation, was also probably recycled during the algal bloom.

Under moderate lighting (E8), fluidisation of the viscera quickly led to the growth of green algae on all the ophiuroid carcasses, covering the disc region (Figures 17Q-R; 18I-L; Video S5). This green cap biased the decay of the skeletons. In some cases, it helped delay disarticulation of the proximal arms compared to conditions without algae (Figure 16A, H). However, in other cases, algae created such a thick barrier that it blocked the decay bubbles from escaping. Some discs were then inflated like balloons, while their arm tips remained anchored in the sediment. This process caused the collapse of the buccal framework, marking the earliest onset of decay stage 5 in just 10 days (Figures 16H; S17). In the long term, all carcasses reached a high degree of disarticulation due to the complex interaction of bottom current, microbial activity, microscavenger disturbance, and exacerbated algal growth.

Due to the higher luminosity, most of the algal bloom occurred within the cycling period in experiment E9. The fluidisation of the ophiuroid viscera led to the growth of microbial caps, but without a thick algal barrier (Figure 17S-T), the disc and proximal arms were more exposed to microscavengers (Video S6). An important feature of experiment E9 was also the production of gases at the innermost levels of the substrate, perhaps due to the microbial reduction of some compounds to methane ( $\text{CH}_4$ ) or molecular nitrogen ( $\text{N}_2$ ). The escape of these bubbles created a minefield for the small decaying skeletons. From day 5 onwards, the bubbles began to deform the sediment daily while migrating until emerging into the water column, creating a series of mini craters in the substrate (Figure S18). The bubbles could also collide below the carcasses, accelerating the disarticulation. In this unstable scenario, all the skeletons reached high levels of decay after 15 days (Figures 16I; 18M-P). Similarly to experiment E8, light radiation also helped to degrade the pigments and whiten all the skeletons.

### *Influence of sediment*

Three experiments (E1, E10-E11) compared decay on different sediment types. Unlike the fine sand used in experiment E1, experiment E10 used a substrate made up of ooids to simulate a carbonate seafloor (Table S10). The surface of the substrate was more unstable than the quartz sand, probably due to the greater sphericity of the ooids, which favoured the transport of the grains by the bottom current. The decay of the ophiuroid carcasses was rapid in these carbonate conditions, although a little slower than in the siliciclastic scenario (E1) (Figure 16A, J). The viscera began to fluidise rapidly in the initial days, leading to the collapse of disc scales, the formation of microbial caps (Figure S19), and the attack of mi-

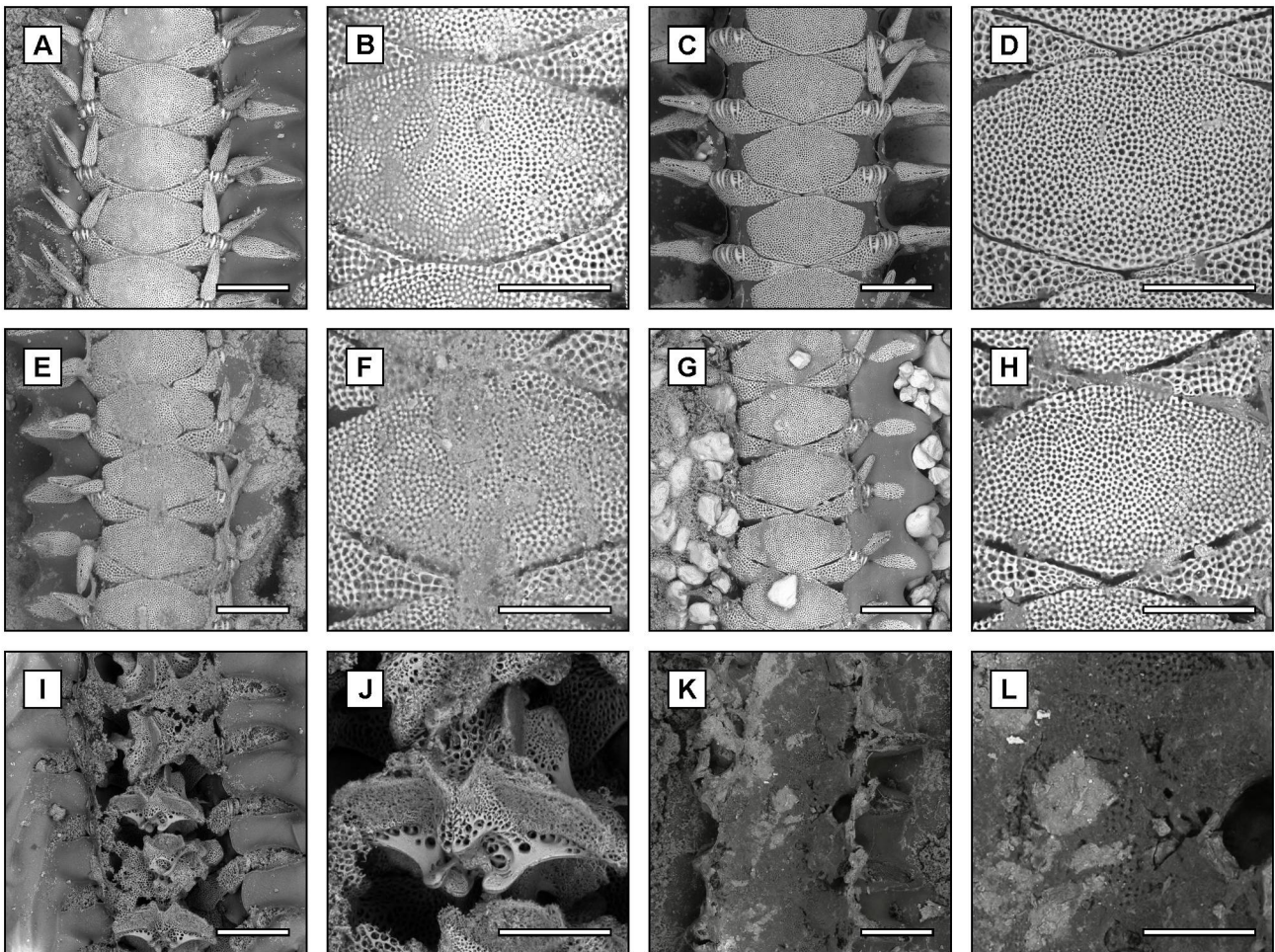


**Figure 19.** Microscopic decay patterns in proximal arm segments of the ophiuroid *Amphipholis januarii*. A, Decay in carbonate sediment (E10). B, Detail of the centre of “A”. C, Decay in mud sediment (E11). D, Detail of the centre of “B”. E, Decay in stagnant water (E12). F, Detail of the centre of “E”. G, Decay under higher bottom current (E13). H, Detail of the centre of “G”. I, Decay in low oxic conditions (E14). J, Detail of the centre of “I”. K, Decay in anoxic conditions (E15). L, Detail of the centre of “K”. All the arm segments were attached to an aluminium stub with cyanoacrylate-based glue. Note that the seawater led to the oxidation of the stubs and the associated growth of aluminium oxides in many cases. The skeleton was also completely dissolved in “K-L”, leaving only a ghost mould in the layer of glue below. Scale bars indicate 500  $\mu\text{m}$  (A, C, E, G, I, K) and 250  $\mu\text{m}$  (B, D, F, H, J, L).

crosscavengers. Some arm segments were also subtly reoriented by the bottom current, but the first signs of disarticulation appeared after 4 days (Figure S20). Most of the carcasses reached a high stage of decay around 20 days (Figure 18Q-T). Organic parts were better preserved in the long term, as were the carbonate elements (Figure 19A-B).

Experiment E11 was realised with a mud substrate rich in fine sand, organic matter, and silt-clay flocculates (Table S11). The sediment was rich in microscavengers, such as ostracods, nematodes, and gastropods. All the ophiuroid carcasses gradually sank into this soft substrate by the higher rates of background sedimentation (Figure 20A-B). The fluidisation of the viscera rapidly led to the growth of microbial caps in the initial days, covering up to the arm tips. These broad caps helped to temporarily armour against the attack by

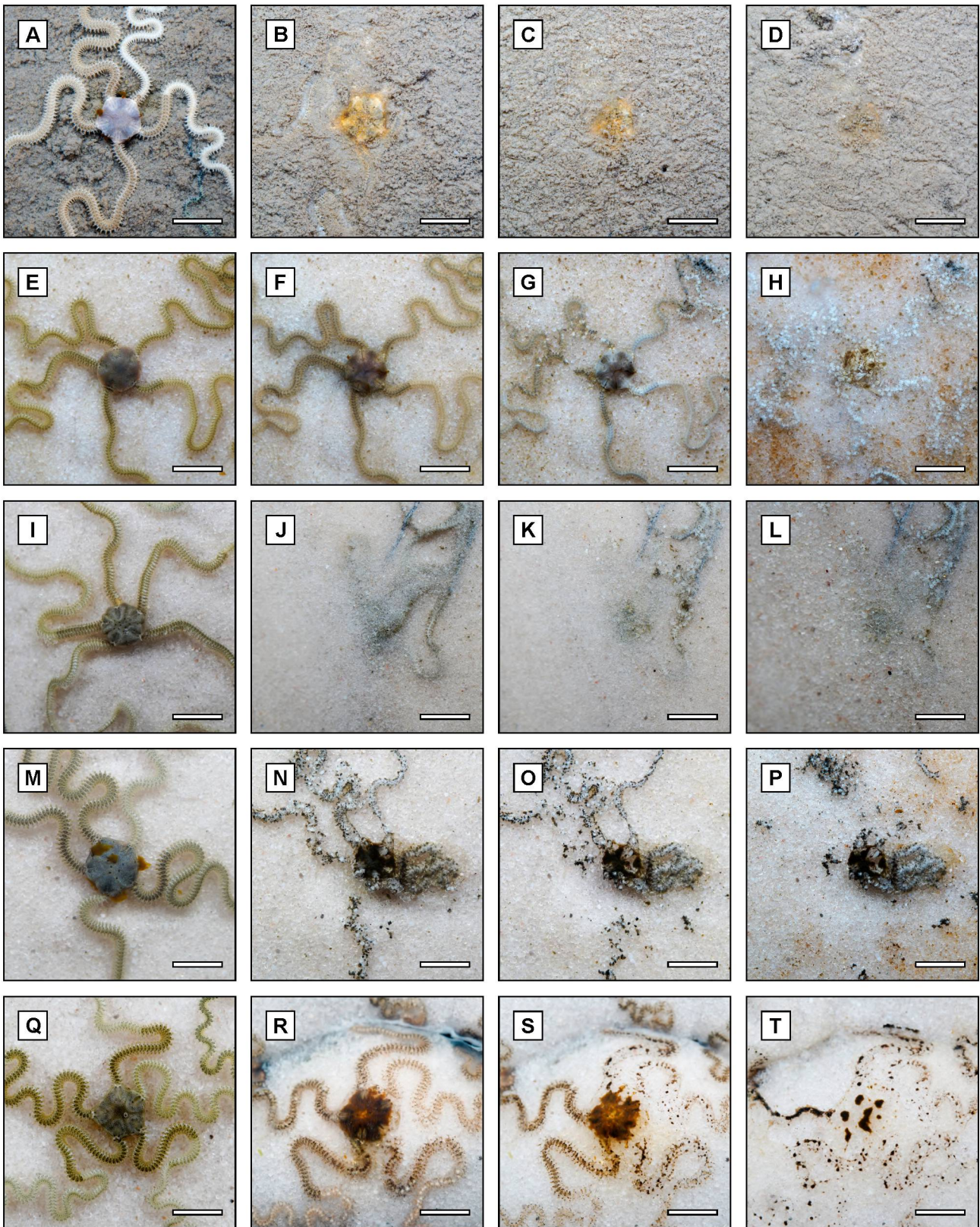


**Figure 20.** Decay pattern of the ophiuroid *Amphipholis januarii* under different marine conditions, without disturbance of macroscavengers. A-D, Decay in mud sediment (E11). A, Day 0 (minutes after death). B, Day 15. C, Day 30. D, Day 45. E-H, Decay in stagnant water (E12). E, Day 0 (minutes after death). F, Day 15. G, Day 30. H, Day 45. I-L, Decay under higher bottom current (E13). I, Day 0 (minutes after death). J, Day 15. K, Day 30. L, Day 45. M-P, Decay in low oxic conditions (E14). M, Day 0 (minutes after death). N, Day 15. O, Day 30. P, Day 45. Q-T, Decay in anoxic conditions (E15). Q, Day 0 (minutes after death). R, Day 15. S, Day 30. T, Day 45. Scale bars indicate 1 cm.

most microscavengers (Video S7). The organic decay also darkened the sediment around the discs in the first week, indicating anaerobic activity beneath the microbial caps (Figure S21). The first signs of arm disarticulation appeared around day 5 due to an attack by microgastropods (Figure 16K). Most of the skeletons reached decay stage 5 after around 35 days (Figure 16K), before the complete burial of the remains. In this muddy setting, the DO dropped to 5.60 mg/L, while the pH fluctuated between 7.8 and 8.2, but without much effect on the carbonate ossicles (Figure 19C-D).<sup>7</sup>

### *Influence of water energy*

Three experiments (E1, E12-E13) studied the role of water energy in decay. Experiment E12 was carried out without a filter to simulate a stagnant seafloor. These conditions led to a drop in DO and a greater increase in dissolved nitrogen compounds, especially ammonia (Table S12). In the initial days, the fluidisation of the viscera also resulted in the stratification of the water column and the settling of a broad microbial viscous layer, covering most of the ophiuroid carcasses (Figure S22). The rapid rupture of the epidermis and the collapse of the disc scales were frequent within decay stage 1. However, the microbial caps temporarily barred the attack of microscavengers, delaying the onset of arm disarticulation by up to 3 times more compared to conditions with a weak bottom current (E1). The disturbance of the organisms became more intense only after about 2 weeks, with the reduction of the microbial caps, leading to the severe collapse of the carcasses. Most skeletons reached decay stage 5 after 40 days (Figures 16L; 20E-H).

In contrast, experiment E13 simulated a higher bottom current ( $\pm 10$  cm/s) (Table S13). This led to the growth and migration of ripple marks within the aquarium, biasing the decay of the ophiuroid carcasses. The skeletons closest to the filter flow had some arms reorientated and began to be buried by sand grains during the initial days (Figures 20I-L; S23). Although the rapid burial has temporarily protected these skeletons, the constant migration of the sediment also led to the exhumation and disarticulation of some arms. Meanwhile, the skeletons farthest from the filter flow remained in a shadow zone, temporarily protected in the trough of the ripple marks. This dynamic scenario resulted in widely varying decay rates, but most of the carcasses reached a high degree of disarticulation after 40 days (Figures 16M; S24). Microscavengers were present throughout the experiment, although observation was more difficult due to the constant movement of sand grains.

### *Influence of oxygenation*

Three experiments (E1, E14-E15) evaluated decay under different oxygenation levels. Experiment E1 analysed high oxic conditions (Table S1), and experiment E14 simulated low

oxic conditions, with DO dropping to 2.12 mg/L (Table S14). The oxidation of nitrogen compounds was very rapid in both scenarios. The decay rates of the ophiuroid carcasses also followed a similar pattern, with an advanced collapse of the skeletons after 8 days (Figure 16A, N). However, the low oxigen reduced the pH to 7.3, the minimum limit of the test used, suggesting that the value could be even lower. This acidification was also supported by substantial signs of carbonate dissolution (Figure 19I-J). The experiment E14 still led to a greater frenzy among microscavengers, accelerating the disarticulation of the buccal framework of all the carcasses. Despite this, the soft tissues decayed into dark masses and persisted better preserved after 45 days than in the high oxigen scenario (Figures 15D; 20P).

In turn, experiment E15 quickly consumed the DO. Ammonia levels remained very high and no nitrite peak was detectable (Table S14), indicating an interruption in the oxidation cycle. The anoxic conditions led to the overgrowth of sulphate-reducing bacteria, darkening the sediment and covering most of the ophiuroid carcasses during the initial weeks (Figure S25). The water showed a strong egg-poor odour in the sampling intervals probably due to the presence of hydrogen sulphide (H<sub>2</sub>S). The high organic load of the substrate boosted the production of bubbles and helped to deform the sediment (Figure S26). The activity of microscavengers surprisingly remained high during the 45 days of observation (Figures S27; S28). The microbial caps delayed the disarticulation of some arms, but the bottom current, the release of gas bubbles, the instability of the sediment, and the attack of microscavengers were enough to break the blockage and quickly disarticulate the skeletons (Figure 16O; Video S8). The pH was also more acidic and led to the complete dissolution of the carbonate elements (Figure 19K-L), as well as a notable increase in the KH (Table S14). The soft tissues were the only remaining parts, maintaining a mould of the dissolved skeletons.

### *Influence of macroscavengers*

Six experiments (E16-E21) analysed the decay under perturbation of different groups of macroscavengers (Tables S16-S21). The physicochemical conditions of the water were similar to those of experiment E1 (Table S1), but the fluidisation of the viscera and the growth of microbial caps were often hindered by macroscavenger activity. Decay sequences were accelerated in most cases. All organisms were very agile in tracking down the fresh remains and initiating a targeted attack on the viscera, mainly affecting the skeletal integrity of the disc ossicles. This often resulted in the disarticulation of arm segments in less than a day, overlapping some stages of the normal decay sequence (Figure 21A-F).

The shrimp *L. ankeri* quickly attacked the disc of all ophiuroid carcasses, consuming the viscera available within the initial hours of experiment E16. The attack was carried out with its small pincers, reorienting the skeletons, pulling the epidermis of the discs, and oc-

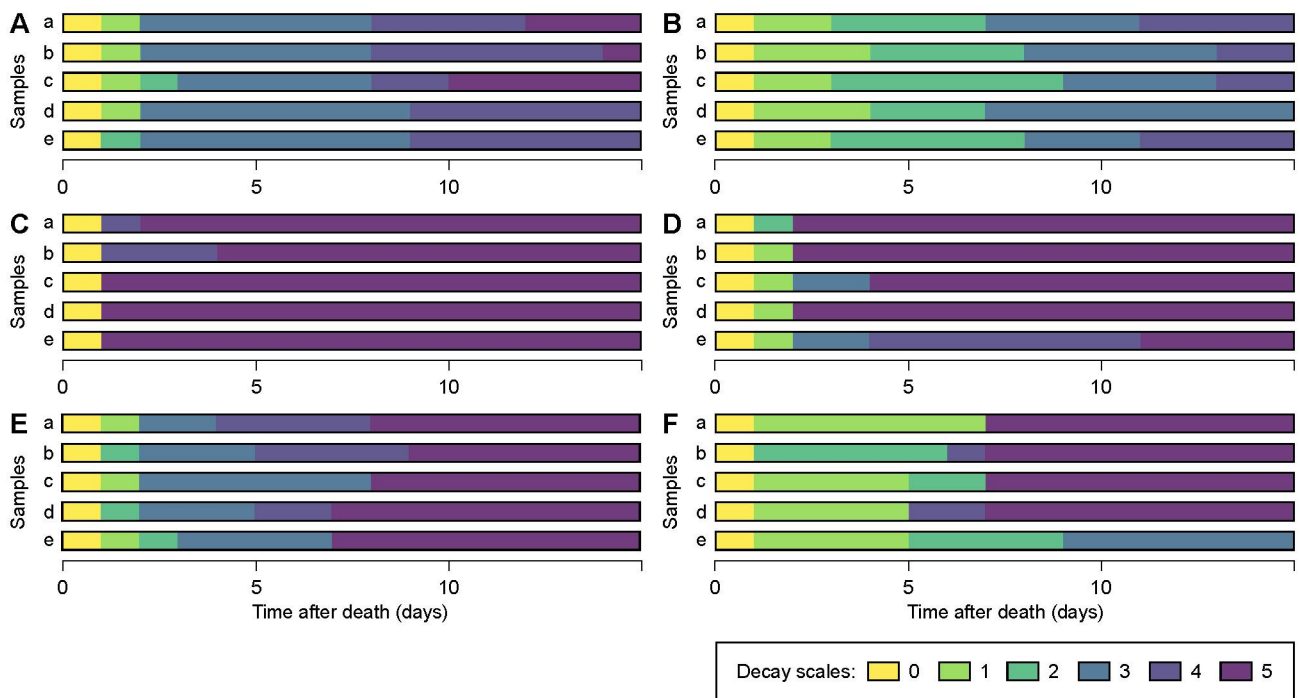


**Figure 21.** Decay stages of five specimens (a–e) of the ophiuroid *Amphipholis januarii* under macroscavenger disturbance. A, Shrimp (E16). B, Sea snail (E17). C, Asteroid (E18). D, Ophiuroid (E19). E, Hermit crab (E20). F, Polychaete (E21).

asionally breaking some arm segments (Figures S29; Video S9). The disturbance was delicate enough to keep the buccal frameworks intact during the first week (Figures 21A; S30; S31). The movement of the specimen was also more frequent through the water column, and the bioturbation of the sediment had little influence on the decay. However, the attacks remained constant in the long term and increasingly focused on the arm segments (Figure S32). All skeletons reached high disarticulation stages in less than 10 days, with the formation of clusters of detached ossicles in the sediment (Figure 22A-D).

The sea snail *P. vibex* produced the most discreet pattern of disturbance. The specimen was quick to track the substances in the water and guide itself to the fresh decaying remains. However, the attack was only directed at one of the ophiuroid carcasses (Figures 22E-H; S33). The proboscis was used to break the epidermis and suck out the viscera in the initial hours of the experiment E17. The disturbance was selective and disarticulated only the disc scales, without altering the decay sequence (Figure 21B). After 2 days, with the fluidisation of the viscera and the greater growth of the microbial caps, the sea snail no longer showed interest in the carcasses, much less in its arm segments. The ophiuroid skeletons then remained more under the effects of the bottom current and other microscavengers, resulting in decay rates very similar to experiment E1 (Figure 16A). Even the bioturbation was also discrete in the long term and accelerated disarticulation very little (Video S10).

In contrast, the disturbance of the asteroid *P. nodosus* led to the fastest decay rates. Seconds after introduction into the aquarium, the specimen moved to the nearest ophiuroid

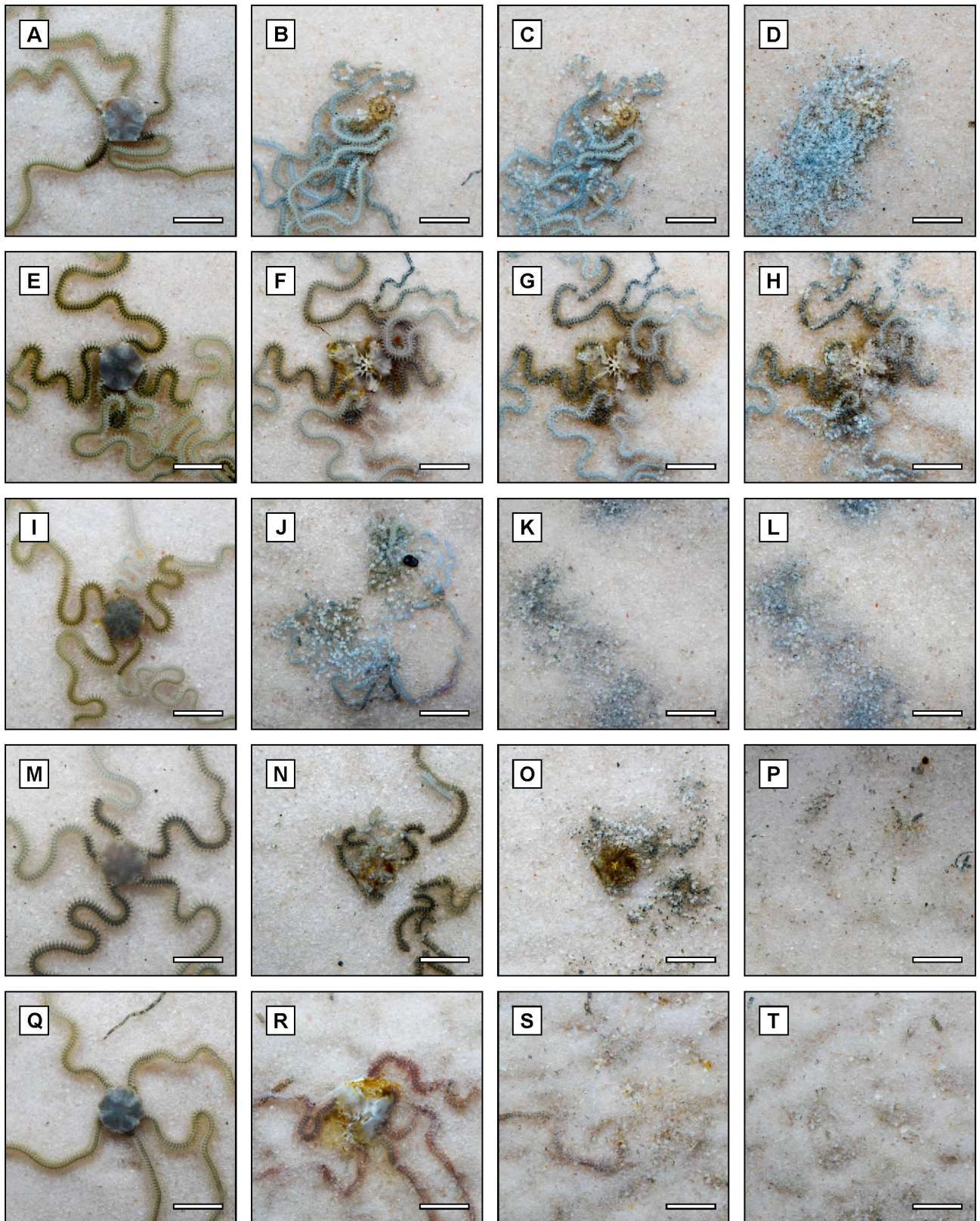


**Figure 22.** Decay pattern of the ophiuroid *Amphipholis januarii* under macrocavenger disturbance. A-D, Decay under shrimp activity (E16). A, Day 0 (minutes after death). B, Day 5. C, Day 10. D, Day 15. E-H, Decay under sea snail activity (E17). E, Day 0 (minutes after death). F, Day 5. G, Day 10. G, Day 15. I-L, Decay under asteroid activity (E18). I, Day 0 (minutes after death). J, Day 5. K, Day 10. L, Day 15. M-P, Decay under ophiuroid activity (E19). M, Day 0 (minutes after death). N, Day 5. O, Day 10. P, Day 15. Q-T, Decay under hermit crab activity (E20). Scale bars indicate 1 cm.

carcass and positioned its body over the disc region (Figure S34; Video S11). The cardiac stomach was expelled and the specimen remained intact until digestion of the soft parts was completed. This process was repeated for all carcasses during the initial hours of experiment E18. All ophiuroid skeletons achieved high disarticulation levels within the first day of observation (Figures 21C; S35). The arm ossicles were detached and most of the buccal frameworks were collapsed, reducing the carcasses to some clusters of small elements (Figure 22I-L). The movement of the asteroid was very active in the two weeks, and the bioturbation of the tube feet helped to disperse the bioclasts in the sediment.

Similarly, the disturbance by the ophiuroid *O. superba* was quite intense. The specimen quickly attacked all the carcasses of *A. januarii* distributed around the edges of the aquarium during the initial days of experiment E19 (Figures 21D; S36). The process was, however, less selective. The ophiuroid scavenged from the disc to the arm segments, consuming some remains and eliminating other parts such as a series of detached ossicles (Figure 22M-P). The movement of the specimen was also frequent and helped it to increasingly disarticulate all the skeletal remains into small bioclasts scattered throughout the sediment (Video S12). Decay was accelerated in these conditions by both scavenging and superficial bioturbation.

The presence of the hermit crab *C. vittatus* also greatly accelerated the decay sequence in the E20 experiment. The specimen was quite active throughout the sediment, dragging its housing shell and creating a large overlap of locomotion tracks (Figures S37; S38). In the initial week, the disarticulation of ophiuroid carcasses was intensified mainly by this expressive bioturbation process (Video S13), breaking most of the arms into a portion of smaller articulated segments. Meanwhile, scavenger activity was recorded only at the end of the first week, probably induced by starvation (Figure 22Q-T). The hermit crab suddenly destroyed all the carcasses with its large claws, removing the microbial caps to reach the organic remains. This attack was much less delicate than the shrimp pincers (E16), disarticulating all the ophiuroid buccal frameworks (Figure 21E).

Last, the polychaete *E. complanata* produced two phases of disturbance. In the early hours of experiment E21, an attack was directed at one of the fresh carcasses (Figure S39). The polychaete wrapped itself around the remains, leaving a series of setae on the ophiuroid skeleton (Video S14). The mandibles were used to break through the disc and consume most of the viscera. The carcass was reoriented and some arms were disarticulated, but the buccal framework remained intact (Figure S40). The polychaete only showed interest in the other carcasses again around day 5. From this point onwards, the attack was much more coarse and less selective. The polychaete destroyed some arms and consumed part of the viscera, leaving damaged discs and a mixture of articulated, semi-articulated, and

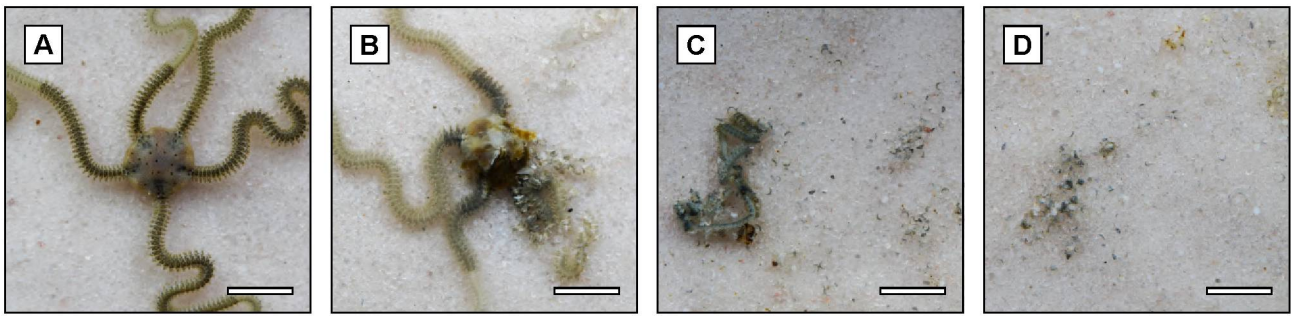


**Figure 23.** Decay pattern of the ophiuroid *Amphipholis januarii* under polychaete activity (E21). A, Day 0 (minutes after death). B, Day 5. C, Day 10. D, Day 15. Scale bars indicate 1 cm.

completely detached arms. The disturbance continued mainly on the remains of the edges of the aquarium. Most skeletons were reduced to a series of isolated ossicles (Figures 21F; 23A-D). The frequent movement of the polychaete also accelerated the decay, but the bioturbation traces in the sand substrate were almost imperceptible.

## Discussion

### *Decay agents*

Our results detail how decay works in small multi-element organisms and how different marine conditions can influence this process. The experimental data are specially calibrated for asterozoan echinoderms because they comprise one of the most complex skeletal arrangements known in nature. After death, the soft tissues of these animals begin to degrade rapidly, and the delicate skeleton soon loses the support necessary to maintain the articulation of the hard parts. The advance of the decay sequence leads to the collapse of hundreds to thousands of carbonate elements in the sediment, destroying the original form of the carcasses usually within a few days. At least seven major decay agents can accelerate this process, most associated with biological activity in marine ecosystems (Table 3). Fossilization then depends on preservation shortcuts that delay or remove most of these destructive agents.

First, macroscavengers play a crucial role because members of all animal phyla can consume dead biomass (Britton & Morton, 1994; King et al., 2007). These organisms are widespread and can thrive under more extreme conditions, such as abyssal depths, poorly oxygenated bottoms, sub-zero water temperatures, and regions with salinity fluctuations (Diaz & Rosenberg, 1995; Dunlop et al., 2021). Many groups are still highly bioturbators and others may use well-developed chemoreceptors to quickly detect carcasses, aggregating in large numbers to consume organic remains (Meyer, 1971; Schäfer, 1972; Plotnick, 1986; Ruxton & Houston, 2004). The fossil record also supports the occurrence of macroscavengers since the Ediacaran, reinforcing the active nutrient cycling even in ancient seas (Gehling & Droser, 2018). For this reason, our data agree that it is unlikely that small car-

**Table 3.** Decay agents and main limiting conditions for the long-term preservation of delicate multi-element skeletons.

<b>Decay agents</b>	<b>Destructive effects</b>	<b>Limiting conditions</b>
Macros scavengers	Removal of soft parts and disarticulation of hard parts	Anoxic waters, fluctuations in salinity or temperature
Microscavengers	Removal of soft parts and disarticulation of hard parts	Fluctuations in salinity or temperature
Microbial activity	Degradation of soft parts and indirect disarticulation of hard parts	Fluctuations in salinity or temperature
Algae growth	Degradation of soft parts, destabilisation and disarticulation of hard parts	Turbid waters or deeper bottoms
Water energy	Transport, reorientation, fragmentation, and disarticulation of hard parts	Stagnation bottoms
Bubble expulsion	Disarticulation of hard parts	Organic-poor bottoms
Acidification	Dissolution of carbonate parts	Oxic waters

casses could have remained intact for more than a day under the complex competition from annelids, molluscs, chordates, arthropods, and echinoderms from most marine ecosystems.

Similarly, microscavengers are also an important agent. Although the effect may not be the same on larger carcasses, our results highlight how the disturbance of these millimetric organisms can accelerate the collapse of delicate multi-element skeletons. Among a diversity of ciliates, arthropods, and nematodes, microscavengers form one of the greatest biomasses on the planet. Many groups can thrive in conditions with annual fluctuations in pH and salinity, and others can tolerate even euxinic environments (Fenchel & Finlay, 1991; Steyaert et al., 2007; Ekau et al., 2010; Kehayias et al., 2012; Wishner et al., 2020; Rotterová et al., 2022), colonising more extreme regions than any other metazoans. Despite their diminutive size, usually smaller than 2 mm, microfossil representatives have been known at least since the Ediacaran (Li et al., 2007; Poinar et al., 2008; Harvey et al., 2012), emphasizing their vital role in the food chain throughout geological time.

Another relevant decay agent is microbial activity. Microorganisms are important pillars of the biosphere because they can adapt to extreme environments and perform biogeochemical steps that other organisms are unable to complete (Hunter-Cevera et al., 2005). In the case of small, weakly articulated carcasses, such as asterozoans, microbial activity destroys the ligament tissues and destabilizes the skeletal arrangement, which can lead to the indirect collapse of unstable hard parts by the simple action of gravity. We also agree with some studies that the differences between aerobic and anaerobic decay are minimal (Plotnick, 1986; Allison, 1988b; Kidwell & Baumiller, 1990). However, due to the greater restriction

of microbial communities under anoxia, anaerobic reduction alone may help to better preserve organic remains in the long term.

Surprisingly, the rapid bloom of filamentous algae can also accelerate the decay under bright conditions. Although some studies have indicated that algal caps protect against disarticulation (e.g., Kidwell & Baumiller, 1989; Klompaker et al., 2017), our results have shown that this is not necessarily a rule. The shape of the carcass and the arrangement of the organic parts can produce a rebound effect. In the multi-armed skeleton of asterozoans, the growth of green and brown algae can occur within a few days and condense mainly over the disc region, where most or all of the viscera are housed. These localised algal caps can trap bubbles and inflate the disc in the water column, while the distal arm segments remain anchored in the sediment. This upright posture destabilises the skeleton and leads to the collapse of the ossicles, rapidly disarticulating even the more protected elements of the buccal framework.

Water turbulence is another relevant agent in marine environments. In shallower regions, the wind can drive the production of strong currents, helping to remobilize sediment and destroy delicate carcasses within hours. However, many currents can still be produced by differences in water density, affecting a wide range of seafloor depths. Our simulations showed that flow velocities of 5 cm/s can be sufficient to disarticulate small unstable skeletal segments, such as some ophiuroid arms oriented against the water flow. Due to high porosity, disarticulated carbonate elements can also be transported more easily than dense sand grains, contributing to the wide dispersion of bioclasts within a few weeks. This disturbance is possible even in euxinic basins, where deep-water circulation can reach 5 to 20 cm/s, as recorded for modern regions of the Black and Baltic Seas (Demyshev et al., 2016; Jędrasik & Kowalewski, 2019), as well as indicated for certain Jurassic bituminous shales (Seilacher et al., 1985).

The expulsion of bubbles can also turn the seafloor into a complex minefield for small multi-element skeletons. Due to microbial reduction of organic compounds in the innermost anoxic layers of the sediment, a substantial volume of dissolved gas can be produced, such as N<sub>2</sub>, H<sub>2</sub>S, and CH<sub>4</sub> (Kaplan, 1974; Orsi, 2018). The recurrent ascent of these gaseous products can lead to overgrowth and agglomeration of bubbles up to 1 cm in diameter within the sediment, as observed here under dark anoxic and well-lit oxic conditions. These bubbles rise and escape abruptly and randomly at the water-sediment interface, deforming the substrate and leaving a series of mini craters. During this process, many bubbles can still collide below the carcasses, leading to the sudden collapse of skeletal segments. For this reason, the articulated preservation of delicate specimens is unlikely on such unstable seafloors.

Finally, with the reduction in the pH of the water, acidification still becomes an efficient agent for destroying hard parts. The process is mainly caused by an increase in CO<sub>2</sub>, in addition to sulphur and nitrogen compounds, which lead to a series of changes in the chemistry of carbonates (Guinotte & Fabry, 2008; Gattuso & Hansson, 2011). These events can be achieved naturally in organic-rich seafloors, where aerobic decay converts DO into high levels of dissolved CO<sub>2</sub> (Golubić & Schneider, 1979; Gobler & Baumann, 2016). Several types of calcified organisms can be affected by this acidification, such as molluscs, cnidarians, arthropods, brachiopods, and echinoderms (Andersson et al., 2011; Pickett & Andersson, 2015). Our experiments demonstrated substantial levels of carbonate dissolution under low oxic waters, as well as complete dissolution under anoxia. Such oxygen-poor settings can rapidly deplete the structure of high-magnesian calcite even before disarticulation progresses, thereby reducing the preservation potential of the hard parts more than the soft parts themselves.

### *Preservation shortcuts*

Even a short period of hours to a few days after death can be enough to damage the fragile structure of small multi-element skeletons in most marine environments. The complex interaction of scavengers, algal blooms, water chemistry, bottom currents, microorganisms, and bubble expulsion can quickly reduce fresh carcasses to just a series of isolated elements. For this reason, rapid burial is the most important condition for the fossilization of these delicate organisms (Fraga & Vega, 2024). While low burial rates prolong the destructive effects of biostratinomy, rapid and definitive burial can protect skeletons against most biotic and abiotic disturbances (Brett & Baird, 1986, 1993; Speyer & Brett, 1988; Brandt, 1989; Donovan, 1991; Brett et al., 1997; Ausich, 2021; Fraga & Vega, 2022). At least three preservation shortcuts can then be established, where the quality of the fossils depends on the time lapse between the deposition event and the death of the organisms.

The first and most relevant shortcut involves the rapid burial of living specimens (Figure 24). This is the most favourable scenario for articulated fossils of multi-element organisms, where death and burial are the result of the same depositional event, under obrution beds. In marine basins, this process can often be caused by tempestites, in proximal zones, or by turbidites, reaching a variety of seafloors. Important taphonomic examples have been recorded throughout the Phanerozoic, such as in the Devonian of Brazil (Fraga & Vega, 2020, 2022), the Jurassic of Germany (Rosenkranz, 1971; Seilacher et al., 1985), and the Neogene of Japan (Ishida & Fujita, 2001; Ishida et al., 2024). Some extrabasinal turbidites, generated by large river discharges, can also transport interstitial freshwater and anaesthetize free-living benthic groups, such as many echinoderms (Fraga & Vega, 2024). Entire as-



**Figure 24.** Idealised reconstruction of the rapid burial of an invertebrate-rich benthic community by a muddy extrabasinal turbidite. Art by Julio Lacerda.

semblies can be paralysed under these events, favouring the preservation of articulated skeletons without escape postures.

Another possible shortcut is the rapid burial of fresh carcasses, minutes to a few days after death. This scenario may occur for individuals that occasionally die of old age, disease, or predation before the obrution of a seafloor. Skeletons can have initial signs of disarticulation due to exposure to microbial decay, scavenger attack, and current disturbance, as reported for some Devonian ophiuroids (Fraga & Vega, 2022). However, in the case of larger autochthonous populations, the chances are more complex because they depend on a combination of mass mortality and rapid deposition events. Although fluctuations in salinity, temperature, or oxygenation can favour this process (Lawrence, 1996), as well as restrict scavengers and microorganisms, rapid and timely burial is still necessary. Alternatives have thus suggested the transport of organisms to inhospitable bottoms, where allochthonous preservation could be promoted by subsequent pulses of deposition, as inferred for certain Triassic ophiuroids (Radwański, 2002; Zatón et al., 2008).

Rapid burial can also sometimes lead to the preservation of delicate carcasses weeks after death. The biggest limitation is the length of time the carcasses remain in the taphonomically active zone. The greater the exposure, the greater the damage to the skeletal structure, and the more difficult it will be to recognise the resulting fossils. The organic remains can be completely degraded and most of the hard elements can be disarticulated, fragmented, or dissolved. The carcasses may be reduced to very small bioclasts, and the

deposition event itself may help to further disperse the remains into the sediment. Even if fossilization occurs in this advanced scenario, bioclasts may go unnoticed in fieldwork or be classified only as a series of indistinguishable fragments. Nevertheless, as supported by our experiments, some exceptional circumstances can delay long-term destruction and surprisingly create a preservation shortcut even for small multi-element skeletons with a high degree of decay.

Abrupt and prolonged changes in salinity and temperature are successful in restraining most biological agents. Mesohaline and hypersaline oscillations can kill microscavengers and slow microbial activity due to osmotic imbalance, which accords with previous remarks (Allison, 1988b, 1990). Although other studies with artificial seawater have suggested that the decay rate increases progressively with temperature (Kidwell & Baumiller, 1990; Kerr & Twitchett, 2004), we identified divergences likely due to the use of plankton-rich natural seawater. Very low temperatures, around 5°C, can exclude microscavengers and drastically delay microorganisms, favouring articulation and preservation of soft tissues for months. However, there is an important window between 15 and 25°C in which the attack by microscavengers can be equally intense. We also observed that very high temperatures, around 35°C, can have the opposite effect, limiting microscavengers and helping to preserve articulated parts in the long term.

Some complementary conditions can inhibit the action of other relevant decay agents. More stagnant seafloors can protect multi-element skeletons against intense disturbance from waves and bottom currents. At the same time, water stratification can limit the distribution of microscavengers, slowing disarticulation rates at least during the initial weeks of decay. Deeper or turbid seafloors can also restrict photosynthetic assemblages, preventing the destabilization of more delicate carcasses by excessive growth of filamentous algal caps. Sediment instability caused by the expulsion of bubbles can still be avoided in oxygenated seafloors that are poorer in organic matter, as well as in dark regions without complex photosynthetic zones.

Organic preservation can also be favoured under hypoxic and anoxic seafloors. Although microbial reduction is high under these conditions, the scarcity of DO limits the complete decay cycle of organic compounds, which is accelerated by the combination of oxidation and reduction processes. Only under reduction, the soft tissues can then be degraded to dark masses with greater potential to remain in the bottom for months. However, unlike the idea that anoxia benefits the preservation of articulated skeletons by excluding scavenging metazoans (Kidwell & Baumiller, 1990), we observed that DO variation is unable to restrict the anaerobic activity of many groups of microscavengers, which can also drastically accelerate the collapse of small hard parts. Moreover, microbial reduction in organic-rich sedi-

ments can lead to the production of bubbles and acidification of the water column, potentiating the destruction and dissolution of carbonate elements under anoxia.

### *Gaps and Recommendations*

Although our results help to better elucidate how many marine variables can influence the decay process, interpretations should be treated with caution because the controlled conditions do not replicate the complexity and variability of natural marine environments. The experiments were focused on the alteration of multi-element organisms, with many small and weakly articulated parts that are very sensitive to decay agents in the taphonomically active zone. Obviously, exceptions may exist and the effects described here may not be the same for other larger and more robust carcasses, such as molluscs or chordates. Additional studies are therefore welcome to expand this understanding. Our data also focuses on fluctuations in water parameters within the same idealised seafloor. This means that we evaluate how sudden in situ changes in the environment can delay or accelerate the main decay agents.

However, it is important to recognize that other well-established environments can have biological assemblages that are well adapted to parameters very different from the temperate seawater of the Paranaguá Estuarine Complex used here as a base. This may be the case for many cold polar seas, warm tropical seas, hypersaline lagoons, and brackish fjords and estuaries. Therefore, our results should not lead to misinterpretations and indicate that these regions with different light, energy, salinity, sediment, oxygenation, or temperature are the key to exceptional preservation. Each of these environments can present unique planktonic and benthic communities, including macroscavengers and microscavengers that can dramatically accelerate decay. Future experiments are therefore thus needed to help clarify the effects and divergences between these exotic ecosystems.

### **Conclusions**

The multi-element skeleton of asterozoan echinoderms is one of the most complex arrangements in nature, as well as an excellent guide for taphonomic studies. The first signs of decay in these delicate skeletons can appear hours to a few days after death, therefore requiring exceptional circumstances for fossilization. Seven decay agents can accelerate the destruction of these carcasses in marine systems, including algae growth, water energy, microbial activity, microscavengers, macroscavengers, bubble production, and water acidification. Rapid burial of living specimens is the main shortcut to fossilization of articulated specimens, but burial after death can sometimes also lead to preservation if most decay agents are timely delayed.

Abrupt and prolonged changes in salinity and temperature can restrict the distribution of scavengers and the activity of microorganisms, helping to preserve carcasses in the long term. Deeper or turbid seafloors can prevent the destabilization of delicate skeletons due to excessive growth of filamentous algal caps. Stagnant seafloors can also protect carcasses against intense disturbance from waves and bottom currents, and water stratification can temporarily dampen attack by microscavengers. Although anoxia favours the preservation of soft parts, it is unable to stop the attack of anaerobic microscavengers, which accelerates the destruction of small hard parts. Microbial reduction of organic-rich anoxic bottoms also drives the expulsion of bubbles in the sediment and acidification of the water column, accelerating the destruction and dissolution of carbonate elements.

## **Acknowledgements**

We would like to thank the Coordenação de Aperfeiçoamento de Pessoal de Nível Superior (CAPES) and the Programa de Apoio à Pós-Graduação (PROAP) for funding the research. We would also like to thank the Centro de Microscopia Eletrônica (CME-UFPR), the Laboratório de Paleontologia (LABPALEO-UFPR), the Laboratório de Pesquisas Hidrogeológicas (LPH-UFPR), and the Instituto Laboratório de Análise de Minerais e Rochas (iLAMIR-UFPR) for providing equipment and laboratory analyses. Special thanks to Liz Agnol, Dhiego Silva, Mauro Fraga, Lucas Szekut, Carolina Freire, Robson Bolzon, Michela Borges, Henrique Rieger, Caro Valenzuela, Nicole Stakowian, Adelita Rodrigues, and Rodrigo Guimarães for their assistance during some of the research activities. Finally, we would like to thank the editorial staff and reviewers for their constructive comments.

## **Author Contributions**

**Conceptualization** Malton Carvalho Fraga (MCF); **Data Curation** MCF; **Formal Analysis** MCF; **Funding Acquisition** MCF; **Investigation** MCF; **Methodology** MCF, Cristina Silveira Vega (CSV); **Project Administration** MCF; **Resources** MCF; **Supervision** CSV; **Validation** MCF, CSV; **Visualization** MCF; **Writing - Original Draft Preparation** MCF; **Writing - Review & Editing** MCF, CSV.

## **Supplementary data**

<https://doi.org/10.1016/j.ibiod.2024.105904>

## CARBONACEOUS COMPRESSIONS IN ECHINODERMS: INSIGHTS FROM FOSSILS AND DIAGENETIC EXPERIMENTS

by MALTON CARVALHO FRAGA<sup>1\*</sup> and CRISTINA SILVEIRA VEGA<sup>1</sup>

<sup>1</sup>Departamento de Geologia, Setor de Ciências da Terra, Universidade Federal do Paraná, Curitiba, PR, Brazil; malton.fraga@ufpr.br, cvega@ufpr.br

\*Corresponding author

**Abstract** - This study investigates the atypical formation of carbonaceous compressions in fossil echinoderms. The analyses focus on Devonian encrinasterids from the Ponta Grossa Lagerstätte and other fossil ophiuroids from laboratory-based diagenetic experiments. The results indicate that the kerogenization potential of organic remains is mainly limited by the skeletal structure and the type of burial sediment. Less protected viscera, such as those beneath the thin disk cover of ophiuroids, are more prone to compression and polymerization than other labile tissues and organs housed within robust calcareous modules. The antibacterial properties of purer kaolinitic clays may also contribute to this process, leading to thicker and more defined carbonaceous compressions compared to those formed in microbially complex mixed clays. Despite chemical and structural alterations during diagenesis, carbonaceous remains assist in mapping the anatomy of extinct groups, such as the disc-restricted viscera in the encrinasterids analyzed. Raman spectra of carbonaceous compressions in these fossils also proved excellent geothermometers, showing that the Ponta Grossa Lagerstätte reached a peak temperature of about 170°C.

**Keywords:** Ophiuroids, Taphonomy, Fossilization, Kerogenization, Geothermometer.

### Introduction

Kerogenization is the main mechanism for the fossilization of organic remains in the geological record. It involves a series of biogeochemical reactions that modify the original structure of organisms from their death until their deep burial in sediment (Summons, 1993; Vandenbroucke & Largeau, 2007; Bushnev & Burdel'naya, 2009). During this process, most light and volatile compounds are lost, transforming organic matter into kerogen - a complex, insoluble, and highly stable macromolecular substance (Durand, 1980). This resulting ker-

ogen is particularly important in sedimentary rocks not only as a precursor of hydrocarbons, but also as a source of formation of two-dimensional carbonaceous compressions in macrofossils (Gupta & Briggs, 2011). From plants to animals, these compressions have played a crucial role in preserving soft tissues from different biotas, covering fossils from the Proterozoic to the Phanerozoic (e.g., Cúneo et al. 2003; Loydell et al. 2004; Cai et al. 2012; Kumaran et al. 2013; Broce & Schiffbauer 2017; Muscente et al. 2016; Osés et al. 2017; Hazra et al. 2020; Mouro et al. 2020; Bezerra et al. 2021; Saleh et al. 2021; Zhang et al. 2021; Fraga et al. 2023; Qin et al. 2023; Jiménez et al. 2024). These records offer paleontologists valuable insights into details far beyond the hard parts of extinct organisms.

Despite its widespread occurrence in many fossils, kerogenization is a rare process in groups without strongly sclerotized or cuticularized parts, as is the case in all representatives of echinoderms. Even after centuries of paleontological research, the exceptional preservation of organic parts in these marine invertebrates has mostly been reported through mineralization. Important examples include the pyritization in crinoids, ophiuroids, holothurians, and stylophorans (Glass & Blake 2004; Glass 2006; Ausich et al. 2013; Smith & Reich 2013; Clark et al. 2017; Lefebvre et al. 2019; Saleh et al. 2023), as well as calcitic and ferruginous filling in crinoids, asteroids, and holothurians (Haugh 1975; Haugh & Bell 1980; Sutton et al. 2005; Briggs et al. 2017; Rahman et al. 2019). Meanwhile, carbonaceous compressions have only been reported for Cambrian gogiids from the Balang Lagerstätte in China (Lin et al. 2008), Devonian ophiuroids from the Ponta Grossa Lagerstätte in Brazil (Fraga & Vega 2022), and Cretaceous crinoids from the Smoky Hill Chalk Lagerstätte in United States (Springer 1901; Meyer & Milsom 2001). However, these fossils provide an opportunity to further understand the original arrangement of soft tissues and the taphonomic shortcuts that led to atypical kerogenization in echinoderms.

Motivated by these findings, we investigate here the process of formation of carbonaceous compressions in small ophiuroids. The analyses are based on both natural fossils from the Ponta Grossa Lagerstätte and artificial fossils from long-term diagenetic experiments conducted in the laboratory. From these samples, we employed scanning electron microscopy to map the morphology, composition, and distribution of elements associated with carbonaceous compressions under different sediments and variable periods of diagenetic maturation. Additionally, we utilized Raman spectroscopy as a fast and practical method to assess and compare the thermal, chemical, and structural signatures of these carbon-rich films preserved in both natural and artificial conditions. The results contribute to a better understanding of the potential pathways of kerogenization in small multi-element organisms, focusing mainly on the influence of time, sediment, and temperature on this process. In this way, we hope this study will encourage further research for new traces of kerogenized soft

tissues in more types of echinoderms and other fossil groups that have been little explored in the literature.

## **Materials and methods**

### *Natural fossils and paleontological sites*

Two small samples of fossil ophiuroids with well-preserved carbonaceous compressions were used as proxies for studying the natural process of kerogenization in echinoderms. These samples were selected to accommodate the size limitations of the non-destructive analytical instruments used in the research. Both fossils originate from the marine siliciclastic sequence of the Ponta Grossa Formation, known as a Devonian Konservat-Lagerstätte with exceptional preservation of echinoderms from the Paraná Basin in Brazil (Figure 25A) (Fraga & Vega, 2022). The specimens are juvenile *Encrinaster pontis*, an epifaunal encrinasterid endemic to the polar epicontinental seas of western Gondwana during the late Pragian to late Emsian (Fraga & Vega, 2020, 2022). Sample UFPR 0621 PI was collected from the silty shale beds of the Rio Caniú site (Figure 25B, D) (25°18'50.9"S, 50°05'32.9"W), while sample UFPR 0587 PI was obtained from the mudstone beds of the Aeroporto Sant'Ana site (Figure 25C, E) (25°10'50.5"S, 50°08'45.8"W), both located in the eastern part of Paraná state, southern Brazil. These fossils are part of the scientific collection of the Laboratório de Paleontologia (LABPALEO) of the Setor de Ciências da Terra (SCT) at the Universidade Federal do Paraná (UFPR).

### *Artificial fossils and experimental protocol*

Four long-term experiments were conducted to evaluate the potential for kerogenization in extant echinoderms under controlled diagenetic conditions. The experiments used adult specimens of *Amphipholis januarii*, an unprotected species of semi-infaunal amphiuroid abundant in the Paranaguá Estuarine Complex, on the coast of Paraná, southern Brazil. This species was chosen for its soft disk, which has a thin, flexible epidermis covered only by small calcite scales, resembling the less skeletonized disk of certain Paleozoic ophiuroids, such as protasterids and encrinasterids (e.g., Spencer & Wright, 1966). Live specimens were manually collected with the help of a small fishing boat during low tide in the estuary, when parts of the muddy bottom emerge, and the ophiuroids burrow into the sediment to avoid dehydration. The specimens were transported in plastic boxes partially filled with the soggy sediment from the region to minimize stress and prevent autotomy of the arm segments. Some gallons of mud and seawater were also sampled for use in the laboratory. All field collections were licensed by the Brazilian biodiversity and genetic heritage regulatory systems, SISBIO and SISGEN, respectively.

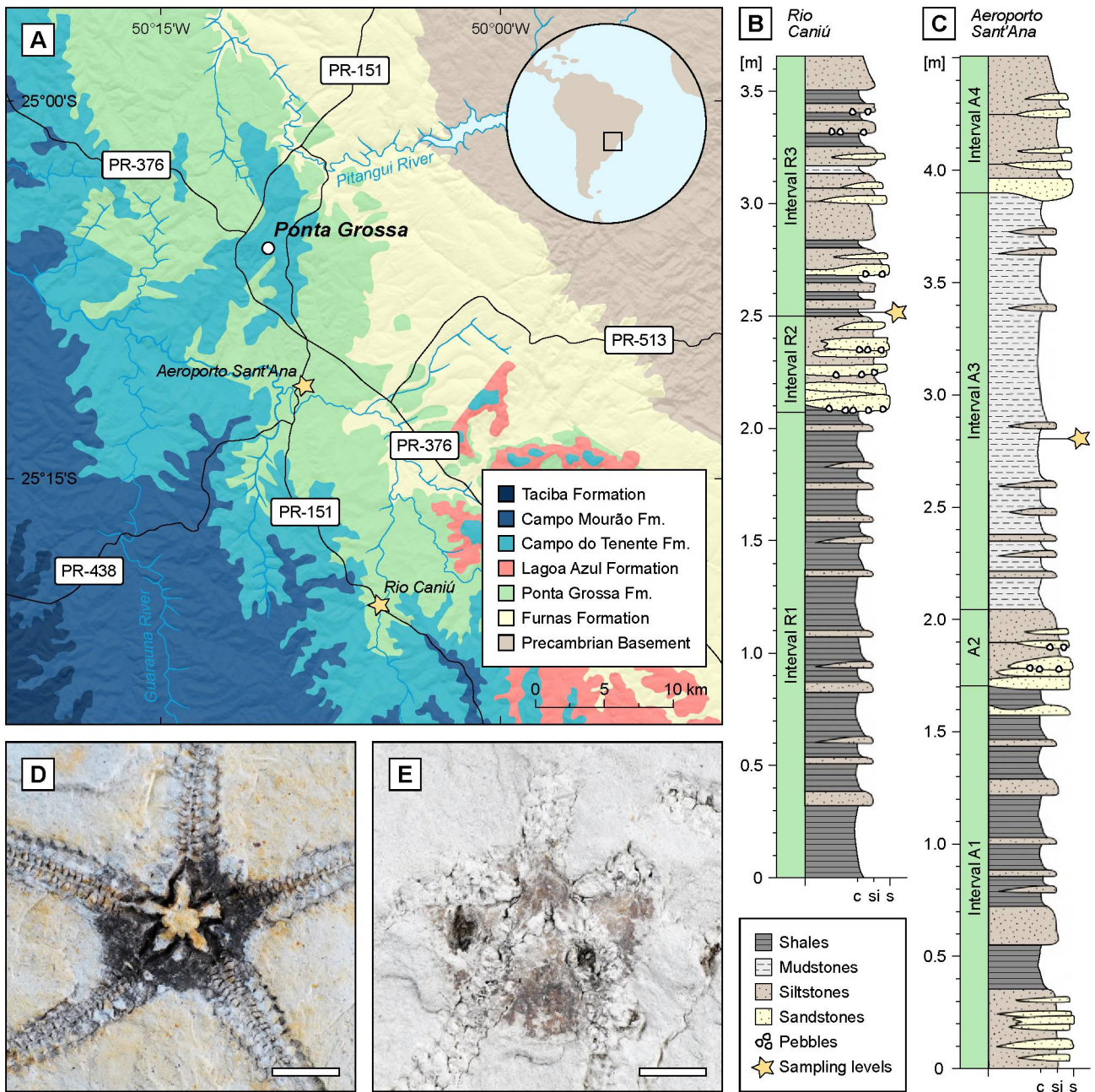


**Figure 25.** Provenance of the Devonian ophiuroids. A, Geological map highlighting the two paleontological sites of interest around the municipality of Ponta Grossa, in the eastern portion of the state of Paraná, southern Brazil. The stratigraphic columns from the Rio Caniú (B) and Aeroporto Sant'Ana (C) sites indicate the collection levels of samples UFPR 0621 PI (D) and UFPR 0587 PI (E), respectively (based on Fraga & Vega, 2022). The fossils preserve the dorsal (D) and ventral (E) surfaces of juvenile specimens of *Encrinaster pontis*, both with carbonaceous compressions. Scale bars represent 3 mm (D-E).

In the laboratory, the ophiuroids were inspected, and four complete specimens with intact disks and five well-preserved arms were selected for the experiments. Following the method of Fraga & Vega (2025), the individuals were laid out on a dry surface and sacrificed by heat shock, using approximately 5 mL of fresh water at  $\pm 85$  °C poured over the disk. With the dorsal side facing upwards, each carcass was then placed at the bottom of one of the four experimental aquariums (Figure 26A). These aquariums were glass cylinders

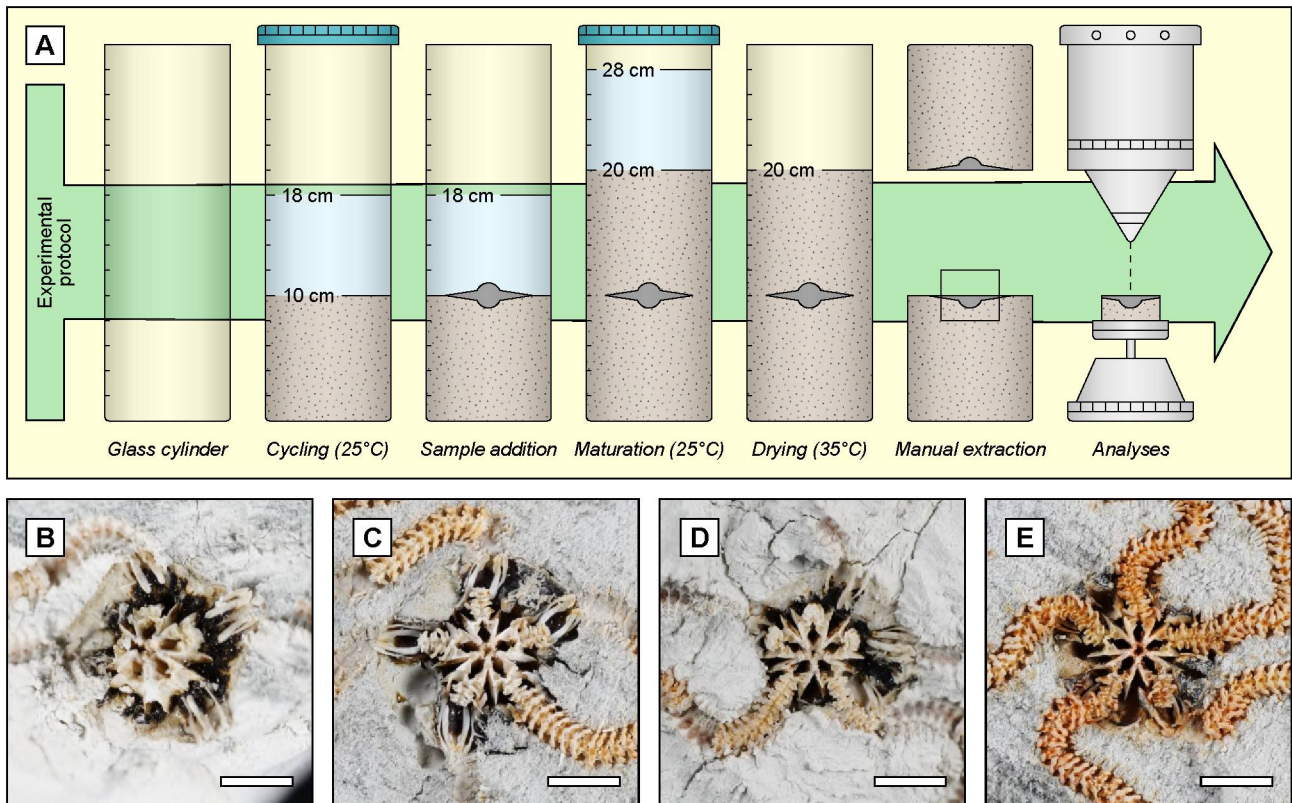


**Figure 26.** Provenance of the artificial fossil ophiuroids. A, Main steps used in the process of creating fossil ophiuroids in the laboratory (see text for explanations). B, 60 days in kaolinitic clay (Setup 1). C, 60 days in a mixture of kaolinite and marine mud (Setup 2). D, 120 days in kaolinitic clay (Setup 3). E, 120 days in a mixture of kaolinite and marine mud (Setup 4). Scale bars represent 3 mm (B-E).

with a diameter of 10 cm and a height of 30 cm, filled with a 10 cm layer of pre-deposited substrate and an 8 cm column of natural seawater ( $\pm 30$  ppt). The sediment used varied between kaolinitic clay or an organic-rich mixture (1:1) of kaolinitic clay and natural marine mud, passed through a 125  $\mu\text{m}$  sieve to remove larger particles (Table 4). The setups were previously kept in the dark to prevent excessive algal growth and in a water bath at 25°C for 30 days to allow the microbial colonies to gradually stabilize before introducing the ophiuroid carcasses. Plastic lids were also used to seal the four cylinders, preventing evaporation and salinity fluctuations during the pre-cycling period (Figure 26A).

After establishing this scenario, the fresh carcasses were buried under a 10 cm column of mud (Figure 26A). The mud was carefully dispersed over the bottom of the aquariums with a large syringe, avoiding disturbing the ophiuroid skeletons. The sediment used for burial was identical to the pre-deposited substrate, both prepared from a previous mixture with natural seawater (Table 4). The aquariums were then sealed with plastic lids and kept in the dark at 25°C for diagenetic maturation over a period of 30 to 90 days (Table 4). After this stage, the setups were opened and the water column was removed, leaving only the saturated sediment in a water bath at 35°C for 30 days to dehydrate and compact naturally (Figure 26A). The mud gradually detached from the aquarium walls during this process, fa-

**Table 4.** Main attributes of the diagenetic experiments.

Main attributes	Diagenetic experiments			
	Setup 1	Setup 2	Setup 3	Setup 4
Water	Seawater (30 ppt)	Seawater (30 ppt)	Seawater (30 ppt)	Seawater (30 ppt)
Sediment	Kaolinitic clay	Kaolinitic clay + marine mud (1:1)	Kaolinitic clay	Kaolinitic clay + marine mud (1:1)
Pre-cycling	30 days at 25°C	30 days at 25°C	30 days at 25°C	30 days at 25°C
Maturation	30 days at 25°C	30 days at 25°C	90 days at 25°C	90 days at 25°C
Drying	30 days at 35°C	30 days at 35°C	30 days at 35°C	30 days at 35°C

cilitating the later removal of compact cylindrical blocks of mudstone without damaging the glass. A small hammer and chisel were utilized to split the four samples in half, revealing the artificial fossils (Figure 26B-E). Only basal blocks were selected for analysis. Excess sediment from their margins was removed, creating cylinders less than 4 cm in diameter preserving the ventral portions of the ophiuroids (Figure 26A).

#### *Laboratory analyses*

A first set of analyses was conducted to evaluate the chemical properties of the sediment associated with both natural and artificial fossils. For this purpose, semi-quantitative XRF was performed on small rock samples extracted from the margins of the fossils from the Ponta Grossa Formation (Tables S1-S2), as well as on the kaolinitic clay and natural marine mud used as substrate sources in the experimental aquariums (Tables S3-S4). These sediment samples were pulverized, and the XRF analyses were carried out using a Panalytical Axios Max available at Instituto Laboratório de Análise de Minerais e Rochas (iLAMIR-UFPR). On the other hand, the physicochemical properties of the water used in the diagenetic experiments were also assessed. A hydrological report was prepared for the seawater collected from the Paranaguá Estuarine Complex, using approximately 1L of sample and following the protocols of the Laboratório de Pesquisas Hidrogeológicas (LPH-UFPR) (Table S5). Furthermore, measurements of pH, kH, nitrite ( $\text{NO}_2^-$ ), and ammonia ( $\text{NH}_3/\text{NH}_4^+$ ) were performed on the water column extracted from the aquariums after the maturation period (Table S6), utilizing a Labcon aquarium chemical kit calibrated for saltwater tests at 25°C.

A second set of analyses was performed to investigate the kerogenization process in both natural and artificial fossils. Scanning electron microscopy (SEM) and energy-dispersive X-ray spectroscopy (EDS) were employed to examine the morphology, composition, and elemental distribution of six samples. These analyses were carried out without metal coating, using a Tescan Vega3 LMU provided by the Centro de Microscopia Eletrônica (CME-

UFPR), to avoid altering the specimens. Raman spectroscopy was also applied to each sample to assess their chemical and structural signatures, utilizing a WiTeC Alpha300R Confocal Raman Microscope equipped with a 10X objective and a 532 nm Nd-YAG green laser. For fossils from the Ponta Grossa Formation, the carbonaceous compressions were still used as a geothermometer to estimate maximum diagenetic temperatures. This estimation followed the automatic method proposed by Kaneki & Kouketsu (2022), which is based on the value of the full width at half maximum (FWHM) of the D1-function within the first-order region (1000 to 1750 cm<sup>-1</sup>) of the Raman spectrum in terrestrial carbonaceous materials. The temperature has an error of ±30°C and follows the equation:

$$T[^\circ\text{C}] = -2.30 \times (\text{FWHM}_{\text{D1}}) + 486$$

## Results

### *Devonian ophiuroids*

Both Devonian fossils studied exhibit carbonaceous compressions that are easily recognized macroscopically. They form dark films concentrated primarily in the disk region, which contrasts sharply with the whitish matrix of the shale and mudstone in which they are preserved (Figure 25D-E). On the dorsal surface of sample UFPR 0621 PI, the film appears black, extending across most of the interrays and outlining nearly all the concave edges of the pentagonal disk of *E. pontis* (Figure 25D). It also fills the large dorsal molds of the dissolved ossicles in the buccal framework, including the circumorals and mouth-angle plates, though it is absent in the large petaloid region of the mouth aperture (Figure 25D). Conversely, the film ranges from lighter shades of gray to brown on the ventral surface of sample UFPR 0587 PI (Figure 25E). It extends asymmetrically across the interrays of this specimen, with diffuse and convex distal margins suggesting a flexible disk stretched into a more elliptical shape (Figure 25E). In this case, even the mouth aperture is also notably infilled by the dark film, although its extension over the small ventral molds of the circumorals and mouth-angle plates is less evident (Figure 25E).

In the BSE images, the compressions display a serous to amorphous texture characteristic of kerogen (Figures 27A-B, J-K; 28A-B, D-E). Their dark gray tones indicate the prevalence of elements with low atomic number, in contrast to the lighter gray tones of the heavier substances in the matrix. Although framboidal clusters were not detected, micrometric grains rich in iron and sulfur suggest the sporadic occurrence of pyrite in specimen UFPR 0621 PI (Figure 28C). Some grains of similar size are also distributed across the dark film in specimen UFPR 0587 PI, but they are atypically enriched in yttrium and phosphorus, highlighting an association with trace amounts of xenotime (Figure 28F). Nonetheless, carbon

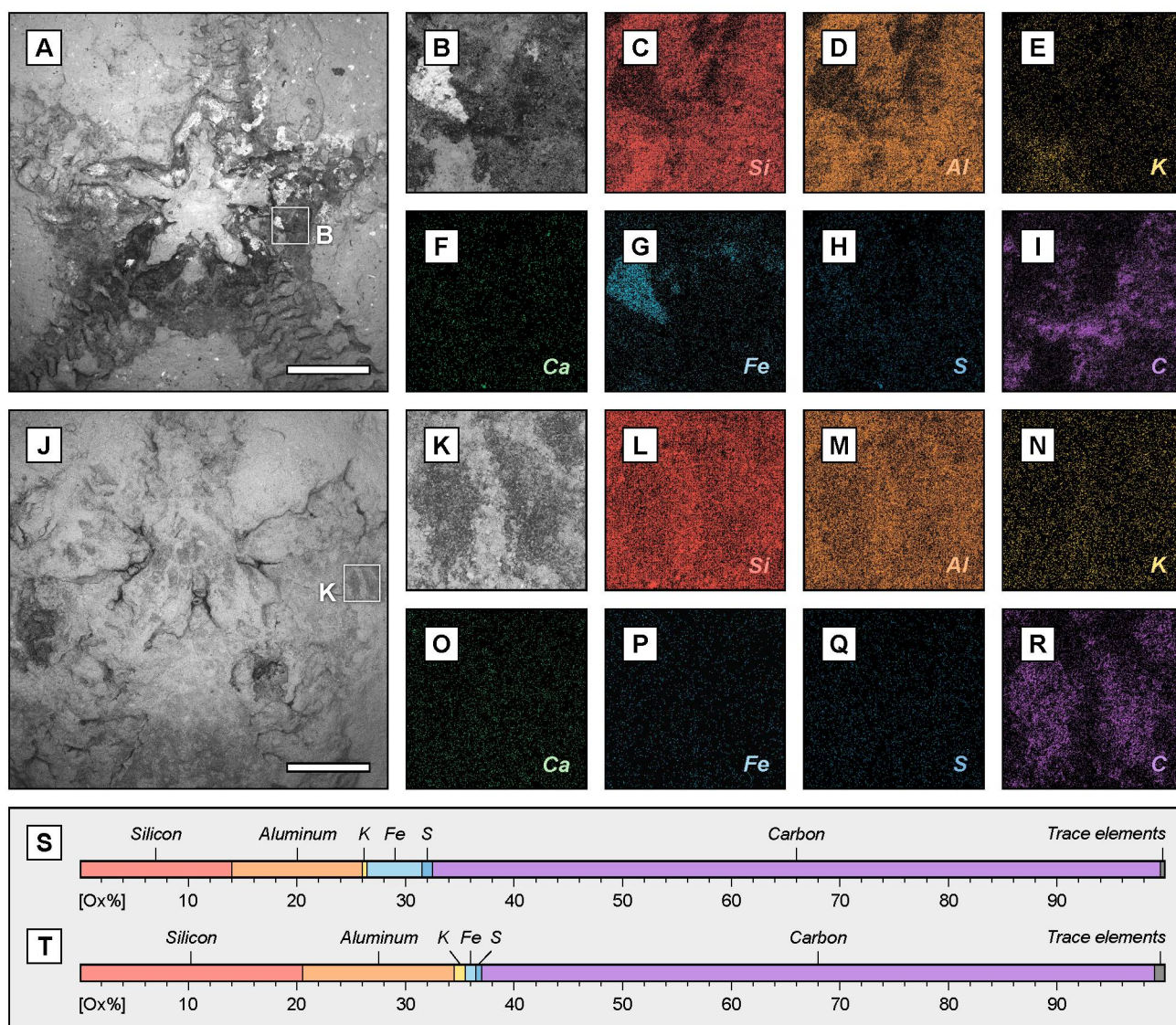


**Figure 27.** Chemical distributions in carbonaceous compressions of *Encrinaster pontis*. A, BSE image of the disk in specimen UFPR 0621 PI. B, BSE image of the region indicated in “A”. C-I, EDS maps of the region indicated in “B”. J, BSE image of the disk in specimen UFPR 0587 PI. K, BSE image of the region indicated in “J”. L-R, EDS maps of the region indicated in “K”. S, EDS map sum spectrum of “B”. T, EDS map sum spectrum of “K”. Scale bars represent 2 mm (A, J).

is the main element of the compressions (Figure 27I, R, S-T). Silica, aluminum, and potassium are more prominent in the sediment (Figure 27C-E, L-N), while sulfur is widespread without association with other elements (Figure 27H, Q). Although some dense accumulations of iron are present in specimen UFPR 0621 PI, they do not replicate biological structures (Figure 27G), pointing more to a product of weathering. In turn, calcium is only a trace element, consistent with the dissolved carbonate skeletons preserved in these siliciclastic beds (Figure 27F, O).

The Raman spectra of the dark films also show similar signatures in the first-order region of terrestrial carbonaceous materials. Two broad, non-deconvoluted bands were present: a dominant G-band centered at about  $1600\text{ cm}^{-1}$  and a subordinate D-band centered

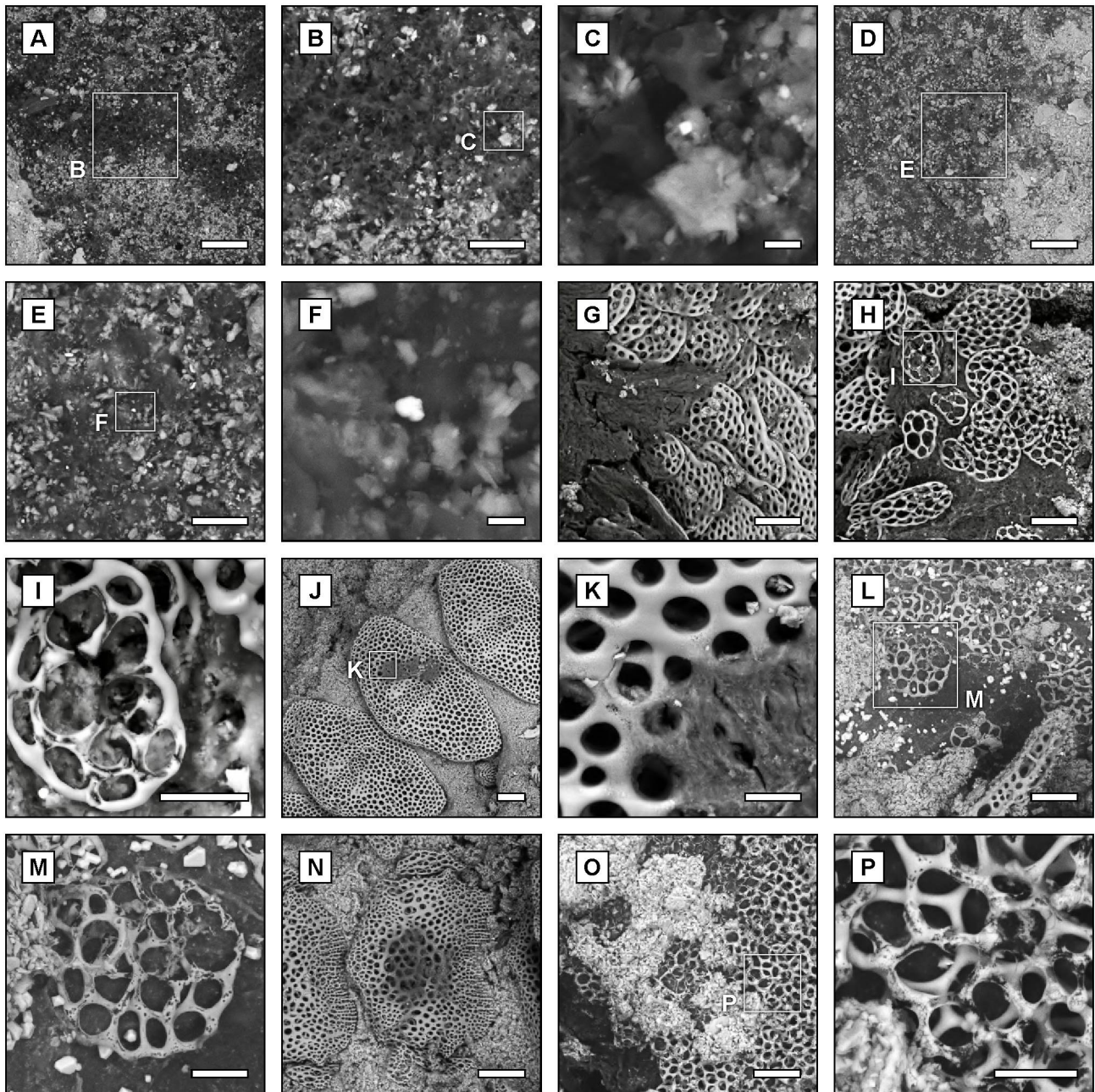


**Figure 28.** BSE images of soft and hard remains in natural and artificial fossil ophiuroids. A-B, Amorphous kerogenized remains preserved in the disk of specimen UFPR 0621 PI. C, Detail of the region indicated in "B" showing a potential pyrite grain enriched in sulfur (13.3 Ox%) and iron (8.3 Ox%). D-E, Amorphous kerogenized remains preserved in the disk of specimen UFPR 0587 PI. F, Detail of the region indicated in "E" showing a potential xenotime grain enriched in yttrium (8.8 Ox%) and phosphorus (7.0 Ox%). G, Viscera and disk scales after 60 days of experimental decay under organic-poor kaolinitic clay. H-I, Viscera and disk scales after 120 days of experimental decay under organic-poor kaolinitic clay. J-K, Organic remains attached to an arm ossicle after 120 days of experimental decay in organic-poor kaolinitic clay. L-M, Viscera and disk scales after 60 days of experimental decay under organic-rich kaolinitic clay. N, Organic remains attached to an arm ossicle after 60 days of experimental decay under organic-rich kaolinitic clay. O-P, Viscera and disk scales after 120 days of experimental decay under organic-rich kaolinitic clay. Scale bars represent 100  $\mu\text{m}$  (J, N), 50  $\mu\text{m}$  (A, D, G, H, L, O), 20  $\mu\text{m}$  (B, E, I, K, M, P), and 2  $\mu\text{m}$  (C, F).

at about  $1360\text{ cm}^{-1}$  (Figure 29A-B). The most notable difference was the decrease in the overall area of the spectrum and the increase in the saddle region between the G- and D-

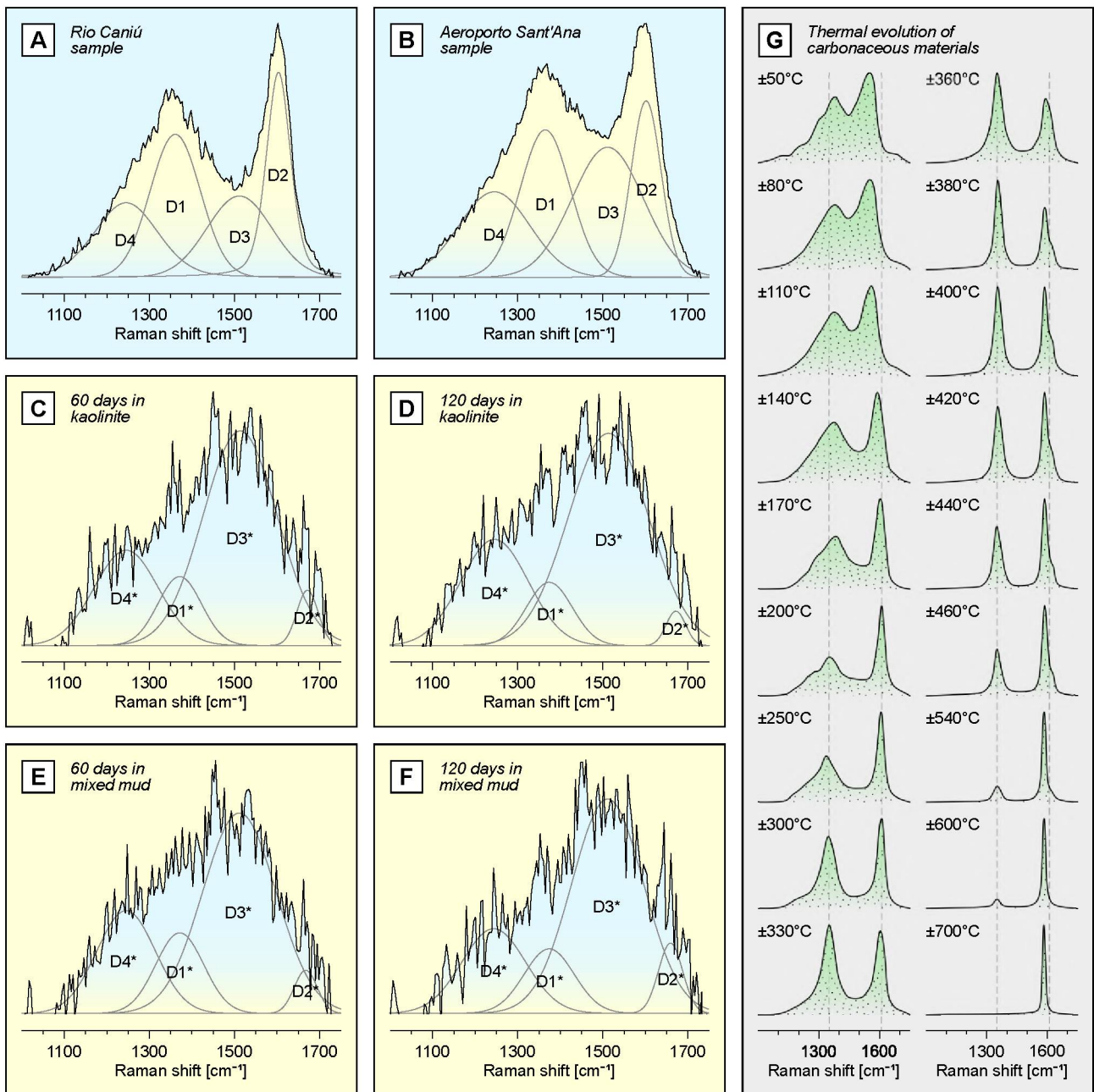


**Figure 29.** Signatures under Raman spectroscopy. Raman spectra of carbonaceous compressions preserved in the disk of specimens UFPR 0621 PI (A) and UFPR 0587 PI (B). Raman spectra of viscera remains in the ophiuroid disk after 60 days (C) and 120 days (D) under organic-poor kaolinitic clay, and after 60 days (E) and 120 days (F) under organic-rich kaolinitic clay, both artificially matured at up to 35°C. (G) Idealized evolution of the Raman spectrum of carbonaceous materials with increasing temperature (from about 50 to 700°C) (adapted from Buseck & Beysac 2014; Schito et al. 2017). Deconvolution method (A-F) based on automatic Fitting G proposed by Kaneki & Kouketsu (2022). In the case of immature experimental samples (D-G), deconvolution (D1\* to D4\* functions) was performed for comparative purposes only.

bands in the sample UFPR 0621 PI (Figure 29A). Despite this, both spectra correspond well to the pattern of amorphous kerogen, especially derived from temperatures below 200°C (Figure 29G). Following the Fitting G of Kaneki & Kouketsu (2022), the automatic deconvolution resulted in only four functions (D1 to D4) (Figure 29A), due to the difficulty of decomposing the G-band into G- and D2-functions in low-grade materials. The FWHM of the

D1-functions was very similar, ranging from  $138.11\text{ cm}^{-1}$  (UFPR 0621 PI) to  $137.59\text{ cm}^{-1}$  (UFPR 0587 PI). Based on this, the peak diagenetic temperature recorded by the carbonaceous compressions was calculated at  $168\pm 30^\circ\text{C}$  for the specimen from the Rio Caniú Site and at  $169\pm 30^\circ\text{C}$  for the specimen from the Aeroporto Sant'Ana Site.

#### *Experimental decay in organic-poor mud*

Under kaolinitic clay, the samples produced artificial fossils with well-preserved carbonaceous remains, regardless of the duration of diagenetic maturation (Figure 26B, D). After 60 days, the carbonate skeleton remained relatively intact (Figure 28G), though initial signs of dissolution became evident after 120 days, leading to partial destruction of the stereom microstructure in smaller ossicles (Figure 28H-I). This process also caused a notable increase in carbonates ( $\text{CO}_3^{2-}$ ) and bicarbonates ( $\text{HCO}_3^-$ ) dissolved in the water column during experiment 2 (Table S6). All disk viscera, in turn, degraded into a black, cracked, amorphous mass that formed a dense film over the mesh of small, imbricated disk scales (Figure 28G-I). These dark films were concentrated in the proximal region of the interrays, surrounding the larger ossicles of the buccal framework (Figure 30A, J). However, their distal edges were diffuse, failing to replicate the disk margins or the precise contour of the viscera. Abundant nanometric nodules were preserved on the dark films, resembling spherical-shaped microorganisms (Figure 28I). Although organic remains also persisted in some areas of the arms, they were very small and sparsely distributed within the cavities of larger ossicles (Figure 28J-K).

In the BSE images, the gray tones emphasize the predominance of lighter elements in the dark films, alongside heavier substances in the carbonate ossicles and the sedimentary matrix (Figure 30A, J). EDS maps indicate that carbon is the primary component of the dark films, but with a significant enrichment in sulfur (Figure 30H-I, Q-R, S-T). Meanwhile, silica, aluminum, and potassium are restricted to the sediment (Figure 30C-E, L-N), and calcium is limited to the carbonate parts of the skeleton (Figure 30F, O). Iron is also scarce and has no obvious association with the dark films (Figure 30G, P; Table S3), suggesting instead the occurrence of some accessory oxide minerals in the kaolinitic sediment, such as goethite or hematite. On the other hand, both Raman spectra of the carbonaceous remains preserved in the disk exhibited a single broad and noisy band, characteristic of highly amorphous carbon, in the first-order range between  $1000$  and  $1750\text{ cm}^{-1}$  (Figure 29C-D). Despite the immaturity of these samples, with a known thermal peak of only  $35^\circ\text{C}$ , deconvolution using the Fitting G method by Kaneki & Kouketsu (2022) indicated in the prevalence of broad D3- and D4-functions over smaller, subordinate D1- and D2-functions.

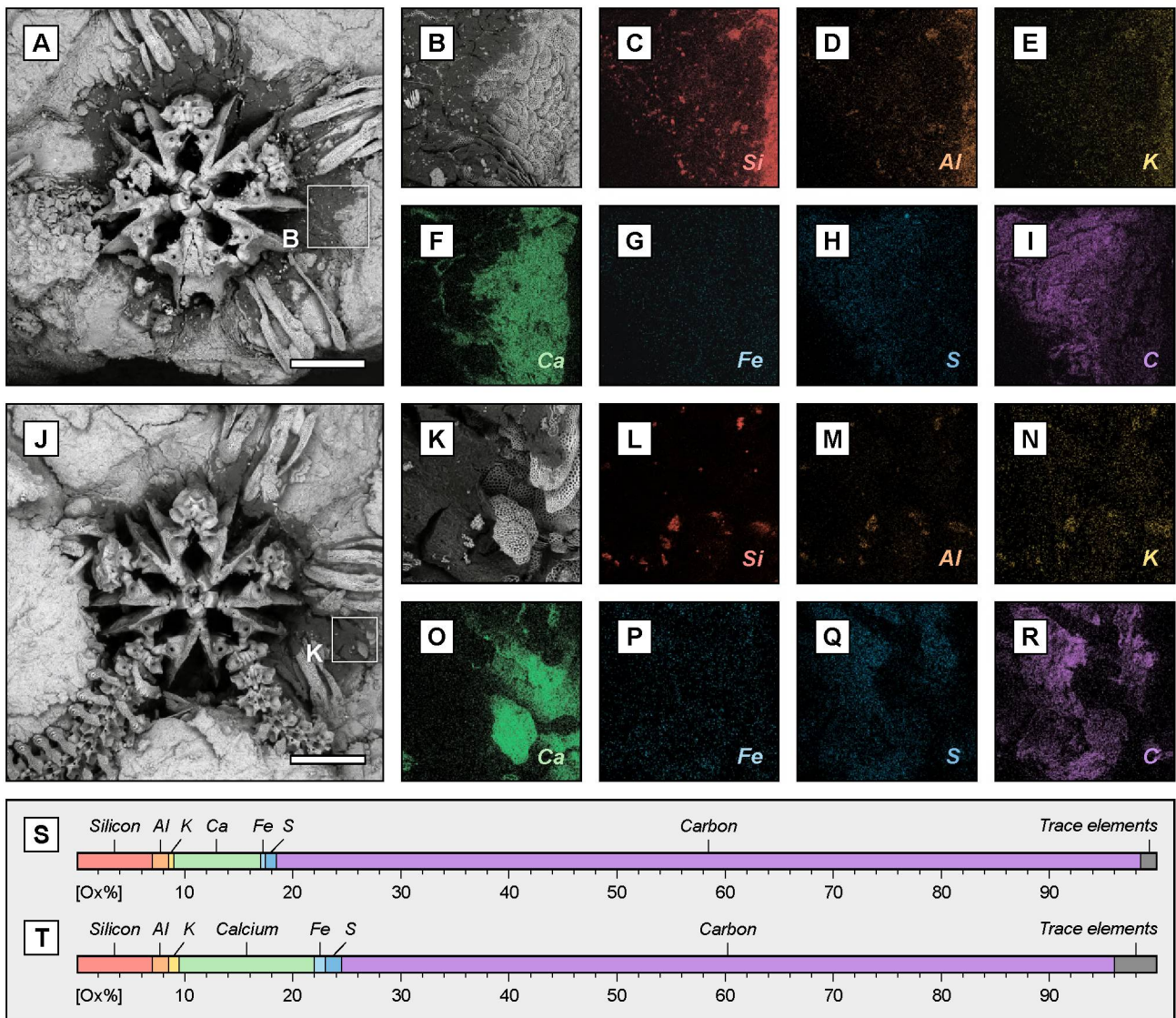


**Figure 30.** Chemical distributions of decayed carbonaceous remains under organic-poor kaolinitic clay. A, BSE image of the ophiuroid disk after 60 days. B, BSE image of the region indicated in “A”. C-I, EDS maps of the region indicated in “B”. J, BSE image of the ophiuroid disk after 120 days. K, BSE image of the region indicated in “J”. L-R, EDS maps of the region indicated in “K”. S, EDS map sum spectrum of “B”. T, EDS map sum spectrum of “K”. Scale bars represent 1 mm (A, J).

### *Experimental decay in organic-rich mud*

Under mixed clay richer in organic matter, both samples produced artificial fossils with only very discrete carbonaceous remains, almost imperceptible macroscopically (Figure 26C, E). Although most of the larger components of the carbonate skeleton remained well preserved, the stereom microstructure of the smaller ossicles was substantially dissolved under these conditions, especially after 120 days (Figure 28L-M, O-P). This coincided with the significant increase in the amount of  $\text{CO}_3^{2-}$  and  $\text{HCO}_3^-$  dissolved in the water column at the end of experiment 4 (Table S6). Meanwhile, all viscera were degraded to an amorphous mass, forming very thin dark films beneath the mesh of small disk scales imbricated with the sediment (Figures 28L-M, O-P; 31A-B, J-K). These dark films were concentrated mainly

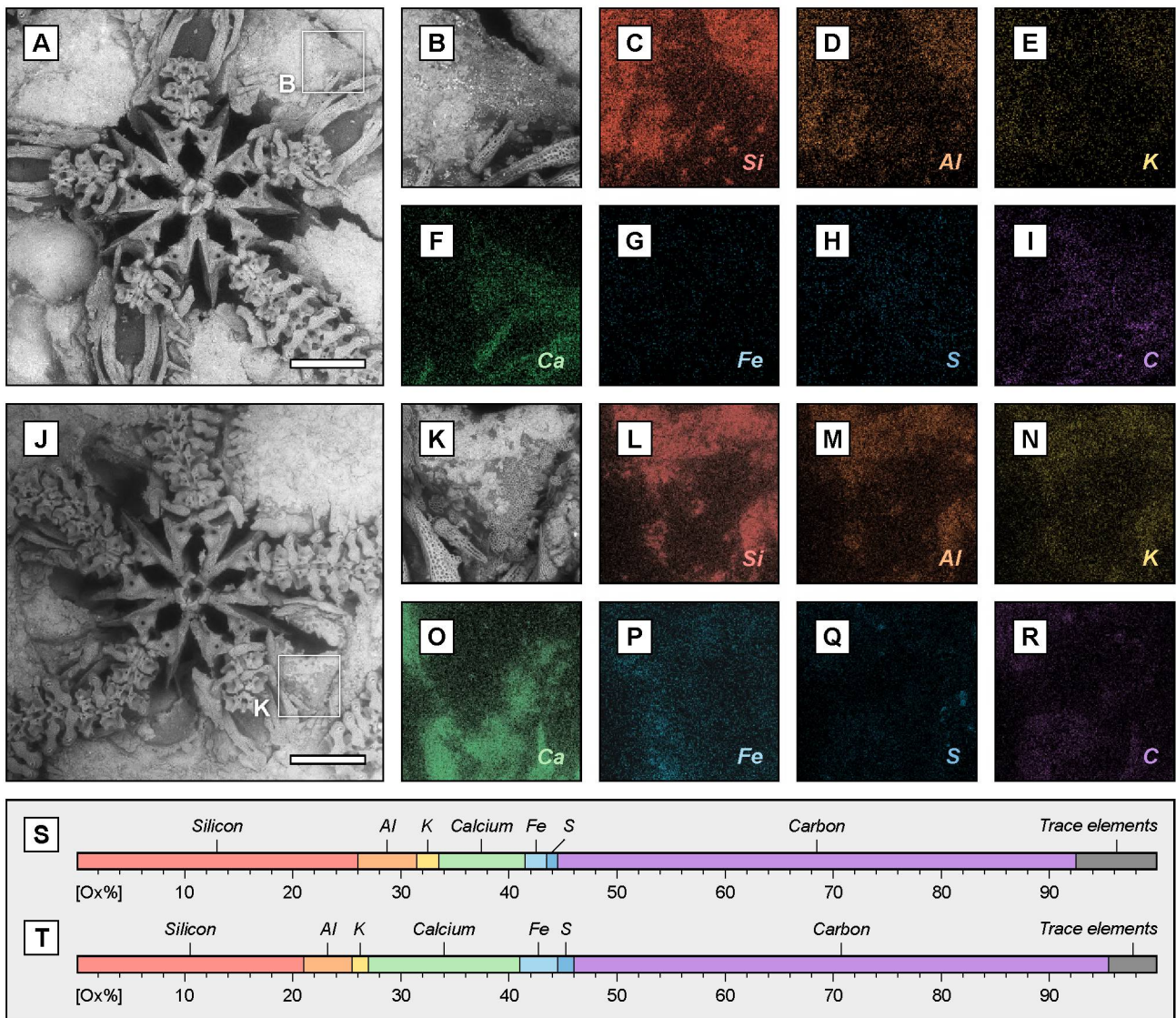


**Figure 31.** Chemical distributions of decayed carbonaceous remains under organic-rich kaolinitic clay. A, BSE image of the ophiuroid disk after 60 days. B, BSE image of the region indicated in “A”. C-I, EDS maps of the region indicated in “B”. J, BSE image of the ophiuroid disk after 120 days. K, BSE image of the region indicated in “J”. L-R, EDS maps of the region indicated in “K”. S, EDS map sum spectrum of “B”. T, EDS map sum spectrum of “K”. Scale bars represent 1 mm (A, J).

around large ossicles, such as the collapsed radial shields and the buccal framework elements (Figure 21A, J). However, the films were diffuse in the flatter region of the interrays, failing to replicate the distal limits of the disk (Figure 21A-B, J-K). Although very small, many oxidized organic remains were also preserved in the stereom pores of the arm segments, as reinforced by the orange coloration of these ossicles (Figures 26E; 28N).

Due to the higher organic load in the sediment, the carbonaceous remains preserved under these conditions show less contrast in the BSE images (Figure 31A-B, J-K). Only on the micrometric scale do dark gray tones better reveal the fine, amorphous, and relatively homogeneous surface of the remains rich in lighter substances (Figure 28L-M, O). Although less intense, carbon is the only significant element in these dark films (Figure 31I, R, S-T).

Silica, aluminum, and potassium are limited to the sediment (Figure 31C-E, L-N), while iron and sulfur are widespread or concentrated in small mono-element patches (Figure 31G-H, P-Q). The calcium signal is also more diffuse, which may reflect either acquisition noise or a greater degree of carbonate dissolution in the investigated regions (Figure 31F, O). Despite the differences in the sediment, the Raman spectra of these carbonaceous remains show a pattern very similar to the result obtained under organic-poor mud. A single broad and noisy band is present in the first-order range of terrestrial carbonaceous materials, indicating very immature carbon (Figure 29E-F). Even the attempt at deconvolution also highlights the presence of broad, dominant D3- and D4-functions over small, secondary D1- and D2-functions.

## Discussions

### *Implications for kerogenization in echinoderms*

In contrast to nonbiomineralized groups, echinoderms have a multi-element skeleton that can consist of hundreds of thousands of small ossicles of Mg-calcite (Lewis, 1980; Donovan, 1991; Brett et al., 1997; Ausich, 2021). This complex skeletal structure is the first barrier in the kerogenization process because it can help retain most of the soft tissues dispersed inside the coelomic cavities even after the burial of living specimens. While other soft-bodied organisms can be more easily compressed in the sediment, echinoderm carcasses have greater potential to resist during early diagenesis, restricting the compaction of the body and the polymerization of organic molecules. Unlike the residual accumulation of large polymers in some fossil groups, such as plants and arthropods, echinoderms also do not possess strongly sclerotized or cuticularized tissues that could promote the selective preservation of compounds more resistant to degradation. Nevertheless, our results highlight that kerogenization of soft parts can still occur in multi-element organisms when adequate conditions coexist. This may lead to the formation of carbonaceous compressions in echinoderms depending mainly on the body structure and burial environment.

First, the degree of skeletonization plays a critical role in kerogenization. Unlike the rigidly sutured body of many echinoderms, such as crinoids and echinoids, the ophiuroids analyzed here possess disks with only small ossicles loosely attached to the epidermis, as in the case of *E. pontis* and *A. januarii* (Fraga & Vega, 2020, 2022, 2025). This thinner covering is more susceptible to flattening caused by the overload of the burial column, favoring the collapse of the disk ossicles, the compression of the tissues, and the accumulation of degraded remains in dark amorphous films. However, an additional important factor is also the type of associated sediment. Our results show that kaolinitic clay can promote the preservation of larger and thicker carbonaceous films even after months of decay. This is con-

sistent with the antibacterial properties of kaolinite, which are mainly attributed to the toxicity of metal cations like  $Al^{+3}$  (Wilson & Butterfield, 2014; McMahon et al., 2016; Naimark et al., 2016; Corthésy et al., 2024). Meanwhile, mixed clays richer in organic matter are less favorable to preservation because they can carry a greater diversity of microbial communities, benefiting the recycling of compounds and further limiting the extent and thickness of carbonaceous remains.

However, even under suitable conditions, the kerogenization potential of echinoderms can vary among their different organic parts. On the one hand, small and labile tissues, such as muscles and tube feet, can be destroyed within hours to a few days by microbial decay, which rapidly restricts their carbon supply (Fraga & Vega, 2025). Preservation in such cases generally requires exceptional mineralization processes, as described for Paleozoic and Mesozoic fossils (Smith & Gallemí, 1991; Glass & Blake, 2004; Sutton et al., 2005; Glass, 2006; Clark et al., 2017; Saleh et al., 2023). Conversely, visceral organs of the digestive and reproductive systems may comprise most of the organic volume in echinoderms, serving as the major source of carbonaceous materials for long-term kerogenization. The gonads are particularly important in this process because they can be enriched in proteins and various reserve lipids, such as sterols, carotenoids, and long-chain fatty acids (Takagi, 1986; Pereira et al., 2014; Zhukova, 2023). But the stomach and the stomach contents themselves can also contribute to kerogenization, helping to form larger carbonaceous compressions that better preserve the region of the coelomic cavity, as in the Devonian encrinasterids evaluated (Figure 25D-E).

As these viscera decay, important chemical changes occur in the early diagenesis. The activity of heterotrophic bacteria helps to transform the organized biopolymers into heterogeneous geopolymers, which are direct precursors of kerogen (Vandenbroucke & Largeau, 2007; Bushnev & Burdel'naya, 2009). Most nitrogenous compounds are rapidly removed by hydrolysis reactions (Schnitzer, 1985). However, our experiments also revealed a significant enrichment of sulfur in the carbonaceous remains preserved in kaolinite. Similar patterns can be common after burial under a depth of a few tens of centimeters, when dissolved sulphate induces the inorganic incorporation of sulphur into hydrolyzed humic fractions (Vandenbroucke & Largeau, 2007). However, all of our experiments simulate shallow burial of only 10 cm, and the kaolinite used contained no detectable sulfur to serve as an inorganic source (Table S3). Even the dissolved sulfate in the experimental water was also well below the levels expected for seawater (Table S5). In this case, it is likely that the sulfur is a biogenic remnant from the tissues of the echinoderms themselves, benefiting from the inhibitory effect of kaolinite on sulphate-reducing bacteria (McMahon et al., 2016; Corthésy et al., 2024).

It is also well known that authigenic pyritization can contribute to the fossilization of organic remains during this stage. This process occurs mainly when reactive iron in the sediment reacts rapidly at low pH with dissolved H<sub>2</sub>S, driving sulfate reduction reactions that are favorable for pyrite formation (Fisher & Hudson, 1985; Canfield & Raiswell, 1999; Vandenbroucke & Largeau, 2007; Schiffbauer et al., 2014). But iron from biological tissues themselves, such as that present in ferritin, may also play a relevant role in the selective replication of some labile tissues (Saleh et al., 2020). Despite this, isolated pyrite microcrystals were noted here only in the carbonaceous compression of the fossil preserved in more iron-rich shale, with 5.2 wt% Fe<sub>2</sub>O<sub>3</sub> (Table S1). Meanwhile, all experimental samples, including those decayed in more ferruginous clays, did not form pyrite, nor did they show obvious association between iron and sulfur in the carbonaceous remains. A likely cause may have been the lower iron availability in these experimental sediments, below about 4.3 wt% of Fe<sub>2</sub>O<sub>3</sub> (Tables S3-S4). However, the scarcity of dissolved sulfate in the experimental water may again have limited some reactions, making pyritization unfeasible in these artificial fossils.

In addition, we have observed that the decay of echinoderm tissues can also indirectly accelerate the onset of the destruction of their own carbonate skeletons in the short term. This is due to the fact that many acidifying compounds can be produced by microbial activity during the degradation of carbonaceous remains, helping to decrease the pH of the micro-environment around buried carcasses (Fraga & Vega, 2025). Although CO<sub>2</sub> is the main acidifying agent, other sulfur and nitrogen compounds can also contribute to the process, such as ammonia (NH<sup>4+</sup>) and hydrogen sulfide (H<sub>2</sub>S), leading to a series of changes in carbonate geochemistry (Guinotte & Fabry, 2008; Gattuso & Hansson, 2011). As a result, the delicate stereom microstructure of small ossicles can begin to dissolve within weeks after death, particularly in mixed organic-rich sediments where microbial activity is intensified. These findings reinforce that carbonate dissolution rates can be significant even during early diagenesis and not only over longer timescales, as also supported by other studies (Walker et al. 2013; Fraga & Vega 2025). Similar cases may also have occurred in siliciclastic units where fossil echinoderms are preserved as negative molds, such as in the Ponta Grossa Lagerstätte (Fraga & Vega 2020, 2022), implying a molding process sufficiently rapid to match the rate of skeleton dissolution.

Although the experimental setup has its limitations, Raman spectra also reveal potential long-term changes in the crystal structure of carbonaceous compressions. Regardless of the clay type or decay period, all artificial fossils produced a single noisy band typical of immature kerogen. The D3-functions were dominant and likely resulted from out-of-plane vibrations caused by defects and heteroatoms (Beyssac et al., 2002; Henry et al., 2019), such as sulfur identified in some EDS maps (Figure 6H, Q). The D4-functions were also

a broad shoulder to the left of the main asymmetric bands, which may be related to the abundance of CH species in aliphatic hydrocarbon chains (Ferralis et al., 2016; Henry et al., 2019). However, larger G- and D-bands appeared as a low-grade kerogen pattern in the Devonian specimens (Kouketsu et al., 2014). Their D1- and D2-functions were more intense, suggesting an increase in the disordered vibration of the graphitic lattice even with the greater thermal maturation of these fossils (Allwood et al., 2006; Henry et al., 2019). Meanwhile, the amplitude of their D3-functions decreased probably with the loss of heteroatoms, as indicated by the purer, carbon-rich films, with no other notably associated elements (Figure 27I, R).

#### *Implications for anatomy in encrinasterids*

Although chemically altered by the kerogenization, carbonaceous compressions may offer valuable insights into the original anatomy of viscera in extinct echinoderms. Unlike most extant ophiuroids, many Paleozoic groups within the order Oegophiurida possessed wider, shorter petaloid arms with deep grooves in the ambulacral ossicles, such as the Devonian encrinasterids studied here. These features were historically used to infer the potential extension of gonads and digestive caeca into the arms, rather than being restricted to the disk (Fell, 1960; Spencer & Wright, 1966). This arrangement would then more closely resemble the visceral distribution seen in asteroides than in modern ophiuroids. Despite this, all carbonaceous compressions known so far for *E. pontis* are limited to the disk region, contradicting this idea. They typically range from relaxed pentagonal disk (Figure 25D) to more deformed disks resulting from escape postures during abrupt burial (Figure 25E) (Fraga & Vega, 2022). In all cases, the compressions do not extend noticeably into the arms, not even in their proximal parts, suggesting that the viscera - and most of the organic material that underwent kerogenization - were confined within the perivisceral coelom of the disk.

#### *Implications for thermal evolution in the Ponta Grossa Formation*

From amorphous carbon to crystalline graphite, another very important point of carbonaceous materials is their excellent potential as geothermometers. This is because the Raman spectrum of these materials exhibits a systematic thermal evolution of geochemical and crystallographic attributes during diagenesis and metamorphism, recording the peak temperature even after the retrograde phase of the associated rocks (Beysac et al., 2002; Kouketsu et al., 2014; Henry et al., 2019). Therefore, based on the automated protocol of Kaneki & Kouketsu (2022), both carbonaceous compressions preserved in the Devonian samples recorded very similar maximum temperatures, around  $170\pm 30^\circ\text{C}$ . This value is an important reference to the diagenetic history of the Ponta Grossa Formation, given its high

potential for gaseous hydrocarbon generation (Milani et al. 1990; Milani et al. 2007). However, considering a geothermal gradient of 25°C/km (Kolawole & Evenick 2023) and a maximum depth of 5 km for the formation (Milani et al. 1990), this paleotemperature exceeds the heating expected from burial alone. Additional heating could then have been associated with Serra Geral igneous event, which affected the region during the Early Cretaceous. Similar evidence has also been identified by clay minerals and fluid inclusions in other Paleozoic units of the Paraná Basin, such as the Furnas, Rio Bonito, Serra Alta, Teresina, and San Miguel formations (De Ros et al. 2000; Sant'Anna et al. 2006; Nomura et al. 2014; Teixeira et al. 2018).

## **Conclusions**

Although rare in multi-element organisms, carbonaceous compressions can also be formed in some fossil echinoderms if suitable conditions coexist. The preservation potential of organic remains is mainly linked to the skeletal structure and the type of burial sediment. On the one hand, we note that less protected viscera are more prone to compression and kerogenization than other labile tissues or organs housed in more robust calcareous modules. On the other hand, we emphasize that the antibacterial properties of kaolinitic clays are more favorable to kerogenization than other mixed sediments richer in organic matter, leading to the formation of thicker and more defined carbonaceous compressions. Despite the chemical and structural changes during decay, we exemplify how carbonaceous remains can also be useful guides to assess the anatomy of some extinct ophiuroids and the maximum paleotemperatures of associated rocks during diagenesis/metamorphism. These results help expand the understanding of kerogenization mechanisms and encourage the search for new carbon-rich films in echinoderms and other less explored groups, beyond just plants and soft-bodied organisms.

## **Acknowledgements**

We would like to thank the Coordenação de Aperfeiçoamento de Pessoal de Nível Superior (CAPES) and the Programa de Apoio à Pós-Graduação (PROAP) for funding the research. We are also grateful to the Centro de Microscopia Eletrônica (CME-UFPR), the Laboratório de Paleontologia (LABPALEO-UFPR), the Laboratório de Pesquisas Hidrogeológicas (LPH-UFPR), and the Instituto Laboratório de Análise de Minerais e Rochas (iLAMIR-UFPR) for providing equipment and laboratory analyses. Special thanks to Dhiego Silva, Lucas Szekut, Carolina Freire, Michela Borges, Gabriel Martins, Caro Valenzuela, Nicole Stakowian, and Adelita Rodrigues for their assistance during some of the research activities.

Finally, we would like to thank the editorial staff and Jih-Pai Lin and Przemysław Gorzelak for their constructive reviews.

### **Author Contributions**

**Conceptualization** Malton Carvalho Fraga (MCF); **Data Curation** MCF; **Formal Analysis** MCF; **Funding Acquisition** MCF; **Investigation** MCF; **Methodology** MCF, Cristina Silveira Vega (CSV); **Project Administration** MCF; **Resources** MCF; **Supervision** CSV; **Validation** MCF, CSV; **Visualization** MCF; **Writing - Original Draft Preparation** MCF; **Writing - Review & Editing** MCF, CSV.

### **Supplementary data**

<https://doi.org/10.1007/s00531-025-02490-6>

#### 4. CONSIDERAÇÕES FINAIS

[1] A espessura mínima para o soterramento definitivo de equinodermos de vida livre, como os ofiuroides, é de 10 cm na maior parte dos casos, independentemente do tipo de sedimento ou fluido intersticial. O soterramento sob camadas mais finas normalmente exige condições deposicionais específicas para evitar o escape de espécimes vivos.

[2] A deposição rápida de sedimentos não produz rapidamente anoxia sob a camada de soterramento. Por isso, é improvável que a morte por asfixia seja suficiente para impedir o escape durante as horas iniciais do soterramento, sobretudo para organismos com baixas taxas metabólicas, como os equinodermos.

[3] O tipo de sedimento de soterramento pode influenciar na qualidade dos esqueletos preservados. A deposição de camadas arenosas promove taxas maiores de autotomia entre os espécimes escapistas, enquanto a deposição de leitos argilosos favorece a preservação de esqueletos multi-elementais intactos.

[4] A deposição de lama não produz por si só um efeito anestésico em equinodermos. Grupos de vida livre podem iniciar rapidamente a escavação sob leitos argilosos ricos em água salgada intersticial. A maior limitação aparece apenas a longo prazo, quando o esforço dos espécimes soterrados é incapaz de refluidizar lamas tixotrópicas consolidadas.

[5] A deposição de sedimentos ricos em água doce intersticial promove um entorpecimento em massa de equinodermos. Devido à mudança brusca na salinidade do ambiente, isso pode resultar em espécimes paralisados por várias horas mesmo abaixo de leitos mais finos de soterramento, como apenas 5 cm de espessura.

[6] Turbiditos extrabacinais são armadilhas eficientes para o soterramento de espécimes vivos de organismos estenoalinos em bacias marinhas. Ao contrário dos turbiditos intrabacinais, eles carregam grandes volumes de água doce intersticial que anestesia assembleias bentônicas e favorece a fossilização sob leitos deposicionais mais finos.

[7] A degradação de pequenas carcaças multi-elementais expostas no fundo marinho pode ser acelerada por sete agentes principais, que incluem micronecrófagos, macronecrófagos, energia da água, atividade microbial, produção de bolhas, crescimento de algas e acidificação da coluna d'água.

[8] Apesar do tamanho diminuto (ca. <2 mm), micronecrófagos podem acelerar o colapso de pequenas carcaças articuladas dentro de poucos dias. Eles são agentes eficientes de degradação que podem prosperar mesmo sob condições euxínicas, colonizando regiões mais extremas que quaisquer outros grupos de metazoários.

[9] Macronecrófagos são os agentes mais eficientes para a degradação de esqueletos multi-elementais. Entre moluscos, anelídeos, artrópodes e equinodermos, diferentes grupos

podem localizar rapidamente restos orgânicos e impulsionar a desarticulação de pequenas carcaças dentro de apenas algumas horas após a morte.

[10] Correntes de apenas 5 cm/s podem ser eficientes para remobilizar e desarticular pequenos segmentos esqueléticos mais instáveis, como braços de ofiuroides orientados contra o fluxo de água. Nessas condições, mesmo ossículos porosos maiores de equinodermos podem ser mais facilmente transportados que grãos de areia densos.

[11] O crescimento rápido de capas bacterianas no disco de carcaças de asterozoários pode proteger temporariamente a estrutura bucal da desarticulação. Porém, a longo prazo, tanto a atividade microbiana aeróbica como anaeróbica são hábeis em destruir tecidos orgânicos, desarticulando indiretamente ossículos instáveis pela ação da gravidade.

[12] A produção de gases nas camadas internas do sedimento pode converter o fundo marinho em um campo minado para pequenos esqueletos multi-elementais. Bolhas de N<sub>2</sub>, H<sub>2</sub>S e CH<sub>4</sub> podem escapar abruptamente, deformando o substrato, colidindo abaixo de carcaças e levando ao colapso imediato de segmentos esqueléticos.

[13] O crescimento rápido de capas de algas filamentosas sobre o disco de carcaças de asterozoários pode reter bolhas e inflar a região proximal do esqueleto na coluna d'água, enquanto os segmentos distais de braço permanecem ancorados no sedimento. Tal postura desestabiliza a carcaça e acelera o colapso dos ossículos.

[14] Em fundos marinhos hipóxicos e anóxicos, o aumento nos níveis de CO<sub>2</sub> e outros compostos sulfurosos e nitrogenados reduz o pH e modifica a química dos carbonatos. Tal acidificação dissolve a estrutura de calcita magnésiana dos equinodermos, destruindo completamente suas partes duras em poucas semanas.

[15] Embora o soterramento rápido de espécimes vivos seja um processo importante para a fossilização de equinodermos, algumas circunstâncias excepcionais podem retardar os principais agentes de destruição, contribuindo para a preservação de carcaças multi-elementais mesmo após um período significativo de exposição no fundo marinho.

[16] Oscilações de salinidade podem eliminar micronecrófagos e retardar a atividade microbiana principalmente devido ao desequilíbrio osmótico. Esse efeito pode ser alcançado tanto por influxos mesohalinos (ca. 15 ppt) e hipersalinos (ca. 45 ppt) em ambientes marinhos dominados por organismos estenohalinos.

[17] Mudanças prolongadas na temperatura também podem limitar os principais agentes biológicos de degradação de carcaças. Tanto condições muito frias (ca. 5°C) como muito quentes (ca. 35°) podem reduzir similarmente a atividade de necrófagos e microrganismos, favorecendo a articulação e preservação dos tecidos moles a longo prazo.

[18] Fundos marinhos estagnados podem proteger carcaças de organismos multi-elementais da perturbação causada por ondas e correntes de fundo. Ao mesmo tempo, a es-

tratificação da coluna d'água pode limitar a distribuição de micronecrófagos, diminuindo as taxas de desarticulação das carcaças nas semanas iniciais de degradação.

[19] Fundos marinhos turvos ou mais profundos também podem restringir a distribuição de comunidades fotossintéticas. Essas condições podem proteger as carcaças delicadas de equinodermos asterozoários da desestabilização provocada pelo crescimento rápido e excessivo de algas filamentosas.

[20] Fundos marinhos oxigenados, pobres em matéria orgânica ou sem zonas fotossintéticas complexas podem restringir a produção intensa de compostos gasosos. Isso pode ajudar a estabilizar o substrato, prevenindo a desarticulação causada pelo impacto de bolhas sob pequenas carcaças multi-elementais expostas na interface água-sedimento.

[21] Fundos marinhos anóxicos e hipóxicos limitam o ciclo completo (oxidação/redução) de degradação dos compostos orgânicos. Somente sob reações de redução, os tecidos moles podem ser degradados para massas amorfas escuras, mas com maior potencial para permanecer no fundo marinho que sob condições normóxicas.

[22] Por outro lado, fundos marinhos oxigenados ajudam a estabilizar o pH da coluna d'água dentro do campo alcalino. Como resultado, as taxas de dissolução carbonática são reduzidas, auxiliando na preservação a longo prazo dos pequenos elementos calcíticos presentes nas carcaças dos equinodermos.

[23] Embora seja um processo raro, a querogenização de tecidos moles também pode beneficiar a formação de compressões carbonáceas em equinodermos durante a diagênese. O tipo de estrutura esquelética e o tipo de sedimento de soterramento são os principais fatores limitantes nesse processo.

[24] Vísceras menos protegidas, como o estômago e as gônadas alojadas sob a fina cobertura do disco dos ofiuroides, são mais propensas ao achatamento causado pela coluna de soterramento. Isso favorece o colapso dos ossículos, a compressão dos tecidos e a polimerização das moléculas orgânicas.

[25] Por sua vez, tecidos mais instáveis, como músculos e pés ambulacrais, são rapidamente degradados, limitando o fornecimento de carbono a longo prazo. Da mesma forma, órgãos alojados em módulos robustos, como em pelmatozoários, podem ficar protegidos durante a diagênese, restringindo a compactação e polimerização.

[26] Devido à toxicidade de cátions metálicos, argilas cauliníticas promovem a preservação de filmes carbonáceos maiores e mais espessos a longo prazo. Enquanto isso, argilas mistas ricas em matéria orgânica carregam comunidades microbiais diversas, o que favorece a reciclagem de nutrientes e reduz a preservação de restos orgânicos.

[27] A redução microbiana ainda pode acelerar indiretamente a destruição do esqueleto de equinodermos soterrados. Sinais de dissolução carbonática podem aparecer em peque-

nos ossículos durante as semanas iniciais de diagênese, especialmente em sedimentos microbiologicamente complexos, com níveis maiores de compostos acidificantes.

[28] Durante a diagênese inicial, os restos carbonáceos de ofiuroides podem mostrar assinaturas típicas de querogênio imaturo enriquecido em heteroátomos, como enxofre. Tal padrão contrasta com os restos carbonáceos mais puros de ofiuroides devonianos da Formação Ponta Grossa, com querogênio de baixo grau maturado em até ca. 170°C.

## REFERÊNCIAS

- ALLISON, P.A. 1986. Soft-bodied animals in the fossil record: The role of decay in fragmentation during transport. *Geology*, **14**, 979-981.
- ALLISON, P.A. 1988a. Konservat-Lagerstätten: cause and classification. *Paleobiology*, **14**, 331-344.
- ALLISON, P.A. 1988b. The role of anoxia in the decay and mineralization of proteinaceous macro-fossils. *Paleobiology*, **14**, 139-154.
- ALLISON, P.A. 1990. Variation in rates of decay and disarticulation of Echinodermata: implications for the application of actualistic data. *Palaios*, **5**, 432-440.
- ALLWOOD, A.C., WALTER, M.R. e MARSHALL, C.P. 2006. Raman spectroscopy reveals thermal palaeoenvironments of c.3.5 billion-year-old organic matter. *Vibrational Spectroscopy*, **41**, 190-197.
- ANDERSSON, A.J., MACKENZIE, F.T. e GATTUSO, J.-P. 2011. Effects of ocean acidification on benthic processes, organisms, and ecosystems. 122-153. Em GATTUSO, J.-P. e HANSSON, L. (eds). *Ocean Acidification*. Oxford University Press, 326 pp.
- AUSICH, W.I. 2021. Disarticulation and preservation of fossil echinoderms: recognition of ecological-time information in the echinoderm fossil record. *Elements of Paleontology*, 1-52.
- AUSICH, W.I., BARTELS, C., KAMMER, T.W. 2013. Tube foot preservation in the Devonian crinoid *Codiocrinus* from the Lower Devonian Hunsrück Slate, Germany. *Lethaia*, **46**, 416-420.
- BARNES, R.D. 1987. Invertebrate Zoology. Saunders College Publishing, 893 pp.
- BEHRENSMEYER, A.K., KIDWELL, S.M. e GASTALDO, R.A. 2000. Taphonomy and paleobiology. *Paleobiology*, **26**, 103-147.
- BEYSSAC, O., GOFFÉ, B., CHOPIN, C. e ROUZAUD, J.N. 2002. Raman spectra of carbonaceous material in metasediments: a new geothermometer. *Journal of Metamorphic Geology*, **20**, 859-871.
- BEZERRA, F.I., AGRESSOT, E.V.H., SOLORZANO-KRAEMER, M.M., FREIRE, P.T.C., PASCHOAL, A.R., SILVA, J.H. e MENDES, M. 2021. Taphonomic analysis of the paleontomofauna assemblage from the Cenozoic of the Fonseca basin, southeastern Brazil. *Palaios*, **36**, 182-192.
- BORGES, M. e AMARAL, A.C.Z. 2005. Classe Ophiuroidea. 237-272. Em AMARAL, A.C.Z., RIZZO, A.E. e ARRUDA, E.P. (eds). Manual de identificação dos invertebrados marinhos da região sudeste sul do Brasil. EdUSP, 288 pp.
- BRANDT, D.S. 1989. Taphonomic grades as a classification for fossiliferous assemblages and implications for paleoecology. *Palaios*, **4**, 303-309.

- BRETT, C.E. e BAIRD, G. 1986. Comparative taphonomy: a key to paleoenvironmental interpretation based on fossil preservation. *Palaios*, **1**, 207-227.
- BRETT, C.E. e BAIRD, G. 1993. Taphonomic approaches to temporal resolution in stratigraphy: Examples from Paleozoic marine mudrocks. *The Paleontological Society Papers*, **1**, 251-274.
- BRETT, C.E., MOFFAT, H.A. e TAYLOR, W.L. 1997. Echinoderm taphonomy, taphofacies, and Lagerstätten. *The Paleontological Society Papers*, **3**, 147-190.
- BRIGGS, D.E.G. e KEAR, A.J. 1993. Decay and preservation of polychaetes: taphonomic thresholds in soft-bodied organisms. *Paleobiology*, **19**, 107-135.
- BRIGGS, D.E.G. e KEAR, A.J. 1994. Decay and mineralization of shrimps. *Palaios*, **9**, 431-456.
- BRIGGS, D.E.G., SIVETER D.J., SIVETER D.J., SUTTON M.D. e RAHMAN I.A. 2017. An edrioasteroid from the Silurian Herefordshire Lagerstätte of England reveals the nature of the water vascular system in an extinct echinoderm. *Proceedings of the Royal Society B*, **284**, 20171189.
- BRITTON, J.C. e MORTON, B. 1994. Marine carrion and scavengers. 369-434. Em ANSELL, A.D., GIBSON, R.N. e BARNES, M. (eds). *Oceanography and Marine Biology: An Annual Review*, 32. Aberdeen University Press/Allen & Unwin, 617 pp.
- BROCE, J.S. e SCHIFFBAUER, J.D. 2017. Taphonomic analysis of Cambrian vermiform fossils of Utah and Nevada, and implications for the chemistry of Burgess shale-type preservation. *Palaios*, **32**, 600-619.
- BROOM, D.M. 1975. Aggregation behaviour of the brittle-star *Ophiothrix fragilis*. *Journal of the Marine Biological Association of the United Kingdom*, **55**, 191-197.
- BUENO, M.L., ALITTO, R.A.S., GUILHERME, P.D.B., DOMENICO, M.D. e BORGERS, M. 2018. Guia ilustrado dos Echinodermata da porção sul do Embaiamento Sul Brasileiro. *Pesquisa e Ensino em Ciências Exatas e da Natureza*, **2**, 169-237.
- BUSECK, P.R. e BEYSSAC, O. 2014. From Organic Matter to Graphite: Graphitization. *Elements*, **10**, 421-426.
- BUSHNEV, D.A. e BURDEL'NAYA, N.S. 2009. Kerogen: chemical structure and formation conditions. *Russian Geology and Geophysics*, **50**, 638-643.
- CAI, Y., SCHIFFBAUER, J.D., HUA, H. e XIAO, S. 2012. Preservational modes in the Ediacaran Gaojiashan Lagerstätte: Pyritization, aluminosilicification, and carbonaceous compression. *Palaeogeography, Palaeoclimatology, Palaeoecology*, **326-328**, 109-117.

- CANFIELD, D.E. e RAISWELL, R. 1991. Pyrite formation and fossil preservation. 337-387. Em ALLISON, P.A. e BRIGGS, D.E.G. (eds). *Taphonomy: Releasing the Data Locked in the Fossil Record*. Plenum Press, 546 pp.
- CHAVE, K.E. 1964. Skeletal durability and preservation. 377-387. em IMBRIE, J. e NEWELL, N.D. (eds). *Approaches to Paleoecology*. John Wiley and Sons, 432 pp.
- CLARK, E.G., BHULLAR, B.-A.S., DARROCH, S.A.F. e BRIGGS, D.E.G. 2017. Water vascular system architecture in an Ordovician ophiuroid. *Biology Letters*, **13**, 20170635.
- CLEMENTS, T., COLLEARY, C., DE BAETS, K. e VINTHER, J. 2017. Buoyancy mechanisms limit preservation of coleoid cephalopod soft tissues in Mesozoic Lagerstätten. *Palaeontology*, **60**, 1-14.
- CORTHÉSY, N., SALEH, F., THOMAS, C., ANTCLIFFE, J.B. e DALEY, A.C. 2024. The effects of clays on bacterial community composition during arthropod decay. *Swiss Journal of Palaeontology*, **143**, 26.
- CÚNEO, N.R., TAYLOR, E.L., TAYLOR, T.N. e KRINGS, M. 2003. In situ fossil forest from the upper Fremouw Formation (Triassic) of Antarctica: paleoenvironmental setting and paleoclimate analysis. *Palaeogeography, Palaeoclimatology, Palaeoecology*, **197**, 239-261.
- DEMYSHEV, S.G., DYMOVA, O.A., MARKOVA, N.V. e PIOTUKH, V.B. 2016. Numerical Experiments on Modeling of the Black Sea Deep Currents. *Physical Oceanography*, **2**, 34-45.
- DE ROS, L.F., MORAD, S., BROMAN, C. e CESERO, P. 2000. Influence of uplift and magmatism on distribution of quartz and illite cementation: evidence from Siluro-Devonian sandstones of the Parana Basin, Brazil. 231-252. Em WORDEN, R. e MORAD, S. (eds). *Quartz Cementation in Sandstones*. International Association of Sedimentologists, Special Publication 29, 352 pp.
- DIAZ, R.J. e ROSENBERG, R. 1995. Marine benthic hypoxia: a review of its ecological effects and the behavioural responses of benthic macrofauna. 245-303. Em ANSELL, A.D., GIBSON, R.N. e BARNES, M. (eds). *Oceanography and Marine Biology: An Annual Review*, 33. UCL Press, 665 pp.
- DICKSON, J.A.D. 2001. Diagenesis and crystal caskets: Echinoderm Mg calcite transformation, Dry Canyon, New Mexico, U.S.A. *Journal of Sedimentary Research*, **71**, 764-777.
- DONOVAN, S.K. 1991. The taphonomy of echinoderms: calcareous multi-element skeletons in the marine environment. 241-269. Em DONOVAN, S.K. (ed). *The Processes of Fossilization*. Belhaven Press, 303 pp.

- DUNLOP, K., RENAUD, P.E., BERGE, J., JONES, D.O.B., HARBOUR, R.P., TANDBERG, A.H.S. e SWEETMAN, A.K., 2021. Benthic scavenger community composition and carrion removal in Arctic and Subarctic fjords. *Polar Biology*, **44**, 31-43.
- DURAND, B. 1980. Sedimentary organic matter and kerogen. Definition and quantitative importance of kerogen. 13-34. Em DURAND, B. (ed). *Kerogen, Insoluble Organic Matter from Sedimentary Rocks*. Éditions Technip, 545 pp.
- EKAU, W., AUDEL, H., PÖRTNER, H.-O., e GILBERT, D. 2010. Impacts of hypoxia on the structure and processes in pelagic communities (zooplankton, macro-invertebrates and fish). *Biogeosciences*, **7**, 1669-1699.
- FELL, H.B. 1960. Synoptic Keys to the Genera of Ophiuroidea. *Zoology Publications*, **26**, 44 pp.
- FENCHEL, T. e FINLAY, B.J., 1991. The biology of free-living anaerobic ciliates. *European Journal of Protistology*, **26**, 201-215.
- FERGUSON, J.C. 1992. The function of the madreporite in body fluid volume maintenance by an intertidal starfish, *Pisaster ochraceus*. *The Biological Bulletin*, **183**, 482-489.
- FERGUSON, J.C. 1995. The structure and mode of function of the water vascular system of a brittlestar, *Ophioderma appressum*. *The Biological Bulletin*, **188**, 98-110.
- FERRALIS, N., MATYS, M.D., KNOLL, A.H., HALLMANN, C. e SUMMONS, R.E. 2016. Rapid, direct and non-destructive assessment of fossil organic matter via microRaman spectroscopy. *Carbon*, **108**, 440e449.
- FISHER, I.S.J. e HUDSON, J.D. 1985. Pyrite geochemistry and fossil preservation in shales. *Philosophical Transactions of the Royal Society B*, **311**, 167-169.
- FLESSA, K.W. e BROWN, T.J. 1983. Selective solution of macroinvertebrate calcareous hard parts: a laboratory study. *Lethaia*, **16**, 193-205.
- FRAGA, M.C., MENDES, F.A., GUIMARÃES, R.A. e BARROS, C.E.M. 2023. Biogenic signatures in the Cryogenian Brusque Metamorphic Complex, Brazil: Geochronological and paleoclimatological implications. *Journal of South American Earth Sciences*, **131**, 104601.
- FRAGA, M.C. e VEGA, C.S. 2020. Asterozoans from the Devonian of the Paraná Basin, South Brazil. *Journal of South American Earth Sciences*, **97**, 102398.
- FRAGA, M.C. e VEGA, C.S. 2022. Preservation models of ophiuroids in epicontinental basins: Examples from a new Devonian echinoderm Lagerstätte from Brazil. *Journal of South American Earth Sciences*, **120**, 104060.
- FRAGA, M.C. e VEGA, C.S. 2024. How does rapid burial work? New insights from experiments with echinoderms. *Palaeontology*, **67**, e12698.

- FRAGA, M.C. e VEGA, C.S. 2025. Decay and preservation in marine basins: a guide to small multi-element skeletons. *International Biodeterioration & Biodegradation*, **196**, 105904.
- GATTUSO, J.-P. e HANSSON, L. 2011. Ocean acidification: background and history. 1-20. Em GATTUSO, J.-P. e HANSSON, L. (eds). *Ocean Acidification*. Oxford University Press, 326 pp.
- GEHLING, J.G. e DROSER, M.L. 2018. Ediacaran scavenging as a prelude to predation. *Emerging Topics in Life Sciences*, **2**, 213-222.
- GIBSON, B.M., SCHIFFBAUER, J.D. e DARROCH, S.A.F. 2018. Ediacaran-style decay experiments using mollusks and sea anemones. *Palaios*, **33**, 185-203.
- GLASS, A. 2006. Pyritized tube feet in a protasterid ophiuroid from the Upper Ordovician of Kentucky, U.S.A. *Palaeontologica Polonica*, **51**, 171-184.
- GLASS, A. e BLAKE, D.B. 2004. Preservation of tube feet in an ophiuroid (Echinodermata) from the Lower Devonian Hunsrück Slate of Germany and a redescription of *Bundenbachia benecke* and *Palaeophiomyxa grandis*. *Paläontologische Zeitschrift*, **78**, 73-95.
- GOBLER, C.J. e BAUMANN, H. 2016. Hypoxia and acidification in ocean ecosystems: coupled dynamics and effects on marine life. *Biology Letters*, **12**, 20150976.
- GOHARIMANESH, M., STÖHR, S., GHASSEMZADEH, F., MIRSHAMSI, O. e ADRIAENS, D. 2023. A methodological exploration to study 2D arm kinematics in Ophiuroidea (Echinodermata). *Frontiers in Zoology*, **20**, 15.
- GOLUBIĆ, S. e SCHNEIDER, J. 1979. Carbonate dissolution. 107-129. Em TRUDINGER, P.A. e SWAINE, D.J. (eds). *Biogeochemical Cycling of Mineral-Forming Elements*. Elsevier, 612 pp.
- GORZELAK, P. e SALAMON, M.A. 2013. Experimental tumbling of echinoderms - taphonomic patterns and implications. *Palaeogeography, Palaeoclimatology, Palaeoecology*, **386**, 569-574.
- GREENSTEIN, B.J. 1991. An Integrated Study of Echinoid Taphonomy: Predictions for the Fossil Record of Four Echinoid Families. *Palaios*, **6**, 519-540.
- GREENSTEIN, B.J., PANDOLFI, J.M. e MORAN, P.J. 1995. Taphonomy of crown-of-thorns starfish: implications for recognizing ancient population outbreaks. *Coral Reefs*, **14**, 91-97.
- GUINOTTE, J.M. e FABRY, V.J., 2008. Ocean Acidification and Its Potential Effects on Marine Ecosystems. *Annals of the New York Academy of Sciences*, **1134**, 320-342.

- GUPTA, N.S. e BRIGGS, D.E.G. 2011. Taphonomy of Animal Organic Skeletons Through Time. 199-222. Em ALLISON, P.A. e BOTTJER, D.J. (eds). *Taphonomy: Process and Bias Through Time*. Springer, 599 pp.
- HARVEY, T.H.P., VÉLEZ, M.I. e BUTTERFIELD, N.J., 2012. Exceptionally preserved crustaceans from western Canada reveal a cryptic Cambrian radiation. *PNAS*, **109**, 1589-1594.
- HAUGH, B.N. 1975. Digestive and coelomic systems of Mississippian camerate crinoids. *Journal of Paleontology*, **49**, 472-493.
- HAUGH, B.N. e BELL, B.M. 1980. Fossilized Viscera in Primitive Echinoderms. *Science*, **209**, 653-657.
- HAZRA, T., SPICER, R.A., HAZRA, M., MAHATO, S., SPICER, T.E.V., BERA, S., VALDES, P.J., FARNSWORTH, A., HUGHES, A.C., JIAN, Y. e KHAN, M.A. 2020. Latest Neogene monsoon of the Chotanagpur Plateau, eastern India, as revealed by fossil leaf architectural signatures. *Palaeogeography, Palaeoclimatology, Palaeoecology*, **545**, 109641.
- HENDLER, G., MILLER, J.E., PAWSON, D.L. e KIER, P.M. 1995. Sea stars, sea urchins, and allies: echinoderms of Florida and the Caribbean. *Smithsonian Institution Press*, 391 pp.
- HENRY, D.G., JARVIS, I., GILLMORE, G. e STEPHENSON, M. 2019. Raman spectroscopy as a tool to determine the thermal maturity of organic matter: Application to sedimentary, metamorphic and structural geology. *Earth-Science Reviews*, **198**, 102936.
- HUGHES, S.J.M., RUHL, H.A., HAWKINS, L.E., HAUTON, C., BOORMAN, B. e BILLET, D.S.M. 2011. Deep-sea echinoderm oxygen consumption rates and an interclass comparison of metabolic rates in Asterozoidea, Crinozoidea, Echinozoidea, Holothurozoidea and Ophiurozoidea. *The Journal of Experimental Biology*, **214**, 2512-2521.
- HUNTER-CEVERA, J., KARL, D. e BUCKLEY, M. 2005. *Marine Microbial Diversity: The Key to Earth's Habitability*. American Society for Microbiology, 22 pp.
- ISHIDA, Y. 2003. Cenozoic ophiuroids from Japan; particularly those conspecific with extant species. 53-59. Em FÉRAL, J.-P. e DAVID, B. (eds). *Echinoderm research 2001: Proceedings of the 6th European conference on echinoderm research*. Swets & Zeitlinger, Lisse, 337 pp.
- ISHIDA, Y. e FUJITA, T. 2001. Escape behavior of epibenthic ophiuroids buried in the sediment: observations of extant and fossil *Ophiura sarsii sarsii*. 285-292. Em BARKER, M. (ed). *Echinoderms 2000: Proceedings of the Tenth International Conference*. A.A. Balkema Publishers, 612 pp.

- ISHIDA, Y., TANABE, T., ITO, T. e HACHIYA, K. 1996. Fossil Ophiuroids from the Plio-Pleistocene Hijikata Formation of the Kakegawa Group, Shizuoka, Central Japan. *Bulletin of the National Science Museum*, **22**, 63-89.
- ISHIDA, Y., FUJITA, T. e THUY, B. 2015. Two ophiuroid species (Echinodermata, Ophiuroidea) from lower Miocene deep-sea sediments of Japan. *Paleontological Research*, **19**, 208-218.
- ISHIDA, Y., TAGIRI, M., KATO, T., TSUNODA, S., NAKAJIMA, Y., THUY, B., NUMBERGER-THUY, L.D. e FUJITA, T. 2024. The new brittle-star species *Stegophiura takaisoensis* (Echinodermata, Ophiuroidea) from the Pliocene of Ibaraki Prefecture, central Japan. *Paleontological Research*, **28**, 82-96.
- JĘDRASIK, J. e KOWALEWSKI, M. 2019. Mean annual and seasonal circulation patterns and long-term variability of currents in the Baltic Sea. *Journal of Marine Systems*, **193**, 1-26.
- JELBY, M. E., GRUNDVÅG, S.-A., HELLAND-HANSEN, W., OLAUSSEN, S. e STEMMERIK, L. 2020. Tempestite facies variability and storm-depositional processes across a wide ramp: towards a polygenetic model for hummocky cross-stratification. *Sedimentology*, **67**, 742-781.
- JIMÉNEZ, V.C., MONFERRAN, M.D., PACE, D.M.D., COPELLO, G.J., PELLERANO, R.G., CABALERI, N.G. e GALLEGGO, O.F., 2024. Preservational analysis of Jurassic clam shrimps from la Matilde formation (Patagonia, Argentina) by libS and Raman spectroscopies. *Palaios*, **39**, 127-144.
- KANEKI, S. e KOUKETSU, Y. 2022. An automatic peak deconvolution method for Raman spectra of terrestrial carbonaceous material for application to the geothermometers of Kouketsu et al. (2014). *Island Arc*, **31**, e12467.
- KAPLAN, I.R., 1974. Natural gases in marine sediments. Plenum Press, 324 pp.
- KEHAYIAS, G., GIANNI, A., DOULKA, E. e ZACHARIAS, I. 2012. Anoxia and its impacts on the vertical distribution of copepods in a deep Mediterranean coastal lake. *Fresenius Environmental Bulletin*, **10**, 2993-3002.
- KERR, T.J.V. e TWITCHETT, R.J. 2004. Experimental decay and disintegration of *Ophiura texturata*: implications for the fossil record of ophiuroids. 439-446. Em HEINZELLER, T. e NEBELSICK, J.H. (eds). *Echinoderms München*. Taylor & Francis, 660 pp.
- KIDWELL, S.M., e BAUMILLER, T. 1989. Post-mortem disintegration of echinoids: effects of temperature, oxygenation, tumbling, and algal coats. *Abstracts of the 28th International Geological Congress*, **2**, 188-189.
- KIDWELL, S.M. e BAUMILLER, T. 1990. Experimental disintegration of regular echinoids: roles of temperature, oxygen, and decay thresholds. *Paleobiology*, **16**, 247-271.

- KING, N.J., BAILEY, D.M. e PRIEDE, I.G. 2007. Role of scavengers in marine ecosystems: Introduction. *Marine Ecology Progress Series*, **350**, 175-178.
- KLOMPMAKER, A.A., PORTELL, R.W. e FRICK, M.G. 2017. Comparative experimental taphonomy of eight marine arthropods indicates distinct differences in preservation potential. *Palaeontology*, **60**, 773-794.
- KOLAWOLE, F. e EVENICK, J.C. 2023. Global distribution of geothermal gradients in sedimentary basins. *Geoscience Frontiers*, **14**, 101685.
- KOUKETSU, Y., MIZUKAMI, T., MORI, H., ENDO, S., AOYA, M., HARA, H., NAKAMURA, D. e WALLIS, S. 2014. Raman CM geothermometer using FWHM. *Island Arc*, **23**, 33-50.
- KUMARAN, K.P.N., LIMAYE, R.B., PUNEKAR, S.A., RAJAGURU, S.N., JOSHI, S.V. e KARLEKAR, S.N. 2013. Vegetation response to South Asian Monsoon variations in Konkan, western India during the Late Quaternary: Evidence from fluvio-lacustrine archives. *Quaternary International*, **286**, 3-18.
- LAWRENCE, J.M. 1996. Mass mortality of echinoderms from abiotic factors. 103-138. Em JANGOUX, M. e LAWRENCE, J.M. (eds). *Echinoderm Studies 5*. A.A. Balkema Publishers, 250 pp.
- LEWIS, R. 1980. Taphonomy. 27-39. Em BROADHEAD, T.W. e WATERS, J.W. (eds). *Echinoderms: Notes for a Short Course*. University of Tennessee, Sciences Studies in Geology, 3, 235 pp.
- LEWIS, R. 1986. Relative Rates of Skeletal Disarticulation in Modern Ophiuroids and Paleozoic Crinoids. *Geological Society of America Abstracts with Programs*, **18**, 672.
- LEWIS, R. 1987. Post-mortem decomposition of ophiuroids from the Mississippi Sound. *Geological Society of America Abstracts with Programs*, **19**, 94-95.
- LI, C.-W., CHEN, J.-Y., LIPPS, J.H., GAO, F., CHI, H.-M. e WU, H.-J. 2007. Ciliated protozoans from the Precambrian Doushantuo Formation, Wengan, South China. *Geological Society, London, Special Publications*, **286**, 151-156.
- LIN, J.-P., AUSICH, W.I., ZHAO, Y.-L., e PENG, J. 2008. Taphonomy, palaeoecological implications, and colouration of Cambrian gogiid echinoderms from Guizhou Province, China. *Geological Magazine*, **145**, 17-36.
- LEFEBVRE, B., GUENSBURG, T.E., MARTIN, E.L.O., MOOI, R., NARDIN, E., NOHEJLOVÁ, M., SALEH, F., KOURAÏSS, K., HARIRI, K.E. e DAVID, B. 2019. Exceptionally preserved soft parts in fossils from the Lower Ordovician of Morocco clarify stylophoran affinities within basal deuterostomes. *Geobios*, **52**, 27-36.

- LEWIS, R. 1980. Taphonomy. 27-39. Em BROADHEAD, T.W. e WATERS, J.W. (eds.). Echinoderms: Notes for a Short Course. *University of Tennessee, Sciences Studies in Geology*, **3**.
- LOYDELL, D.K., ORR, P. e KEARNS, S. 2004. Preservation of soft tissues in Silurian graptolites from Latvia. *Palaeontology*, **47**, 503-513.
- MARTIN, R.E. 1999. Taphonomy: A Process Approach. Cambridge University Press, 508 pp.
- MCCMAHON, S., ANDERSON, R.P., SAUPE, E.E. e BRIGGS, D.E.G. 2016. Experimental evidence that clay inhibits bacterial decomposers: Implications for preservation of organic fossils. *Geology*, **44**, 867-870.
- MEYER, D.L. 1971. Post-mortem disintegration of Recent crinoids and ophiuroids under natural conditions. *Geological Society of America Abstracts with Programs*, **3**, 645-646.
- MEYER, D.L. e MILSON, C.V. 2001. Microbial sealing in the biostratigraphy of *Uintacrinus* Lagerstätten in the Upper Cretaceous of Kansas and Colorado, USA. *Palaios*, **16**, 535-546.
- MILANI, E.J., KINOSHITA, E.M., ARAÚJO, L.M. e CUNHA, P.R.C. 1990. Bacia do Paraná: possibilidades petrolíferas da calha central. *Boletim de Geociências da Petrobrás*, **4**, 21-34.
- MILANI, E.J., MELO, J.H.G., SOUZA, P.A., FERNANDES, L.A. e FRANÇA, A.B. 2007. Bacia do Paraná. *Boletim de Geociências da Petrobras*, **15**, 265-287.
- MOURO, L.D., PACHECO, M.L.A.F., RICETTI, J.H.Z., SCOMAZZON, A.K., HORODYSKI, R.S., FERNANDES, A.C.S., CARVALHO, M.A., WEINSCHÜTZ, L.C., Silva, M.S., WAICHEL, B.L. e SCHERER, C.M.S. 2020. Lontras Shale (Paraná Basin, Brazil): Insightful analysis and commentaries on paleoenvironment and fossil preservation into a deglaciation pulse of the late Paleozoic Ice Age. *Palaeogeography, Palaeoclimatology, Palaeoecology*, **555**, 109850.
- MULDER, T., SYVITSKI, J.P.M., MIGEON, S., FAUGÈRES, J.C. e SAVOYE, S. 2003. Marine hyperpycnal flows: Initiation, behavior and related deposits. A review. *Marine and Petroleum Geology*, **20**, 861-882.
- MULDER, T. e CHAPRON, E. 2011. Flood deposits in continental and marine environments: character and significance. 1-30. Em SLATT, R.M. e ZAVALA, C. (eds.). Sediment transfer from shelf to deep water - Revisiting the delivery system. *AAPG Studies in Geology*, **61**, 214 pp.

- MÜLLER, A.H. 1979. Fossilization (taphonomy). 2-78. Em ROBISON, R.A. e Teichert, C. (eds). *Treatise on Invertebrate Paleontology. Part A. Introduction*. Geological Society of America and University of Kansas Press, 569 pp.
- MUSCENTE, A.D., ALLMON, W.D. e XIAO, S. 2016. The hydroid fossil record and analytical techniques for assessing the affinities of putative hydrozoans and possible hemichordates. *Palaeontology*, **59**, 71-87.
- NAIMARK, E.B. e BOEVA, N.M. 2016. The role of iron in the formation of fossils of soft-bodied organisms: Results of long-term experiments. *Doklady Earth Sciences*, **490**, 72-75.
- NEBELSICK, J.H. 2004. Taphonomy of Echinoderms: introduction and outlook. 471-477. Em HEINZELLER, T. e NEBELSICK, J.H. (eds). *Echinoderms: München*. Taylor & Francis Group, 664 pp.
- NEBELSICK, J.H. e KAMPFER, S. 1994. Taphonomy of *Clypeaster humilis* and *Echinodiscus auritus* (Echinoidea, Clypeasteroidea) from the Red Sea. 803-808. Em DAVID, B., GUILLE, A., FÉRAL, J.-P. e ROUX, M. (eds). *Echinoderms through Time*. A.A. Balkema Publishers, 940 pp.
- NICHOLS, J.A., ROWE, G.T., CLIFFORD, C.H. e YOUNG, R.A. 1978. In situ experiments on the burial of marine invertebrates. *Journal of Sedimentary Petrology*, **48**, 419-425.
- NOMURA, S.F., SAWAKUCHI, A.O., BELLO, R.M.S., MÉNDEZ-DUQUE, J., FUZIKAWA, K., GIANNINI, P.C.F. e DANTAS, M.S.S. 2014. Paleotemperatures and paleofluids recorded in fluid inclusions from calcite veins from the northern flank of the Ponta Grossa dyke swarm: Implications for hydrocarbon generation and migration in the Paraná Basin. *Marine and Petroleum Geology*, **52**, 107-124.
- ORSI, W.D. 2018. Ecology and evolution of seafloor and subseafloor microbial communities. *Nature Reviews Microbiology*, **16**, 671-683.
- OSÉS, G.L., PETRI, S., VOLTANI, C.G. PRADO, G.M.E.M., GALANTE, D., RIZZUTTO, M.A., RUDNITZKI, I.D. SILVA, E.P.S., RODRIGUES, F., RANGEL, E.C., SUCERQUIA, P.A. e PACHECO, M.L.A.F. 2017. Deciphering pyritization-kerogenization gradient for fish soft-tissue preservation. *Scientific Reports*, **7**, 1468.
- PARRY, L. A., SMITHWICK, F., NORDEN, K. K., SAITTA, E. T., LOZANO-FERNANDEZ, J., TANNER, A. R., CARON, J.-B., EDGE-COMBE, G. D., BRIGGS, D. E. G. e VINTHER, J. 2017. Soft bodied fossils are not simply rotten carcasses - toward a holistic understanding of exceptional fossil preservation. *BioEssays*, **40**, 1700167.
- PEREIRA, D.A., ANDRADE, P.B., PIRES, R.A. e REIS, R.L. 2014. Chemical ecology of echinoderms: impact of environment and diet in metabolomic profile. 57-76. Em WHITMORE, E. (ed). *Echinoderms: Ecology, habitats and reproductive biology*. Nova Science Publishers, 163 pp.

- PICKETT, M. e ANDERSSON, A.J. 2015. Dissolution rates of biogenic carbonates in natural seawater at different pCO<sub>2</sub> conditions: A laboratory study. *Aquatic Geochemistry*, **21**, 459-485.
- PLOTNICK, R.E. 1986. Taphonomy of a Modern Shrimp: Implications for the Arthropod Fossil Record. *Palaios*, **1**, 286-293.
- POINAR, G., KERP, H. e HASS, H. 2008. *Palaeonema phyticum* gen. n., sp. n. (Nematoda: Palaeonematidae fam. n.), a Devonian nematode associated with early land plants. *Nematology*, **10**, 9-14.
- PURNELL, M.A., DONOGHUE, P.J.C., GABBOTT, S.E., MCNAMARA, M.E., MURDOCK, D.J.E. e SANSOM, R.S. 2018. Experimental analysis of soft-tissue fossilization: opening the black box. *Palaeontology*, **61**, 317-323.
- QIN, S., DONG, L., LIU, X., TANG, F. e LIU, H. 2023. Macroscopic carbonaceous compression fossils from the Tonian Liulaobei Formation in the Huainan region of North China. *Precambrian Research*, **393**, 107076.
- RADWAŃSKI, A. 2002. Triassic brittlestar beds of Poland: a case study of *Aspiduriella ludeni* (v. Hagenow, 1846) and *Arenorbis squamosus* (E. Picard, 1858). *Acta Geologica Polonica*, **52**, 395-410.
- RAHMAN, I.A., THOMPSON, J.R., BRIGGS, D.E.G., SIVETER, D.J., SIVETER, D.J. e SUTTON, M.D. 2019. A new ophiocistioid with soft-tissue preservation from the Silurian Herefordshire Lagerstätte, and the evolution of the holothurian body plan. *Proceedings of the Royal Society B*, **286**, 20182792.
- REID, M., TAYLOR, W.L., BRETT, C.E., HUNTER, A.W. e BORDY, E.M. 2019. Taphonomy and paleoecology of an ophiuroid-stylophoran obrution deposit from the lower Devonian Bokkeveld Group, South Africa. *Palaios*, **34**, 212-228.
- RIJN, L.V. 2023. Fluid mud formation. Disponível em: [www.leovanrijn-sediment.com](http://www.leovanrijn-sediment.com).
- ROSENKRANZ, D. 1971. Zur Sedimentologie und Okologie von Echinodermen Lagerstätten. *Neues Jahrbuch für Geologie und Paläontologie*, **138**, 221-258. [em alemão]
- ROTTEROVÁ, J., EDGCOMB, V.P., ČEPIČKA, I. e BEINART, R., 2022. Anaerobic ciliates as a model group for studying symbioses in oxygen-depleted environments. *Journal of Eukaryotic Microbiology*, **69**, e12912.
- RUSSELL, M. P. 2013. Echinoderm responses to variation in salinity. 171–212. Em LESSER, M. (ed.) *Advances in marine biology*, 66. Academic Press, 301 pp.
- RUXTON, G.D. e HOUSTON, D.C. 2004. Energetic feasibility of an obligate marine scavenger. *Marine Ecology Progress Series*, **266**, 59-63.

- SALAMON, M.A., GORZELAK, P., NIEDŹWIEDZKI, R., TRZEŚIOK, D. e BAUMILLER, T.K. 2014. Trends in shell fragmentation as evidence of mid-Paleozoic changes in marine predation. *Paleobiology*, **40**, 14-23.
- SALAMON, M. A., NIEDŹWIEDZKI, R., LACH, R., BRACHANIEC, T. e GORZELAK, P. 2012. Ophiuroids discovered in the middle triassic hypersaline environment. *PLoS One*, **7**, e49798.
- SALDANHA, L. 1972. Preparação e conservação de animais marinhos. *Arquivos do Museu Bocage, Série Extensão Cultural e Ensino*, **9**, 1-16.
- SCHÄFER, W. 1972. Ecology and Palaeoecology of Marine Environments. University of Chicago Press, 584 pp.
- SALEH, F., DALEY, A.C., LEFEBVRE, B., PITTET, B. e PERRILLAT, J.P. 2020. Biogenic iron preserves structures during fossilization: A hypothesis. *BioEssays*, **42**, 1900243.
- SALEH, F., LEFEBVRE, B., DUPICHAUD, C., MARTIN, E.L.O., NOHEJLOVÁ, M. e SPACCESI, L. 2023. Skeletal elements controlled soft-tissue preservation in echinoderms from the Early Ordovician Fezouata Biota. *Geobios*, **81**, 51-66.
- SALEH, F., VAUCHER, R., ANTCLIFFE, J.B., DALEY, A.C., HARIRI, K.E., KOURAISS, K., LEFEBVRE, B., MARTIN, E.L.O., PERRILLAT, J.-P., SANSJOFRE, P., VIDAL, M. e PITTET, B. 2021. Insights into soft-part preservation from the Early Ordovician Fezouata Biota. *Earth-Science Reviews*, **213**, 103464.
- SANT'ANNA, L.G., CLAUER, N., CORDANI, U.G., RICCOMINI, C., VELÁZQUEZ, V.F. e LIEWIG, N. 2006. Origin and migration timing of hydrothermal fluids in sedimentary rocks of the Paraná Basin, South America. *Chemical Geology*, **230**, 1-21.
- SCHIFFBAUER, J., XIAO, S., CAI, Y., WALLACE, A.F., HUA, H., HUNTER, J., XU, H., PENG, Y. e KAUFMAN, A.J. 2014. A unifying model for Neoproterozoic-Palaeozoic exceptional fossil preservation through pyritization and carbonaceous compression. *Nature Communications*, **5**, 5754.
- SCHITO, A., ROMANO, C., CORRADO, S., GRIGO, D. e POE, B. 2017. Diagenetic thermal evolution of organic matter by Raman spectroscopy. *Organic Geochemistry*, **106**, 57-67.
- SCHNITZER, M. 1985. Nature of nitrogen in humic substances. 303-325. Em MC KNIGHT, D.M., AIKEN, G.R., WERSHAW, R.L. e MacCARTHY, P. (eds). *Humic Substances in Soil, Sediment and Water: Geochemistry, Isolation and Characterization*. Wiley & Sons, 708 pp.
- SEILACHER, A. 1982. General Remarks About Event Deposits. 161-174. Em EINSELE, G. e Seilacher, A. (eds). *Cyclic and Event Stratification*. Springer Verlag, 536 pp.

- SEILACHER, A., REIF, W.-E. e WESTPHAL, F. 1985. Sedimentological, ecological and temporal patterns of fossil Lagerstätten. *Philosophical Transactions of the Royal Society of London*, **B311**, 5-24.
- SMITH, A.B. e GALLEMÍ, J. 1991. Middle Triassic holothurians from northern Spain. *Palaeontology*, **34**, 49-76.
- SMITH, A.B. e REICH, M. 2013. Tracing the evolution of the holothurian body plan through stem-group fossils. *Biological Journal of the Linnean Society*, **109**, 670-681.
- SPENCER, W.K. e WRIGHT, C.W. 1966. Asterozoans. 4-107. Em Moore, R.C. (ed). *Treatise on Invertebrate Paleontology, Part U, Echinodermata 3*. The Geological Society of America and The University of Kansas Press, Lawrence, 366 pp.
- SPEYER, S.E. e BRETT, C.E. 1988. Taphofacies models for epeiric sea environments: Middle Paleozoic examples. *Palaeogeography, Palaeoclimatology, Palaeoecology*, **63**, 225-262.
- SPRINGER, F. 1901. *Uintacrinus*, its structure and relations. *Memoirs of the Museum of Comparative Zoology, Harvard University*, **25**, 1-89.
- STEYAERT, M., MOODLEY, L., NADONG, T., MOENS, T., SOETAERT, K. e VINCX, M. 2007. Responses of intertidal nematodes to short-term anoxic events. *Journal of Experimental Marine Biology and Ecology*, **345**, 175-184.
- STÖHR, S., O'HARA, T.D. e THUY, B. 2012. Global Diversity of Brittle Stars (Echinodermata: Ophiuroidea). *PLoS ONE*, **7**, e31940.
- SUMMONS, R.E. 1993. Biogeochemical cycles: A review of fundamental aspects of organic matter formation, preservation, and composition. 3-21. Em STEHLI, F.G. e JONES, D.S. (eds). *Organic Geochemistry Principles and Applications*. Springer Science+Business Media, 861 pp.
- SUTTON, M.D., BRIGGS, D.E.G., SIVETER, D.J., SIVETER, D.J., e GLADWELL, D.J. 2005. A starfish with three-dimensionally preserved soft parts from the Silurian of England. *Proceedings of the Royal Society B*, **272**, 1001-1006.
- TAKAGI, T., KANENIWA, M. e ITABASHI, Y. 1986. Fatty acids in Crinoidea and Ophiuroidea: Occurrence of all-cis-6,9,12,15,18,21-tetracosahexaenoic acid. *Lipids*, **21**, 430-433.
- TEIXEIRA, C.A.S., SAWAKUCHI, A.O., BELLO, R.M.S., NOMURA, S.F., BERTASSOLI, D.J. e CHAMANI, M.A.C. 2018. Fluid inclusions in calcite filled opening fractures of the Serra Alta Formation reveal paleotemperatures and composition of diagenetic fluids percolating Permian shales of the Paraná Basin. *Journal of South American Earth Sciences*, **84**, 242-254.
- TOMHOLT, L., FRIESEN, L.J., BERDICHEVSKY, D., FERNANDESA, M.C., PIERRE, C., WOOD, R.J. e WEAVER, J.C., 2020. The structural origins of brittle star arm kine-

- matics: An integrated tomographic, additive manufacturing, and parametric modeling-based approach. *Journal of Structural Biology*, **211**, 107481.
- VANDENBROUCKE, M. e LARGEAU, C. 2007. Kerogen origin, evolution and structure. *Organic Geochemistry*, **38**, 719-833.
- WALKER, B.J., MILLER, M.F., BOWSER, S.S., FURBISH, D.J. e GUALDA, G.A.R. 2013. Dissolution of ophiuroid ossicles on the shallow Antarctic shelf: implications for the fossil record and ocean acidification. *Palaios*, **28**, 317-332.
- WARNER, G.F. 1971. On the ecology of a dense bed of the brittle-star *Ophiothrix fragilis*. *Journal of the Marine Biological Association of the United Kingdom*, **51**, 267-282.
- WILSON, L.A. e BUTTERFIELD, N.J. 2014. Sediment effects on the preservation of Burgess Shale-type compression fossils. *Palaios*, **29**, 145-153.
- WISHNER, K.F., SEIBEL, B. e OUTRAM, D. 2020. Ocean deoxygenation and copepods: coping with oxygen minimum zone variability. *Biogeosciences*, **17**, 2315-2339.
- ZATÓN, M., SALAMON, M.A., BOCZAROWSKI, A. e SITEK, S., 2008. Taphonomy of dense ophiuroid accumulations from the Middle Triassic of Poland. *Lethaia*, **41**, 47-58.
- ZAVALA, C. 2020. Hyperpycnal (over density) flows and deposits. *Journal of Palaeogeography*, **9**, 1-21.
- ZAVALA, C. e ARCURI, M. 2016. Intrabasinal and extrabasinal turbidites: origin and distinctive characteristics. *Sedimentary Geology*, **337**, 36-54.
- ZAVALA, C., ARCURI, M., DI MEGLIO, M., DIAZ, H.G. e CONTRERAS, C. 2011. A genetic facies tract for the analysis of sustained hyperpycnal flow deposits. 31-51. Em SLATT, R.M. e Zavala, C. (eds). *Sediment transfer from shelf to deep water - Revisiting the delivery system*. AAPG Studies in Geology, 61, 214 pp.
- ZAVALA, C., ARCURI, M. e VALIENTE, L.B. 2012. The importance of plant remains as diagnostic criteria for the recognition of ancient hyperpycnites. *Revue de Paléobiologie*, **11**, 457-469.
- ZHANG, F., WANG, H., YE, Y., DENG, Y., LYU, Y., WANG, X., YU, Z., LYU, D., LU, Y., ZHOU, C., BI, L., DENG, S., ZHANG, S. e CANFIELD, D.E. 2021. The environmental context of carbonaceous compressions and implications for organism preservation 1.40 Ga and 0.63 Ga. *Palaeogeography, Palaeoclimatology, Palaeoecology*, **573**, 110449.
- ZHUKOVA, N.V. 2022. Fatty acids of echinoderms: Diversity, current applications and future opportunities. *Marine Drugs*, **21**, 21.

How does rapid burial work? New insights from experiments with echinoderms

RAPID COMMUNICATION  
How does rapid burial work? New insights from experiments with echinoderms

by MALTON CARVALHO FRAGA\* and CRISTINA SILVEIRA VEGA  
Departamento de Geologia, Universidade Federal do Paraná, Curitiba, PR, Brazil. malton.carvalho@ufpr.br, cristina@ufpr.br

Manuscript received 14 October 2023; accepted in revised form 15 March 2024  
\*Corresponding author

**Abstract:** This research explores the significance of rapid burial in preserving fossils, with a particular focus on free-living echinoderms. Experiments were based on ophiuroid skeletons buried under different turbidite flows, ranging from 10 cm to 100 cm, to simulate burial under thicknesses of around 10 cm. The results showed that a bed thickness of around 10 cm is a limit for the preservation of whole skeletons in most cases. The type of sediment can affect the integrity of the buried skeletons, with sand deposition resulting in higher rates of autolysis. However, mud deposition did not show any numbing effect, as previously believed for echinoderms. In contrast, freshwater-rich sediments can play a

critical role, paralyzing specimens and preventing escape postures through rapid changes in salinity. From this, the study highlights the importance of extrabasinal turbidites, generated outside the marine basin, in the fossilization of water and can be more efficient burial traps compared to other intrabasinal deposits generated by storm waves or submarine landslides.

**Key words:** ophiuroid, escape posture, turbidite, intrabasinal, extrabasinal, experimental taphonomy.

BURIAL is a critical factor in the preservation of most fossils. On the one hand, low burial rates keep the remains of organisms under the destructive effects of bioturbation, resulting in the decay of soft parts and disarticulation of hard elements (Brandt 1989; Brett & Baird 1986, 1993; Speyer & Brett 1988; Donovan 1991; Parry et al. 2017). These rapid depositional events can produce obstruction beds with well-preserved fossils, including delicate records of soft-bodied and multi-elemental organisms (Sclacher et al. 1985; Allison 1988).

Although this exceptional preservation is often attributed to the rapid burial of live specimens, the type of depositional process associated is still an underexplored variable in taphonomic studies. As important case occurs in epicontinental basins, where tempestites are considered the main burial agent of articulated invertebrates (Lewis 1980; Brett & Baird 1986; Speyer & Brett 1988; Brett et al. 1997; Audech 2021), even in the absence of direct sedimentological evidence of storm influence. However, although storm waves also can produce potential burial events, they carry a paradox: post-depositional

reworking is high in proximal sandy tempestites, while the frequency and thickness of beds are limited in distal muddy depositional scenarios (Fraga & Vega 2022). In the case of free-living echinoderms, such as asteroids and ophiuroids, even a rapid influx of sediment still depends on a special condition to prevent the escape of specimens buried alive. The burial thickness when the sediment column overloads exceeds a critical point (Schäfer 1972; Nichols et al. 1978). Another limiting effect is historically inferred to be mud deposition, in which clay particles could obstruct the madreporite (Rosenkranz 1971; Sclacher 1982; Sclacher et al. 1985). However, since modern echinoderms can remain active for prolonged periods without access to madreporite (e.g. Ferguson 1992, 1995), it is uncertain whether mud obstruction alone could rapidly inhibit escape behaviours. A more recent alternative for the burial may be also related to sediment flows derived from river discharges, which are well known for their extensive sedimentary contribution to modern seas. These events can generate long-duration hyperpycnal flows capable of transferring large loads of freshwater-rich sediments hundreds of kilometres from the river mouth (Mulder et al. 2003; Mulder

2 PALAEOLOGY

& Chapron 2011; Zavala et al. 2011; Zavala & Arcuri 2016; Zavala 2020). Considering that fresh water is an anaesthetic for echinoderms (Saldanha 1972; Henders et al. 1995), these hyperpycnal flows may have the potential for mass immobilization of live specimens, favouring preservation under thinner burial beds (Fraga & Vega 2022). However, due to the lack of experimental studies, many effects of these processes are still speculative for the burial of free-living echinoderms. Therefore, here we review the influence of salinity, oxygenation, sediment size, and thickness of the deposited bed on the burial potential of modern ophiuroids. The results are based on laboratory simulations of extrabasinal flows generated outside marine basins, and intrabasinal turbidites, to cover depositional events generated within the marine basins, such as storm waves and submarine landslides. From this, we hope to explore how echinoderms can be buried alive and how different depositional events can influence the preservation of these delicate organisms in the geological record.

MATERIAL AND METHOD

The experiments were based on *Amphipholis januaria*, a small semi-infaunal ophiuroid abundant along the Paraná Estuarine Complex, on the coast of Paraná, in southern Brazil. With the help of a small boat to access the region, some specimens were collected manually during low tide hours, when parts of this estuary are submerged in a thermal box partially filled with sediment from the site. Some gallons of natural sea water were also sampled in the estuary for laboratory use. A total of nine field collections were conducted, one before each burial experiment, all licensed by the Brazilian regulatory systems for biodiversity and genetic heritage, SISBIO and SISGEN, respectively.

In the laboratory, the ophiuroids were carefully inspected to remove dead, moribund, or autotomized specimens. After initial screening, 10 adult and active specimens, capable of quickly turning over when placed on their backs, were selected to be used in each of the experiments. These specimens were acclimatized for 3 h inside a 40 L aquarium with sand substrate and natural saline water from the collection site (Fig. 1A). A thermometer was installed to maintain the temperature at 25°C, while a dissolved oxygen sensor was attached next to the substrate to analyse the oxygenation (Table S1). The ophiuroids remained free during the acclimatization,

while some buried themselves in the sand substrate, while others walked most actively through the aquarium. After the acclimatization interval, the ophiuroids were again inspected and any specimen that had gone up to the region of the sand substrate. Once this process was established, the burial of the ophiuroids was started, always on the same day of the nine pre-depositional scenarios was established, the burial process was started. The main attributes of the burial experiments are indicated in Table 1. The sediment used in the burial flow varied between dolomitic clay or fine quartz sand, the same as the aquarium mixture was fresh water (±0.5 ppt) or natural saline water. In turn, the final thickness of the burial bed varied between 1.5, 5 or 10 cm, with a margin of error of ±0.5 cm in the 10 cm experiments.

In the mud burial, clay powder and water (fresh or saline) were previously mixed in a plastic bucket and then poured on top of the aquarium ramp. The process resulted in a non-erosive turbidite flow head, with interstitial fluid used in the burial mixture was fresh water (±0.5 ppt) or natural saline water. In turn, the final thickness of the burial bed varied between 1.5, 5 or 10 cm, with a margin of error of ±0.5 cm in the 10 cm experiments. In the mud burial, clay powder and water (fresh or saline) were previously mixed in a plastic bucket and then poured on top of the aquarium ramp. The process resulted in a non-erosive turbidite flow head, with interstitial fluid used in the burial mixture was fresh water (±0.5 ppt) or natural saline water. In turn, the final thickness of the burial bed varied between 1.5, 5 or 10 cm, with a margin of error of ±0.5 cm in the 10 cm experiments.

As an alternative, sand burial was produced only by depositing dry sand directly above the region of the aquarium bottom (Fig. 1C). After burial, the aquarium was observed continuously during the first 8 h. During this period, the salinity of the water and the internal oxygenation of the burial bed were recorded every 30 min. Two 9 W LED lamps were also turned on just above the aquarium to facilitate photography during these initial hours. The aquarium was subsequently covered with a black cloth and left in semi-darkness. After 24 h of burial, all specimens that escaped were carefully removed for inspection of potential patterns resulting from burial stress. The same was repeated after 48 h of burial and then the experiment was ended. Only specimens that completely died above the burial bed were considered for analysis. No buried specimens were recovered for analysis.

RESULTS

**Burial by sandy intrabasinal turbidites**  
Three experiments were conducted with echinoderms under sand

Palaeontology  
VOLUME 67 | ISSUE 2 | MARCH/APRIL 2024





